Studies on Oxidative Degradation of Biomass in Alkaline Water

王, 敬賢

Studies on Oxidative Degradation of Biomass in Alkaline Water

By

Wang Jingxian

Department of Applied Science for Electronic and Materials

Interdisciplinary Graduate School of Engineering Sciences

Kyushu University

2020

ABSTRACT

The energy crisis caused by the depletion of fossil fuels is globally recognized as a serious threat to humanity in the near future. Moving away from fossil fuels in favor of reliance on renewable sources is an inevitable trend in development. Among renewable resources, lignocellulosic biomass is the most abundant renewable organic resource on the earth which has been used as an alternative to fossil fuels for the extensive production of sustainable fuels, chemicals, materials, and biological products. Global researchers have devoted their great efforts to develop effective technologies for biomass conversion in the past decades, the economic transformation and utilization of biomass is restricted by the efficiency and selectivity due to the complexity and resistance structure. High lignin content biomass has stronger resistance than low lignin content biomass. A pretreatment process to reduce its recalcitrance or to fractionate lignocellulose into its main components that improves the conversion efficiency is considered to be the foundation step for the establishment of an economical and sustainable lignocellulosic biorefinery. Alkaline wet oxidation, which allows milder conditions than thermochemical conversion and higher efficiency than bioconversion, is a popular technology to treat biomass for delignification and has been widely used in commercial paper and pulp processes. However, there are still problems such as severe loss of carbohydrates, unclear mechanism of biomass degradation, and the use of expensive or toxic reagents.

A main focus of the present study is the alkaline wet oxidation of biomass under mild conditions using the green oxidant O_2 to achieve deep delignification and thus recover cellulose residue. We achieved deep delignification (96%) of a kind of high lignin content woody biomass, Japanese cedar, using NaOH solution and pressurized O_2 under mild conditions (90 ℃). Chemical mechanisms were explored via investigating the degradation of carbohydrates and establishing the removal relationship between lignin and carbohydrates. Polysaccharides (hemicellulose) were directly decomposed into small molecules without forming monosaccharides.

Delignification consists of three stages (early, mid, and late stages) and the late-stage (removal rate >65%) requires cellulose decomposition for making the lignin accessible to oxidizing agents. Secondary reactions of products dissolved in liquid have a detrimental effect on delignification. Repeated short-time oxidation with renewal of alkaline water suppressed the lignin condensation enhancing the delignification. It is very difficult, even impossible, to analyze the primary reaction using a batch reactor, due to the inevitable secondary reactions of the dissolved products in the aqueous phase. A newly developed flow-through fixed-bed reactor (percolator) was thus employed for the primary extraction. Quantitative kinetic analysis revealed that the cedar consisted of three kinetic components (C1, C2, and C3) that underwent extraction in parallel following first-order kinetics with different rate constants. C1 was converted most rapidly by non-oxidative reactions such as alkali-catalyzed hydrolysis, while C2 by oxidative degradation. C3 was the most refractory component, consisting mainly of glucan and very minimally of the lignin and hemicellulose. Although the hemicellulose was converted into organic acids, it is more valuable if it can be recovered as monosaccharides or oligosaccharides. Hydrothermal treatment and alkaline wet oxidation were combined to recover hemicellulose as oligosaccharides and then to deeply delignify under mild conditions. Most hemicellulose in cedar was recovered as mannose-oligosaccharides with molecular weight (200-10000 Da) by hydrothermal extraction using H_2O at 180 ℃. In the subsequent alkaline wet oxidation, the comparison between NaOH and Na_2CO_3 revealed that Na_2CO_3 was more favorable for the oxidative depolymerization of lignin and removed 98.9% lignin at 120 ℃ recovering a high-cellulose residue (98.8%). As a typical herbaceous and agricultural waste, rice husk was also treated with hydrothermal treatment and alkaline wet oxidation to prepare high-purity pulp. High-purity cellulose fibers (98.1%) were obtained in a high yield (>83 wt%) by using Na_2CO_3 solution and O_2 at 120 ℃ for 120 min. The Na_2CO_3 solution maintained a good delignification effect (84%) even after being reused four times.

CHAPTER I

General Introduction

1.1. World Energy Consumption

Fossil fuels (coal, oil, natural gas) have always been the predominant energy and chemicals sources. Fossil fuels account for more than 80% of the world's total energy consumption and this situation will continue for a long time if no breakthrough innovation in the utilization of renewables. [1] Their increasing consumption has caused serious environmental problems, atmospheric pollution, global warming, etc. The reserves of fossil fuels are limited and non-renewable. An optimistic estimate is that crude oil could last until 2100 based on the current growth in energy consumption and other potential oil resources. [2] It is globally recognized that the energy crisis owing to the fossil fuels depletion is a serious threat that humanity are facing in the near future. Many researchers are continuously working in developing advanced technologies and exploring alternatives to fossil fuels. Moving away from fossil fuels in favor of reliance on renewable sources such as hydropower, wind, solar, biomass, and nuclear energy is now attracting considerable attention. [3] Biomass, nuclear, hydroelectric, and other renewables (geothermal, solar, and wind) provides 9.7%, 4.9%, 2.5% and 1.5% of the world's primary energy requirements, respectively. Many governments and organizations push their heads toward this goal. The EU is eager to provide 20% and 55% of its total energy consumptions from renewable sources by 2020 and 2050, respectively. Germany and the United States plan to reach 80% renewable electricity by 2050 while Denmark proposes to completely eliminate fossil energy by 2050. Aggressive studies reveal that it is possible for China to achieve 26% renewable energy by 2030 and 60% renewable energy and 86% renewable electricity by 2050. [4] Among renewable resources, lignocellulosic biomass is the most abundant renewable organic resource on the earth. It has been exploited for the extensive production of sustainable fuels, chemicals, materials, and biological products that underpin our modern societies owing to its renewability and availability. [5] A remarkable advantage is that conversion of biomass can achieve zero emission of CO_2 due to the fixation of CO_2 through the photosynthesis during its growth.

1.2. Lignocellulosic Biomass

Biomass includes agricultural/forestry residues, herbaceous crops, aquatic, and marine biomass (e.g., algae and seaweed), and organic wastes (e.g., sewage sludge and industrial waste). Lignocellulosic biomass is the most commonly employed type of biomass used for biofuel production. [2] It is mainly composed of three constituent biopolymers (**Figure 1.1**): cellulose (35–55wt%), lignin (15–30wt%), and hemicellulose (10–35wt%). [6]

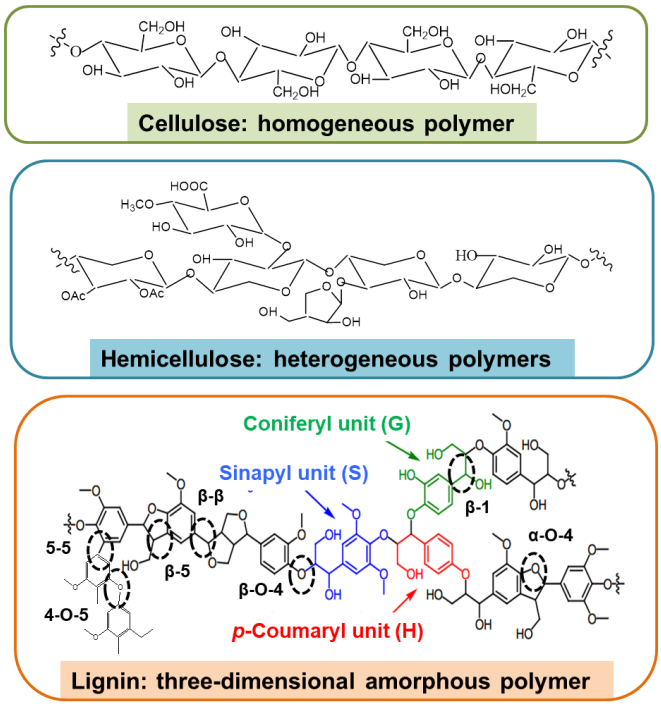

Figure 1.1. Structures of cellulose, hemicellulose, and lignin. [13]

Hemicelluloses give a complex network of bonds by linking cellulose fibres into microfibrils and cross-linking with lignin. [7] Cellulose is a homogeneous polymer composed of glucose long chains that are connected by *β*-glycosidic linkages with reducing and non-reducing ends. Hemicelluloses are heterogeneous polymers consisting of pyranoses and furanoses units, including xylose, mannose, arabinose, glucose, and galacturonic acid. [8] Hemicellulose varies in different biomass; hardwood hemicellulose contains mainly xylan, whereas softwood hemicellulose contains mainly glucomannan. [9] Generally, cellulose and hemicellulose have been fed into already-developed biorefinery product streams for pulp, monosaccharide products or bioethanol. [5] Lignin is a three-dimensional

amorphous polymer comprised of aromatic rings of varying functionalization, primarily hydroxyl, methoxy, and propyl groups. The structure of lignin within different biomasses varies considerably, especially in the composition of its three monolignols, *p*-coumaryl (H), coniferyl (G), and sinapyl units (S). [10] Lignin is the most abundant aromatic renewable resource in the nature. The lignin depolymerization produces phenolic compounds (such as coniferyl, sinapyl, *p*-coumaryl alcohol, and their derivates) which are the potential feedstocks for chemical industry. [11] However, it is very hard to depolymerize lignin into monomers effectively due to its chemical recalcitrance and structural complexity. [12]

These biopolymers are organized into complex inhomogeneous three-dimensional structures in the cell wall which makes the robustness and recalcitrance of lignocellulose. The crystallinity of cellulose, hydrophobicity of lignin, and encapsulation of cellulose by the lignin-hemicellulose matrix all contribute to the resistance of biomass to degradation. [13] The intricate structure and natural recalcitrance often leads to low productivity and complex unstable products, seriously restricting its effective utilization in biochemical and biofuel technologies. [7]

1.3. Biofuel Production Processes

Biomass can be transformed into the desired forms of energy by different technologies. Combustion, pyrolysis, catalytic pyrolysis, gasification, liquefaction, and enzymatic digestion are the mature biomass utilization technologies developed in the past decades. These technologies allow the direct conversion of biomass into heat, mixture of gaseous products (CO_2, CO, H_2, CH_4, etc), char, bio-oils, and chemicals as needed. [5]

Biomass combustion has received widespread attention to provide electric power due to its comparable calorific value to coal (HHV: 10–20 MJ/kg) as well as the trace nitrogen and sulphur. Biomass burning mainly releases CO_2 and H_2O which is friendly to the environment. The combustion systems are constantly being improved to increase combustion efficiency. [14] Along with an apparent growing trend, the biofuels provided 421131.0 GWh in 2018. [15]

Biomass pyrolysis occurs in an oxygen-free atmosphere at 300–600 ℃ under atmospheric pressure primarily converting feedstock into liquid bio-oils and char with a minority of gas. [16] The main decomposition temperature ranges for the three components of biomass, cellulose, hemicellulose, and lignin, are 315–400, 220–315, and 200–600 ℃, respectively. [17] Pyrolysis is categorised to slow and fast pyrolysis (heating rate > 10–200 ℃/s, residence time = 0.5–10 s) according to the heating rate, where mainly produce char and bio-oils, respectively. [18] Char is the residual solid product with low volatility and high carbon content. The carbonaceous residue can be employed as a catalyst carrier or be burned to provide heat. Bio-oils is an organic mixture of alcohols, ketones, aldehydes, phenols, ethers, esters, sugars, furans, alkenes, nitrogen and oxygen compounds, which fine chemicals can be recovered. [18] Bio-oil has some deleterious properties including high oxygen content, thermal instability, high corrosiveness, and correspondingly low heating value, which prevents it from being utilized directly as an engine fuel. To overcome such issues, bio-oils has to be further upgraded by hydrodeoxygenation which requires the involvement of catalysts and high pressure H_2. [19]

Catalytic pyrolysis is a promising technology developed to upgrade the bio-oil in situ during the pyrolysis, where the catalyst was added directly in the reactor for removing the oxygen of oxygenates and cracking the heavy species. [20] Many kinds of catalysts have been developed for catalytic pyrolysis, such as transition metal catalysts (Fe, Ni, Co, Mo, Pa), noble metal catalysts (Pt, Au, Ru), and zeolite catalysts (ZSM-5, Y-zeolite, Beta-zeolite, MCM-41, CM-22, Mordenite, SAPO-34), etc. [21]

Gasification converts biomass into syngas at 800-1500 ℃ (CO, H_2, CH_4, CO_2, and light hydrocarbons) via multi-stages: drying, pyrolysis, oxidation, reduction, and cracking. [22] The conversion is usually performed in the presences of the catalysts and a gasifying carrier, such as oxygen, steam, air, or CO_2. [23] In the past decades, steam was the most popular gasifying agent. Recently, gasification employing CO_2 as a gasifying agent has attracted a considerable attention in the academic and industrial fields of biomass conversion due to its potential advantages in reducing carbon emissions. [24] Syngas is primarily used as chemical feedstock, power generation, or biofuel production.

Biomass liquefaction is a thermochemical process carried out at low temperature (250-400 ℃) and high pressure (1-20 MPa) suitable solvents, in which the wet biomass is converted into bio-oil fractions (target product), gases, and solid residues. [25] Water, organic solvents (methanol, ethanol, acetone, and 2-butanol etc.), and ionic liquids are widely used liquefaction solvents. Among them, water is the most favored thanks to its advantages of environmental benign, cheap, and safety. But it usually yields a relatively low yield of bio-oil (20 wt%). Higher bio-oil yields (30-70 wt%) can be recovered with organic solvents than water, but this could also cause a high cost and some environmental concerns. [26] Although the ionic liquids give the highest conversion rate (>90 wt%), their high cost and non-recyclability prevent them from a large-scale utilization. [27]

Biochemical conversion is a technology to convert biomass into bioethanol, biogas, biological hydrogen, or fermentable sugars etc., using microorganisms or enzymes under mild conditions. [28, 29] Unlike the thermochemical conversion method, this technology is well adapted to the organic waste with a high moisture (>50%). [30] It often takes several days or weeks to degrade the majority of the organic material owing to its low conversion efficiency.

1.4. Biomass Pretreatment Procedures

Using biomass to provide heat is a relatively low-level utilization mode compared to obtaining biomass-based platform chemicals. It is, however, difficult to efficiently and selectively convert biomass into targeted chemicals by a single step treatment method, like pyrolysis and liquefaction, because of the complex and diverse structures of the three-components. [11] Bio-oil is a complex mixture of hundreds of compounds. The three components interact with each other in the process of biomass conversion. It is a consensus that lignin can seriously restrict the efficiently conversion of carbohydrate (cellulose and hemicellulose). [31] The C_5 and C_6 sugars derived from cellulose and hemicellulose can be converted into a variety of platform chemicals, such as 1,4-diacids (succinic acid, fumaric acid, malic acid), 2,5-furan dicarboxylic acid, 3-hydroxy propionic acid, aspartic acid, glucaric acid, glutamic acid, itaconic acid, levulinic acid, 3-hydroxybutyrolactone, glycerol,

sorbitol, and xylitol/arabinitol. [1, 32, 33] Unique structure and chemical properties of lignin allow the production of a wide variety of aromatic compounds. [11, 34, 35] Therefore, an integrated pretreatment process to reduce its recalcitrance or to fractionate lignocellulose into its main components that improves the conversion efficiency is considered to be the foundation step for the establishment of an economical and sustainable lignocellulosic biorefinery. [36] Although it is difficult to completely separate and collect the three components, it is valuable to recover high-quality streams of the major biomass components. Pretreatments generally achieve destruction of the crosslinking structure, increasing pore volume and accessibility, hemicellulose removal and/or degradation, lignin delignification and/or modification, and reducing the crystallinity and polymerization of cellulose etc. [37] Various pretreatment technologies have been extensively studied and are still in development, which can be classified into three categories, including physical, chemical, biological, and combination of these pretreatments.

Common physical pretreatments include steam explosion, hydrothermal treatment, and mechanical comminution. For the steam explosion treatment, biomass particles are rapidly heated by a high-pressure saturated steam at 160-270 ℃ for several seconds or minute, and then achieve an explosive decompression state by swift release of pressure. [38] Although the steam-explosion can effectively improve the digestibility of the residue, it suffers from high voltage equipment and energy consumption. Another desirable alternative is the steam pretreatment where the biomass is treated by superheated steam at atmospheric pressure. [39] The partial hemicellulose can be decomposed by the superheated steam (190-240 ℃) which is crucial for the downstream fractionation. [40, 41] Hydrothermal treatment is a popular pretreatment method for recovering hemicellulose by using hot liquid water, with the advantage of producing hardly any inhibitors of sugar fermentation. Cleavage of O-acetyl and uronic acid substitutions from hemicellulose during the hydrothermal treatment produces organic acids (mainly acetic acid) that contribute to the hydrolysis of hemicellulose into soluble monomeric and oligomeric sugars. [42] A lot of monosaccharides are produced due to the further hydrolysis of dissolved hemicellulose in a batch reactor, while mainly hemicellulosic oligomers are recovered in a flow-through reactor. [43] Although the

pretreatments using steam or hot water show attractive features, including low capital investment, low environmental influence, and low cost of the solvent, it cannot eliminate the negative effect of lignin on the subsequent treatment. Biomass materials are crushed by various chipping, grinding and milling which is known as mechanical comminution. [44] The decreases of cellulose crystallinity and the degree of polymerization, and the increase of specific surface area are achieved by breaking down the biomass into smaller particles. However, it is seldom used exclusively due to the time-consuming, energy-intensive, and expensive. [45]

In general, chemical pretreatment has higher efficiency in removing hemicellulose and lignin compared to the physical treatments. Chemicals were extensively studied, such as acids, alkali, organic solvents, and ionic liquids, etc., for the treatment of biomass. [37] Dilute acid (H_2SO_4, HCl, H_3PO_4, HNO_3, or organic acids) has been used to effectively hydrolyze most of the hemicellulose at moderate temperatures (140-190 ℃). [38] Hemicellulose is recovered mainly in the form of monosaccharides after dilute acid treatment of biomass and the hydrolysate requires neutralization before further conversion. The alkaline pretreatment with NaOH, KOH, $Ca(OH)_2$, or ammonia is basically a delignification process, in which a large amount of hemicellulose is dissolved as well. The mechanism is believed to be the saponification of intermolecular ester bonds that cross-link xylan hemicellulose and lignin, resulting in swelling, increasing internal surface area, and separation of structural bonds between lignin and carbohydrates. [46, 47] It has been shown that alkaline pretreatment is more effective on the low lignin content biomass (hardwood, herbaceous crops, and agricultural residues) than on the biomass with high lignin content (softwood). [48] A significant advantage of alkaline pretreatment is that it can be performed at low temperatures and pressures, even under ambient conditions. Organic solvents (methanol, ethanol, acetone, ethylene glycol, etc.) with and without acid or alkali catalysts are also employed to remove lignin and hemicellulose from biomass. [49] During the pretreatment process, lignin was degraded due to the breaking of ether bond at the side chains carbon position, hemicellulose and minor cellulose were depolymerized to oligosaccharides and monosaccharides due to the disrupting of glycosidic bonds. [50, 51]

Dehydration of saccharides produced furans and HMF, which were further degraded into organic acids. Methanol and ethanol are the most favored organic solvents for biomass pretreatment for economic reasons. [31] Nevertheless, organic pretreatment is still too complex and expensive to attract industrial interests. Ionic liquids, generally defined as salts that melt at or below 100 ℃, can dissolve large amounts of cellulose under mild conditions and have therefore received extensive research attention recently. [52] The interaction of ionic liquids with cellulose hydroxyl groups leads to the disruption of hydrogen bonds between molecular chains of the cellulose resulting in the dissolution of cellulose. [53] Application of ionic liquids has been described as a new potentially development in this area, but there are still many challenges, for example, high price of ionic liquids, regeneration requirement, and lack of toxicological data.

The biological treatment using fungi, bacteria or enzymes is a comparatively green and low energy consumption technology for degrading the biomass components to enhance its degradability or to produce bioethanol and biomethane directly. [54] Biological reagents are usually selective for the three components, especially cellulase, hemicellulases, and ligninase. [55] White-rot fungi selectively degrade lignin with minimum sugar loss while the brown-rot fungi prefer to digest polysaccharides over lignin. [56] Bacteria that work under both aerobic and anaerobic conditions have shown an excellent performance in degrading lignin. [57] Hydrolytic enzymes are the most commonly used biological agents in biological pretreatment to reduce cellulose polymerization, hydrolyze hemicellulose, and remove lignin due to their high selectivity. [58] Usually the biological treatment technology should be combined with other treatment technologies to obtain more desirable results, such as the combination of biological treatment and chemical, physical, or thermal approach.

Normally, a single method of pretreatment is difficult to achieve a desired result for maximum biomass conversion, which requires a combination of these methods for overcoming the limitations of each approach. [37] In terms of chemical and structural changes, previous studies have shown that combined pretreatment methods of two or more stages are more effective than single-stage pretreatment. [58] However, among the many

combined treatment technologies (acid/base-catalyzed organic process, [59] combined fungal physicochemical pretreatment, [60] ammonia fibre/freeze explosion, [61] alkaline wet oxidation, [37] etc.), only alkaline wet oxidation has achieved commercial application in the pulp and paper industry.

1.5. Alkaline Wet Oxidation

Wet oxidation was first applied to remove organic compounds in the wastewater by oxidizing them completely to CO_2 and H_2O using an oxidant such as O_2 or air. [62] Biomass pretreatment using H_2O and high-pressure O_2 was first proposed in 1983 by McGinnis et al. [63] Alkali treatment of biomass is an effective method to delignify with little loss of cellulose and hemicellulose. [36, 64] Adding oxidant in the reaction mixture of alkaline treatment (alkaline wet oxidation) greatly improves the delignification, especially for highly lignified materials. [65] As a typical commercial operation, it is capable of removing about 50% of the lignin from kraft pulp [66] and up to 67% from softwoods. [67] The combination of base and wet oxidation has been shown to reduce the production of inhibitory compounds. [68] It is, therefore, generally considered that the alkaline wet oxidation is a potentially effective pretreatment or fractionation technology which can provide cellulose rich fraction and a soluble stream of hemicellulose/lignin with minimum inhibitor formation. [36, 69-71] The pretreatment technology significantly improves the efficiency of subsequent enzymatic digestion or fermentation due to the decrease in crystallinity and the increase in accessibility of cellulose. [67, 72, 73] In order to obtain high delignification efficiency in a short time, high temperature (>150 ^{o}C), or strong oxidants are generally used. [74]

1.5.1 Oxidants of alkaline wet oxidation

Many oxidants have been reported for alkaline wet oxidation to delignify including chlorine, chlorine dioxide, hypochlorite, hydrogen peroxide, ozone, oxygen, peroxy acids, etc. [75] Chlorine-containing oxidants are efficient in delignification and bleaching pulp but they are environmentally hazardous. Ozone and peroxy acids are highly effective oxidants, but their high cost limits their large-scale application. [76] Although peroxides are

environmentally benign, they have the drawbacks of poor stability, weak oxidative power, and high cost. Molecular oxygen is the most attractive oxidant due to its abundance, low cost, nontoxicity, and environment-friendly nature compared with other oxidants. [74] In addition to delignification and bleaching, oxygen has also been used to oxidatively depolymerize lignin to produce aromatic aldehydes or acids, although in relatively low yields. [74, 77, 78] Since oxygen is a relatively weak oxidant, strong base (such as NaOH) is usually required. Electron transfer between the high electron density centers in substrate and molecular O_2 results in the formation of reactive oxidation species (superoxide anion radical), as shown in the Formula 1.1. The O_2-derived active species directly contribute to the oxidation reaction. [79]

$$O_2 + e^- \text{ (from substrate)} = O_2^- + \text{substrate radical} \qquad \text{(Formula 1.1)}$$

1.5.2 Carbohydrates fate during alkaline wet oxidation

After oxygen delignification most of the cellulose is generally well retained in the solid residue for subsequent production of monosaccharides, bioethanol, and other biochemicals. The cellulose that undergoes degradation is mainly its non-crystalline fraction. Cellulose is first oxidized to carbonyl-containing oxidized cellulose (oxycelluloses) and then subsequently degraded by alkali, which is usually accompanied by chain scission. [80] Cellulose is also attacked by oxygen based radicals generated by the lignin degradation in the late stages of delignification. [81] Curls, kinks, and fiber bonding of the cellulose fibers increased slightly after oxygen delignification. [82] Oxygen delignification has also been reported to change the content of fiber acid group content. [83] The degradation of cellulose is very weak due to its biphasic structure and intracrystalline regions, as well as the encapsulation of hemicellulose and lignin.

In addition, oxygen delignification is always accompanied by the serious loss and degradation of hemicellulose. [84-86] Loss of hemicellulose is mainly caused by alkaline hydrolysis, peeling of end-groups, and oxidative degradation reactions. [7] Alvarez-Vasco et al. [87] investigated softwood hemicelluloses degradation during alkaline wet oxidation and elucidated that an endwise depolymerization and termination reactions are the predominant

degradation pathway. Shi et al. [85] found that 57.67% hemicelluloses were removed from the corn stalk during the heating-up period, while 15% hemicelluloses were removed during at temperature holding period. Studies have shown that most of the dissolved hemicellulose is degraded to organic acids, but little effort has been made to obtain a detailed understanding of the formation pathways of organic acids during hemicellulose degradation. [68, 85]

1.5.3 Lignin fate during alkaline wet oxidation

Alkaline treatment dissolves lignin by cleaving the α-ether linkages and ester bonds between lignin and hemicelluloses. [88] The dissolved lignin could be ionized and then oxidized and depolymerized by O_2 to soluble fragments, aromatic aldehydes, and small molecule organic acids. [71, 74] A portion of the benzene ring structure was severely ruptured and formed low molecular organic acids (formic, acetic, oxalic, and glycolic acids) due to a deep oxidative degradation. [78, 89] The functionalization of lignin can also occur during oxidation by several reactions, such as electrophilic substitution, cleavage of Ar-O-alkyl linkages, rearrangement of side chains, and the oxidative cracking of aromatic nuclei. [7, 77] Thus, the alkaline wet oxidation effectively extracted and separated the lignin from biomass while largely prohibiting the undesired repolymerization and condensation. Several investigators have claimed that the oxidation and partial depolymerization of lignin are helpful for its further catalytic conversion to produce fine chemicals. [90-92] Liquid product containing large amounts of lignin fragments is a good feedstock for further depolymerization to recover aromatic aldehydes. The lignin separation methods that provide more reactive lignin fragments are expected for efficiency depolymerization with high selectivity and yield. [93] Lignin can also be oxidized and degraded directly in the matrix as a solid form. Mittal et al. [94] characterized the residue obtained after alkaline oxidation treatment of the corn stover and found that most of the side-chain structures and aryl-ether bonds in the residual lignin were oxidized and cleaved.

1.5.4 Delignification process during alkaline wet oxidation

It is generally accepted that O_2 delignification process of biomass can be described using as three phases obeying single first-order kinetics: initial, bulk, and residual delignification, as shown in **Figure 1.2**. [95] Different bonds and units (S, G, and H) within the lignin macromolecule have different reactivity thus causing heterogeneity in the delignification process. The phenolic α-O-4-bonds and some phenolic β-O-4-bonds in lignin are quickly cleaved during the initial delignification stage. In the bulk stage, the main reaction is the cleavage of the non-phenolic and phenolic β-O-4-linkages. The most stable C-C bonds in lignin are slowly broken in the residual stage, which is accompanied by the serious carbohydrate degradation. [96] These three stages remove about 15-25%, 70%, and 10-15% of the lignin, respectively.

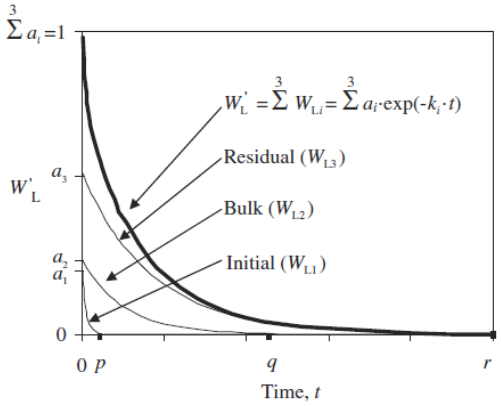

Figure 1.2 Delignification of lignocellulosic biomass described in three simultaneous stages (initial, bulk, and residual). [95]

The absence of methoxyl at C5 in the aromatic ring of guaiacyl-lignin makes it more resistant to cleavage. For this reason lignin rich in G-units is more difficult to remove, while lignin rich in S/H-units is more easily cleaved and solubilized. [97] S-units and G-units had similar reactivity during the main delignification stage, while the higher reactivity of S-units relative to G-units was observed in the later stage. [98] Lignin mainly exists in two types of lignin-carbohydrate complexes as glucomannan-linked and xylan-linked lignins, and the former one has a higher resistance than the latter one. [99] Although the kinetics of delignification during O_2 delignification has been well studied,

delignification is accompanied by carbohydrates removal and therefore it does not accurately reflect the overall degradation of biomass. To the best of our knowledge, there are no reports on the kinetics of the overall degradation of biomass during alkaline wet oxidation.

1.5.5 Reactor of alkaline wet oxidation

In the past, most of the experiments were performed in the batch reactor, where the reaction environment is continuously changing due to the consumption of alkali and the accumulation of products, result in the decrease of alkalinity and the deterioration of oxygen transfer. [100-102] It is usually necessary to perform many experiments at different time intervals for calculating the reaction rate via the chemical composition of residue. Another limitation is that the products cannot be collected timely which does not prevent the secondary reaction. [71] This causes serious inconvenience to the exploration of the primary products and reactions.

Based on the disadvantages of the batch reactor, a continuous flow-through reactor (percolator) was adopted where the feed is loaded into the reactor and a fresh oxygenated alkaline solution is passed through the packed bed at a set temperature. [81, 103] This not only ensures constant alkalinity and oxygen concentration in the reactor, but also discharges and collects the degradation products timely. The employment of the flow-through reactor makes it possible to study the primary reactions of oxidative degradation.

1.6 Objective of This Study

Lignocellulosic biomass is the most important renewable source of chemicals and energy. It is inefficient to convert and utilize it as biofuels and chemicals directly due to its complex composition and natural recalcitrance. In particular, biomass with high lignin content is more recalcitrant and difficult to be converted than that with low lignin content. Biomass pretreatment aimed at destroying its recalcitrant structure or fractionating biomass into its components (cellulose, hemicellulose, and lignin) is desirable to improve the conversion efficiency. Steam pretreatment destroys the stubborn structure by decomposing part of hemicellulose, and hydrothermal treatment recovers most of hemicellulose as

oligosaccharides and monosaccharides. Alkaline wet oxidation is a promising method for biomass delignification and providing cellulose-rich residue and liquid stream of lignin. Japanese cedar is a high-lignin biomass resource and widely distributed in Japan. The lignin in cedar is composed of only G units (99.5%) [104] and the hemicellulose is mainly composed of mannan (46.4 wt% based on hemicellulose), which makes it considerably resistant. It is a challenge to effectively remove the lignin from cedar under mild conditions. We achieved a deep delignification of cedar by repeated mild alkaline treatments with pressurized O_2. The relationship between carbohydrates (cellulose and hemicellulose) degradation and delignification rate was established for revealing the delignification process, the results are presented in **Chapter 2**. The dissolved lignin and hemicellulose underwent severe degradation during alkaline wet oxidation. Timely collection of the products is not possible in a batch reactor which causes secondary reactions limiting the exploration of the primary reactions. A newly developed flow-through fixed-bed reactor (percolator) that achieves constant reaction conditions and timely products collection was employed in **Chapter 3** for the analysis of primary reactions. Although the hemicellulose was converted into organic acids, it is more valuable if it can be recovered as monosaccharides or oligosaccharides. In **Chapter 4**, the combination of hydrothermal treatment and alkaline wet oxidation achieved hemicellulose recovery and deep delignification under mild conditions. The effects of strong bases (NaOH) versus milder bases (Na_2CO_3) were investigated. Rice husk contains high levels of lignin and ash (Si). The removal of lignin and ash from rice husk along with a high yield of cellulose was investigated in **Chapter 5**.

1.7 Outline of This Study

- **Chapter 1** clarified the importance of biomass as an ideal alternative to fossil fuels for providing renewable biofuels and chemicals. The common conversion and pretreatment technologies of biomass are briefly introduced. Specifically, a promising biomass delignification technology i.e. alkaline wet oxidation, as well as the removal and degradation of carbohydrates and lignin are interpreted. Finally, the objectives of the present work are clarified.

- **Chapter 2** investigated extensive delignification of cedar at low temperatures and its chemical mechanism. Even at 90 ℃, O_2 greatly promotes the lignin dissolution while decomposing carbohydrates. Polysaccharides are decomposed into small molecules without forming monosaccharides. The delignification process, in terms of the delignification rate against cellulose degradation, is mostly dominated by the chemical structure of the cedar. However, the delignification rate is greatly influenced by the operating conditions. The chemical condensation of dissolved lignin fragments greatly impedes the delignification. Repeated short-time oxidation with renewal of alkaline water suppressed the condensation enhancing the delignification. Four times repetition of 2-h treatments achieved 96% delignification, which was even 8% higher than a single 8-h treatment at 130 ℃.
- **Chapter 3** explored oxidation of Japanese cedar with O_2 in hot compressed alkaline water, employing not a batch reactor but a newly developed flow-through fixed-bed reactor (percolator). It enabled to determine the rate of the primary extraction that was free from the secondary reactions of extract in the aqueous phase and those over the residual solid, solubility of extractable matter, and mass transport processes. Quantitative kinetic analysis revealed that the cedar consisted of three kinetic components (C1, C2, and C3) that underwent extraction in parallel following first-order kinetics with different rate constants. Further analysis revealed the chemical compositions of the kinetic components, which were mixtures of carbohydrates and lignin. C1 was converted most rapidly by non-oxidative reactions such as alkali-catalyzed hydrolysis, while C2 by oxidative degradation. The product distributions from C1 and C2 (CO_2, lower organic acids, oligosaccharides, acid-soluble and acid-insoluble lignins) were steady throughout their conversion. Both C1 and C2 thus behaved as single reactants, nevertheless those were lignin/carbohydrates mixtures. It was also demonstrated that the extraction rate of C2 was proportional to the concentration of dissolved O_2. C3 was the most refractory component, consisting mainly of glucan and very minimally of the lignin, xylan, mannan, galactan, and arabinan.

- **Chapter 4** combined hydrothermal treatment and alkaline wet oxidation to recover hemicellulose as oligosaccharides and then to deeply delignify under mild conditions. Most hemicellulose was recovered as mannose-oligosaccharides with high molecular weight (200-10000 Da) by hydrothermal extraction using H_2O at 180 ℃. The results of subsequent alkaline wet oxidation showed that 0.8 mol/L NaOH removed 91.3% lignin at 90 ℃, while the Na_2CO_3 can effectively remove lignin (98.9%) only at a higher temperature (120 ℃). Moreover, the depolymerization and oxidation are dominant reactions during lignin removal resulting 65-95% of the lignin dissolved by Na_2CO_3 was degraded into small lignin fragments (<1000 Da) and organic acids. Furthermore, the degraded carbohydrates were selectively converted to organic acids with the highest yield of 24.7%-C using Na_2CO_3 at 120 ℃. Finally, the high-cellulose residue contenting 98.88% glucose was obtained.
- **Chapter 5** prepared cellulose fibers from rice husk (high lignin and ash content) by using Na_2CO_3 and O_2 under mild conditions. The rice husk was hydrothermally treated to facilitate the removal of lignin and ash in the subsequent alkaline wet oxidation. The use of Na_2CO_3 rather than NaOH prevented severe cellulose loss. High-purity cellulose fiber (98.1%) was obtained in a high yield (>83 wt%) by using Na_2CO_3 solution and O_2 at 120 ℃ for 120 min. The Na_2CO_3 solution maintained a good delignification effect (84%) even after being reused four times.
- **Chapter 6** summarizes the general conclusions based on the finding in the preceding chapters.

1.8 References

[1] J.J. Bozell. G.R. Petersen, Technology development for the production of biobased products from biorefinery carbohydrates-the US Department of Energy's "Top 10" revisited, *Green Chem.*, 12 (2010) 539-554.

[2] T.E. Amidon, C.D. Wood, A.M. Shupe, Y. Wang, M. Graves, S. Liu, Biorefinery: Conversion of woody biomass to chemicals, energy and materials, *J. Biobased Mater. Bio.*, 2 (2008) 100-120.

[3] S.R. Bull, Renewable energy today and tomorrow, Proceedings of the IEEE, 89 (2001) 1216-1226.

[4] X.J. Yang, H.J. Hu, T.W. Tan, J.Y. Li, China's renewable energy goals by 2050, *Environ. Dev.*, 20 (2016) 83-90.

[5] N. Gaurav, S. Sivasankari, G.S. Kiran, A. Ninawe, J. Selvin, Utilization of bioresources for sustainable biofuels: A Review, *Renew. Sust. Energ. Rev.*, 73 (2017) 205-214.

[6] M.T. Amiri, G.R. Dick, Y.M. Questell-Santiago, J.S. Luterbacher, Fractionation of lignocellulosic biomass to produce uncondensed aldehyde-stabilized lignin, *Nat. Protoc.*, 14 (2019) 921-954.

[7] A.T.W.M. Hendriks, G. Zeeman, Pretreatments to enhance the digestibility of lignocellulosic biomass, *Bioresource Technol.*, 100 (2009) 10-18.

[8] Q. Zheng, T.T. Zhou, Y.B. Wang, X.H. Cao, S.Q. Wu, M.L. Zhao, H.Y. Wang, M. Xu, B.D. Zheng, J.G. Zheng, X. Guan, Pretreatment of wheat straw leads to structural changes and improved enzymatic hydrolysis, *Sci. Rep.*, 8 (2018) 1321.

[9] B.C. Saha, Hemicellulose bioconversion, *J. Ind. Microbiol. Biot.*, 30 (2003) 279-291.

[10] M.J. Cocero, Á. Cabeza, N. Abad, T. Adamovic, L. Vaquerizo, C.M. Mart ínez, M.V. Pazo-Cepeda, Understanding biomass fractionation in subcritical & supercritical water, *J. Supercrit. Fluid.*, 133 (2018) 550-565.

[11] W. Schutyser, T. Renders, S.V.D. Bosch, S.F. Koelewijn, G.T. Beckham, B.F. Sels, Chemicals from lignin: an interplay of lignocellulose fractionation, depolymerisation, and upgrading, *Chem. Soc. Rev.*, 47 (2018) 852-908.

[12] H. Wang, Y. Pu, A. Ragauskas, B. Yang, From lignin to valuable products-strategies,

challenges, and prospects, *Bioresource Technol.*, 271 (2019) 449-461.

[13] F.H. Isikgor, C.R. Becer, Lignocellulosic biomass: a sustainable platform for the production of bio-based chemicals and polymers, *Polym. Chem.*, 6 (2015) 4497-4559.

[14] J.D. Smith, V. Sreedharan, M. Landon, Z.P. Smith, Advanced design optimization of combustion equipment for biomass combustion, *Renew. Energ.*, 145 (2020) 1597-1607.

[15] I.E. Agency, Renewables 2019, IEA, Paris. (2019) https://www.iea.org/reports/renewables-2019.

[16] X. Hu, M. Gholizadeh, Biomass pyrolysis: A review of the process development and challenges from initial researches up to the commercialisation stage, *J. Energy Chem.*, 39 (2019) 109-143.

[17] H.P. Yang, R. Yan, H.P. Chen, D.H. Lee, C.G. Zheng, Characteristics of hemicellulose, cellulose and lignin pyrolysis, Fuel, 86 (2007) 1781-1788.

[18] P. Roy, G. Dias, Prospects for pyrolysis technologies in the bioenergy sector: A review, *Renew. Sust. Energ. Rev.*, 77 (2017) 59-69.

[19] T.V. Choudhary, C.B. Phillips, Renewable fuels via catalytic hydrodeoxygenation, *Appl.Catal. A-Gen.*, 397 (2011) 1-12.

[20] R. French, S. Czernik, Catalytic pyrolysis of biomass for biofuels production, *Fuel Process. Technol.*, 91 (2010) 25-32.

[21] T. Dickerson, J. Soria, Catalytic fast pyrolysis: A review, *Energies*, 6 (2013) 514-538.

[22] S. Safarian, R. Unnþórsson, C. Richter, A review of biomass gasification modelling, *Renew. Sust. Energ. Rev.*, 110 (2019) 378-391.

[23] A. Molino, S. Chianese, D. Musmarra, Biomass gasification technology: The state of the art overview, *J. Energ. Chem.*, 25 (2016) 10-25.

[24] Z.F. Zahara, S. Kudo, Daniyanto, U.P.M. Ashik, K. Norinaga, A. Budiman, J.-i. Hayashi, CO_2 gasification of sugar cane bagasse: quantitative understanding of kinetics and catalytic roles of inherent metallic species, *Energy Fuel.*, 32 (2017) 4255-4268.

[25] F. Behrendt, Y. Neubauer, M. Oevermann, B. Wilmes, N. Zobel, Direct Liquefaction of biomass, *Chem. Eng. Technol.*, 31 (2008) 667-677.

[26] H.J. Huang, X.Z. Yuan, Recent progress in the direct liquefaction of typical biomass,

Prog. Energ. Combust., 49 (2015) 59-80.

[27] Z.J. Chen, J.X. Long, Organosolv liquefaction of sugarcane bagasse catalyzed by acidic ionic liquids, *Bioresource Technol.*, 214 (2016) 16-23.

[28] R.C. Saxena, D.K. Adhikari, H.B. Goyal, Biomass-based energy fuel through biochemical routes: A review, *Renew. Sust. Energ. Rev.*, 13 (2009) 167-178.

[29] R. Kumar, S. Singh, O.V. Singh, Bioconversion of lignocellulosic biomass: biochemical and molecular perspectives, *J. Ind. Microbiol. Biotechnol.*, 35 (2008) 377-391.

[30] S.M.Z. Hossain, Biochemical conversion of microalgae biomass into biofuel, *Chem. Eng. Technol.*, 42 (2019) 2594-2607.

[31] P. Sannigrahi, A.J. Ragauskas, Fundamentals of biomass pretreatment by fractionation, aqueous pretreatment of plant biomass for biological and chemical conversion to fuels and chemicals, *Charles E. Wyman (editor)* 10 (2013) 201-222.

[32] T.A. Werpy, J.E. Holladay, J.F.White, Top value added chemicals from biomass: I. results of screening for potential candidates from sugars and synthesis gas, United States: N. p. 2004 Web. doi:10.2172/926125. (2004).

[33] P. Gallezot, Conversion of biomass to selected chemical products, *Chem. Soc. Rev.* 41 (2012) 1538-1558.

[34] J. Zakzeski, Pieter P.C.A. Bruijnincx, A.L. Jongerius, B.M. Weckhuysen, The catalytic valorization of lignin for the production of renewable chemicals, *Chem. Rev.* 110 (2010) 3552–3599.

[35] R. Katahira, A. Mittal, K. McKinney, X.W. Chen, M.P. Tucker, D.K. Johnson, G.T. Beckham, Base-catalyzed depolymerization of biorefinery lignins, *ACS Sustainable Chem. Eng.* 4 (2016) 1474-1486.

[36] E.M. Karp, B.S. Donohoe, M.H. O'Brien, P.N. Ciesielski, A. Mittal, M.J. Biddy, G.T. Beckham, Alkaline pretreatment of corn stover: bench-scale fractionation and stream characterization, *ACS Sustainable Chem. Eng.* 2 (2014) 1481-1491.

[37] S. Rahmati, W. Doherty, D. Dubal, L. Atanda, L. Moghaddam, P. Sonar, V. Hessel, K. Ostrikov, Pretreatment and fermentation of lignocellulosic biomass: reaction mechanisms and process engineering, *React. Chem. Eng.* 5 (2020) 2017-2047.

[38] S. Singh, G. Cheng, N. Sathitsuksanoh, D. Wu, P. Varanasi, A. George, V. Balan, X. Gao, R. Kumar, B.E. Dale, C.E. Wyman, B.A. Simmons, Comparison of different biomass pretreatment techniques and their impact on chemistry and structure, *Front. Energy Res.* 2 (2015) 62.

[39] M. Sagehashi, T. Nomura, H. Shishido, A. Sakoda, Separation of phenols and furfural by pervaporation and reverse osmosis membranes from biomass--superheated steam pyrolysis-derived aqueous solution, *Bioresource Technol.*, 98 (2007) 2018-2026.

[40] M. Nishida, T. Tanaka, T. Miki, T. Ito, K. Kanayama, Multi-scale instrumental analyses for structural changes in steam-treated bamboo using a combination of several solid-state NMR methods, *Ind. Crop. Prod.*, 103 (2017) 89-98.

[41] M. Nishida, T. Tanaka, T. Miki, T. Ito, K. Kanayama, Instrumental analyses of nanostructures and interactions with bound water of superheated steam treated plant materials, *Ind. Crop. Prod.*, 114 (2018) 1-13.

[42] G. Gallina, E.R. Alfageme, P. Biasi, J. Garcia-Serna, Hydrothermal extraction of hemicellulose: from lab to pilot scale, *Bioresource Technol.*, 247 (2018) 980-991.

[43] T. Ingram, T. Rogalinski, V. Bockemühl, G. Antranikian, G. Brunner, Semi-continuous liquid hot water pretreatment of rye straw, *J. Supercrit. Fluid.*, 48 (2009) 238-246.

[44] L. Kratky, T. Jirout, Biomass size reduction machines for enhancing biogas production, *Chem. Eng. Technol.* 34 (2011) 391-399.

[45] Z. Miao, T.E. Grift, A.C. Hansen, K.C. Ting, Energy requirement for comminution of biomass in relation to particle physical properties, *Ind. Crop. Prod.*, 33 (2011) 504-513.

[46] Y. Zheng, Z.L. Pan, R.H. Zhang, Overview of biomass pretreatment for cellulosic ethanol production, *Int. J. Agric. Biol.*, 2 (2009) 51.

[47] B.C. Saha, M.A. Cotta, Enzymatic saccharification and fermentation of alkaline peroxide pretreated rice hulls to ethanol, *Enzyme Microb. Tech.*, 41 (2007) 528-532.

[48] J.S. Kim, Y.Y. Lee, T.H. Kim, A review on alkaline pretreatment technology for bioconversion of lignocellulosic biomass, *Bioresource Technol.*, 199 (2016) 42-48.

[49] K. Zhang, Z.J. Pei, D.H. Wang, Organic solvent pretreatment of lignocellulosic biomass for biofuels and biochemicals: A review, *Bioresource Technol.*, 199 (2016) 21-33.

[50] D.E. Kim, X.J. Pan, Preliminary study on converting hybrid poplar to high-value chemicals and lignin using organosolv ethanol process, *Ind. Eng. Chem. Res.*, 49 (2010) 12156–12163.

[51] M.F. Li, S.N. Sun, F. Xu, R.C. Sun, Ultrasound-enhanced extraction of lignin from bamboo (Neosinocalamus affinis): characterization of the ethanol-soluble fractions, *Ultrason. Sonochem.*, 19 (2012) 243-249.

[52] H. Tadesse, R. Luque, Advances on biomass pretreatment using ionic liquids: An overview, *Energy Environ. Sci.*, 4 (2011) 3913.

[53] L. Feng, Z.L. Chen, Research progress on dissolution and functional modification of cellulose in ionic liquids, *J. Mol. Liq.*, 142 (2008) 1-5.

[54] M. Yadav, A. Singh, V. Balan, N. Pareek, V. Vivekanand, Biological treatment of lignocellulosic biomass by chaetomium globosporum: Process derivation and improved biogas production, *Int. J. Biol. Macromol.*, 128 (2019) 176-183.

[55] R. Kumar, Effects of cellulase and xylanase enzymes on the deconstruction of solids from pretreatment of poplar by leading technologies, *Biotechnol. Progr.*, 25 (2009) 302-314.

[56] E. Rouches, I. Herpoël-Gimbert, J.P. Steyer, H. Carrere, Improvement of anaerobic degradation by white-rot fungi pretreatment of lignocellulosic biomass: A review, *Renew. Sust. Energ. Rev.*, 59 (2016) 179-198.

[57] B. Tsegaye, C. Balomajumder, P. Roy, Microbial delignification and hydrolysis of lignocellulosic biomass to enhance biofuel production: an overview and future prospect, *Bulletin of the National Research Centre* 43 (2019).

[58] S.K. Singh, Biological treatment of plant biomass and factors affecting bioactivity, *J. Clean. Prod.*, 279 (2021) 123546.

[59] P.P. Thoresen, L. Matsakas, U. Rova, P. Christakopoulos, Recent advances in organosolv fractionation: Towards biomass fractionation technology of the future, *Bioresource Technol.*, 306 (2020) 123189.

[60] E. Shirkavand, S. Baroutian, D.J. Gapes, B.R. Young, Combination of fungal and physicochemical processes for lignocellulosic biomass pretreatment – A review, *Renew.*

Sust. Energ. Rev., 54 (2016) 217-234.

[61] V. Balan, B. Bals, S.P.S. Chundawat, D. M arshall, B.E. Dale, Lignocellulosic biomass pretreatment using AFEX, *Biofuels Methods and Protocols* 581 (2009) 61-77.

[62] S.K. Bhargava, J. Tardio, J. Prasad, K. Fo1ger, D.B. Akolekar, S.C. Grocott, Wet oxidation and catalytic wet oxidation, *Ind. Eng. Chem. Res.*, 45 (2006) 1221-1258.

[63] G.D. McGinnis, W.W. Wilson, S.E. Prince, C.C. Chen, Conversion of biomass into chemicals with high-temperature wet oxidation, *Ind. Eng. Chem. Prod. Res. Dev.*, 22 (1983) 633-636.

[64] W.H. Geng, T. Huang, Y.G. Jin, J.L. Song, H.M. Chang, H. Jameel, Comparison of sodium carbonate-oxygen and sodium hydroxide-oxygen pretreatments on the chemical composition and enzymatic saccharification of wheat straw, *Bioresource Technol.*, 161 (2014) 63-68.

[65] V.S. Chang, M. Nagwani, C.H. Kim, M.T. Holtzapple, Oxidative lime pretreatment of high-lignin biomass, *Appl. Biochem. Biotech.*, 94 (2001) 28.

[66] X.J. Pan, X. Zhang, D.J. Gregg, J.N. Saddler, Enhanced enzymatic hydrolysis of steam-exploded douglas fir wood by alkali-oxygen post-treatment, *Appl. Biochem. Biotech.*, 115 (2004) 12.

[67] K.M. Draude, C.B. Kurniawan, S.J.B. Duff, Effect of oxygen delignification on the rate and extent of enzymatic hydrolysis of lignocellulosic material, *Bioresource Technol.*, 79 (2001) 113-120.

[68] H.B. Klinke, B.K. Ahring, A.S. Schmidt, A.B. Thomsen, Characterization of degradation products from alkaline wet oxidation of wheat straw, *Bioresource Technol.*, 82 (2002) 12.

[69] Y.T. Jiang, X.H. Zeng, R. Luque, X. Tang, Y. Sun, T.Z. Lei, S.J. Liu, L. Lin, Cooking with active oxygen and solid alkali: A promising alternative approach for lignocellulosic biorefineries, *ChemSusChem*, 10 (2017) 3982-3993.

[70] S.X. An, W.Z. Li, Q.Y. Liu, Y. Xia, T.W. Zhang, F. Huang, Q.Z. Lin, L. Chen, Combined dilute hydrochloric acid and alkaline wet oxidation pretreatment to improve sugar recovery of corn stover, *Bioresource Technol.*, 271 (2019) 283-288.

[71] N. Ding, X.Q. Song, Y.T. Jiang, B. Luo, X.H. Zeng, Y. Sun, X. Tang, T.Z. Lei, L. Lin, Cooking with active oxygen and solid alkali facilitates lignin degradation in bamboo pretreatment, *Sustain. Energ. Fuels*, 2 (2018) 2206-2214.

[72] E. Arvaniti, A.B. Bjerre, J.E. Schmidt, Wet oxidation pretreatment of rape straw for ethanol production, *Biomass Bioenerg.*, 39 (2012) 94-105.

[73] M. Li, J. Wang, Y.Z. Yang, G.H. Xie, Alkali-based pretreatments distinctively extract lignin and pectin for enhancing biomass saccharification by altering cellulose features in sugar-rich Jerusalem artichoke stem, *Bioresource Technol.*,208 (2016) 31-41.

[74] G. Lyu, C.G. Yoo, X. Pan, Alkaline oxidative cracking for effective depolymerization of biorefining lignin to mono-aromatic compounds and organic acids with molecular oxygen, *Biomass Bioenerg.*, 108 (2018) 7-14.

[75] P. Bajpai, Pulp and Paper Industry: Chemicals, (2015) 49-80.

[76] S. Tripathi, N. Sharma, I. Alam, N.K. Bhardwaj, Effectiveness of different green chemistry approaches during mixed hardwood bamboo pulp bleaching and their impact on environment, *Int. J. Environ. Sci. Te.*, 16 (2018) 4327-4338.

[77] A. Das, A. Rahimi, A. Ulbrich, M. Alherech, A.H. Motagamwala, A. Bhalla, L. da Costa Sousa, V. Balan, J.A. Dumesic, E.L. Hegg, B.E. Dale, J. Ralph, J.J. Coon, S.S. Stahl, Lignin conversion to low-molecular-weight aromatics via an aerobic oxidation-hydrolysis sequence: Comparison of different lignin sources, *ACS Sustain. Chem. Eng.*, 6 (2018) 3367-3374.

[78] K. Srinivas, F. de Carvalho Oliveira, P.J. Teller, A.R. Gonalves, G.L. Helms, B.K. Ahring, Oxidative degradation of biorefinery lignin obtained after pretreatment of forest residues of Douglas Fir, *Bioresource Technol.*, 221 (2016) 394-404.

[79] P. Posoknistakul, T. Akiyama, T. Yokoyama, Y. Matsumoto, Stereo-preference in the degradation of the erythroand threoIsomers of *β*-O-4-type lignin model compounds in oxidation processes: Part 1: In the reaction with active oxygen species under oxygen delignification conditions, *J. Wood Chem. Technol.*, 36 (2016) 288-303.

[80] J.F.K. Charles J. Knill, Degradation of cellulose under alkaline conditions, *Carbohyd. Polym.*, 51 (2003) 20.

[81] V. Jafari, K. Nieminen, H. Sixta, A. van Heiningen, Delignification and cellulose degradation kinetics models for high lignin content softwood Kraft pulp during flow-through oxygen delignification, *Cellulose* 22 (2015) 2055-2066.

[82] R. Yang, L. Lucia, A.J. Ragauskas, H. Jameel, Oxygen delignification chemistry and its impact on pulp fibers, *J. Wood Chem. Technol.*, 23 (2003) 13-29.

[83] D.C. Zhang, X.S. Chai, Q.X. Hou, Arthur Ragauskas, Characterization of fiber carboxylic acid development during one-stage oxygen delignification, *Ind. Eng. Chem. Res.*, 44 (2005) 9279–9285.

[84] X. Chen, R. Katahira, Z. Ge, L. Lu, D.X. Hou, D.J. Peterson, M.P. Tucker, X.W. Chen, Z.J. Ren, Microbial electrochemical treatment of biorefinery black liquor and resource recovery, *Green Chem.*, 21 (2019) 1258-1266.

[85] J. Shi, Q. Yang, L. Lin, The structural features of hemicelluloses dissolved out at different cooking stages of active oxygen cooking process, *Carbohydr. Polym.*, 104 (2014) 182-190.

[86] W. Farhat, R. Venditti, A. Quick, M. Taha, N. Mignard, F. Becquart, A. Ayoub, Hemicellulose extraction and characterization for applications in paper coatings and adhesives, *Ind. Crop. Prod.*, 107 (2017) 370-377.

[87] C. Alvarez-Vasco, X. Zhang, Alkaline hydrogen peroxide pretreatment of softwood: hemicellulose degradation pathways, *Bioresource Technol.*, 150 (2013) 321-327.

[88] B. Xiao, X.F. Sun, R.C. Sun, Chemical, structural, and thermal characterizations of alkali-soluble lignins and hemicelluloses, and cellulose from maize stems, rye straw, and rice straw, *Polym. Degrad. Stabil.*, 74 (2001) 307-319.

[89] F.D.C. Oliveira, K. Srinivas, G.L. Helms, N.G. Isern, J.R. Cort, A.R. Goncalves, B.K. Ahring, Characterization of coffee (coffea arabica) husk lignin and degradation products obtained after oxygen and alkali addition, *Bioresource Technol.*, 257 (2018) 172-180.

[90] S.C. Qi, J.-i. Hayashi, S. Kudo, L. Zhang, Catalytic hydrogenolysis of Kraft lignin to monomers at high yield in alkaline water, *Green Chem.*, 19 (2017) 11.

[91] C.F. Zhang, H.J. Li, J.M. Lu, X.C. Zhang, K.E. MacArthur, M. Heggen, F. Wang,

Promoting lignin depolymerization and restraining the condensation via an oxidation−hydrogenation strategy, *ACS Catal.*, 7 (2017) 3419-3429.

[92] R.S. Ma, M. Guo, X. Zhang, Recent advances in oxidative valorization of lignin, *Catal. Today*, 302 (2018) 50-60.

[93] L. da Costa Sousa, M. Foston, V. Bokade, A. Azarpira, F. Lu, A.J. Ragauskas, J. Ralph, B. Dale, V. Balan, Isolation and characterization of new lignin streams derived from extractive-ammonia (EA) pretreatment, *Green Chem.*, 18 (2016) 4205-4215.

[94] A. Mittal, R. Katahira, B.S. Donohoe, B.A. Black, S. Pattathil, J.M. Stringer, G.T. Beckham, Alkaline peroxide delignification of corn stover, *ACS Sustain. Chem. Eng.*, 5 (2017) 6310-6321.

[95] S. Kim, M.T. Holtzapple, Delignification kinetics of corn stover in lime pretreatment, *Bioresource Technol.*, 97 (2006) 778-785.

[96] B.D. Groot, J.E.G.V. Dam, K.V. Riet, Alkaline pulping of hemp woody core kinetic modelling of lignin, xylan and cellulose extraction and degradation., *Holzforschung*, 49 (1995) 332-342.

[97] A. Guti érrez, I.M. Rodr guez, J.C.D. R ó, Chemical characterization of lignin and lipid fractions in industrial hemp bast fibers used for manufacturing high-quality paper pulps, *J. Agric. Food Chem.*, 54 (2006) 2138–2144.

[98] A. Lourenco, J. Gominho, A.V. Marques, H. Pereira, Reactivity of syringyl and guaiacyl lignin units and delignification kinetics in the kraft pulping of Eucalyptus globulus wood using Py-GC-MS/FID, *Bioresource Technol.*, 123 (2012) 296-302.

[99] M. Lawoko, G. Henriksson, G. Gellerstedt, Structural differences between the lignin-carbohydrate complexes present in wood and in chemical pulps, *Biomacromolecules*, 6 (2005) 6.

[100] I. Dogan, G. Guruz, Dimensionless parameter approach for oxygen delignification kinetics, *Ind. Eng. Chem. Res.*, 47 (2008) 5871–5878.

[101] V.Q. Dang, K.L. Nguyen, A universal kinetic model for characterisation of the effect of chip thickness on kraft pulping, *Bioresource Technol.*, 99 (2008) 1486-1490.

[102] Y. Ji, M.C. Wheeler, A. van Heiningen, Oxygen delignification kinetics: CSTR and

batch reactor comparison, *AIChE J.*, 53 (2007) 2681-2687.

[103] V. Jafari, H. Sixta, A. van Heiningen, Kinetics of oxygen delignification of high-kappa pulp in a continuous flow-through reactor, *Ind. Eng. Chem. Res.*, 53 (2014) 8385-8394.

[104] D. Tarmadi, Y. Tobimatsu, M. Yamamura, T. Miyamoto, Y. Miyagawa, T. Umezawa, T. Yoshimura, NMR studies on lignocellulose deconstructions in the digestive system of the lower termite coptotermes formosanus Shiraki, *Sci. Rep.*, 8 (2018) 1290.

CHAPTER 2

Deep Delignification of Woody Biomass by Repeated Mild Alkaline Treatments with Pressurized O_2

2.1. Introduction

Lignocellulosic biomass is a promising carbonaceous resource to produce sustainable fuels, chemicals, and biological products owing to its renewability and availability. Economically feasible chemical production from lignocellulosic biomass has, however, yet to be achieved. Lignin is a critical obstacle to the production of bioethanol- [1] and carbohydrate-derived chemicals [2] as well as materials, while it can be converted into value-added products. [3]

Alkaline treatment with O_2 has great potential for industrial delignification with economic and environmental feasibilities. [4] Dissolving oxidizing agents such as H_2O_2 and O_2 into alkaline water leads to formation of active species such as OH^- radicals and then decomposition of hemicellulose and lignin by reactions such as electrophilic substitution, side-chain displacement, and oxidative cleavage of aromatic nuclei. [5–7] This combination of an alkaline environment and an oxidizing agent is thus effective for the delignification. [8] Due to lower reactivity than H_2O_2, O_2 is normally used with high temperatures over 150 ℃ to promote the delignification. Klinke et al. [9] reported 62% delignification from wheat straw at 195 ℃ with Na_2CO_3 under 1.2 MPa O_2. Another study by Chang et al. reported 78% delignification from a poplar wood that was treated at 150 ℃ for 6 h under 1.4 MPa O_2 with $Ca(OH)_2$. [10]

Some reports showed that delignification at lower temperatures was effective for reducing the loss of carbohydrates. [11,12] For example, Geng et al. [11] achieved 50% delignification at 110 ℃ with a carbohydrate loss of 4.2% from another wheat straw. In those previous studies, the delignification rate was not necessarily maximized because the delignification was investigated as a pretreatment for enzymatic saccharification, which often required a delignification rate as low as 20–65%. [13,14] However, deeper removal of lignin is desirable for more production of sugar per consumption of enzyme because the enzyme has a high propensity to be adsorbed to the lignin. [13,15] Minimization of the residual lignin is hence effective for reducing the consumption of enzymes. In addition, rapidly developing technologies of cellulose nanofibers will demand cellulose with higher

purity. [14,16]

This study aimed to investigate delignification by a low-temperature alkaline treatment with O_2 and its chemical mechanism. A typical Japanese cedar was chosen as feedstock because it had a most refractory type of lignin. [17] The hemicellulose of the cedar consists mainly of glucomannan. [18] Removal of glucomannan-linked lignin was more difficult than that of xylan-linked lignin. [19] Thus, deep delignification of a Japanese cedar with high carbohydrate retention was challenging. For example, Yoshioka et al. had treated another type of Japanese cedar with an ionic liquid. [20] It removed 40% of the original lignin but allowed the loss of hemicellulose (>90%) and that of cellulose (10%). In contrast, Wang et al. removed 98.7% lignin from a red pine with another ionic liquid while preserving 95% of cellulose. [21] Such a refractory feature of a Japanese cedar was appropriate for investigating the possibility of extensive delignification under mild conditions.

2.2. Experimental Section

2.2.1. Materials

Cellulose, monosaccharides (glucose, xylose, arabinose, galactose, mannose), lower organic acids, NaOH, and Na_2CO_3 were purchased from Wako Pure Chemical Industries. A type of xylan, derived from beech wood, was purchased from SERVA Electrophoresis. Ultrapurified water with electrical resistance over 18.2 MΩ was prepared with a Milli-Q water purification system (Merck, MPGP02001). Japanese cedar in form of particles sized 0.85–2 mm was used as the starting material. It was subjected to a steam pretreatment at 220 ℃ under atmospheric pressure. This pretreatment was performed to cause structural relaxation of hemicellulose and thereby promote the delignification. [22]

The setup of the pretreatment is shown in **Figure S2.1**. Superheated steam pretreatment was carried out at 220 ℃ in a SUS reactor with under ordinary pressure. Briefly, about 5 g of cedar was placed in the reactor which was placed in an oven. After the temperature in incubator reached the desired temperature (220 ℃), keep it for 30 minutes to ensure that the target temperature is reached in reaction tube. Then water was injected into another SUS

tube with a syringe pump at the flow rate of 0.36 mL/min. Two stainless steel tubes were connected in series. Generated steam was introduced to the reactor with carrier gas of N_2 with a flow rate of 10 mL/min. After the completion of 10 mL water injection, temperature and N_2 flow were maintained for 10 min to ensure that the complete discharge of steam. Then, the reactor was rapidly cooled to ambient temperature. The compositions of the original and pretreated cedars are listed in **Table 2.1**.

Table 2.1. Compositions of cedar before and after pretreatment (unit; wt %, dry).

Sample	Mass loss from raw cedar	Lignin	Cellulose	Hemicellulose			Ash
				Xylan	Galactan	Mannan	
Original cedar	-	36.6	43.5	6.11	4.13	7.49	0.38
Pretreated cedar	3.29	38.6	44.3	6.90	2.97	6.36	0.34

2.2.2. Alkaline treatment with O_2

The steam-treated cedar was subjected to oxidation in an autoclave (Taiatsu Techno, TVS-N_2, internal volume; 120 mL). In a typical run, 2 ± 0.1 g the dry steam-treated cedar and 20 ± 1 mL of 0.8 mol/L NaOH aqueous solution were charged in the autoclave. The air in the autoclave was replaced completely by O_2 before its charging at 2 MPa. The autoclave was then heated to 90 ℃, which was held for a prescribed time with stirring of the slurry at 100 rpm. At the end of the holding time, the autoclave was quenched in an ice bath.

Repetitive 2- or 12-h treatments were performed to examine the effect of the alkali solution renewal. For example, in the case of 2×2-h treatments, the residual solid after 2-h treatments was collected and treated again for 2 h. To collect the residual solid, slurry after a 2-h treatment was filtered to remove the liquid portion. The filtered solid was washed with water at 80 ℃ to remove the residual water-soluble material completely and dried at 60 ℃ under vacuum. Then, 2 ± 0.1 g of residual solid collected from several 2-h treatments was subjected to the next 2-h treatment with 20 ± 1 mL of 0.8 mol/L fresh NaOH aqueous solution.

2.2.3. Characterization of products

The workflow of the analyses of gas, liquid, and solid products is shown in **Figure 2.1**. The gaseous product was collected in a gasbag, and analyzed by gas chromatography with an Agilent micro GC 490. The solid and liquid of the slurry were separated by vacuum filtration. The solid was washed with water at 80 ℃ to remove the residual water-soluble material completely and dried at 60 ℃ under vacuum, and then subjected to analyses to quantify glucan, xylan, arabinan, galactan, mannan, and lignin, according to a report by the National Renewable Energy Laboratory (NREL). [23] The content of cellulose was represented by the amount of glucan, assuming that most of the glucan units belonged to the cellulose. [24]

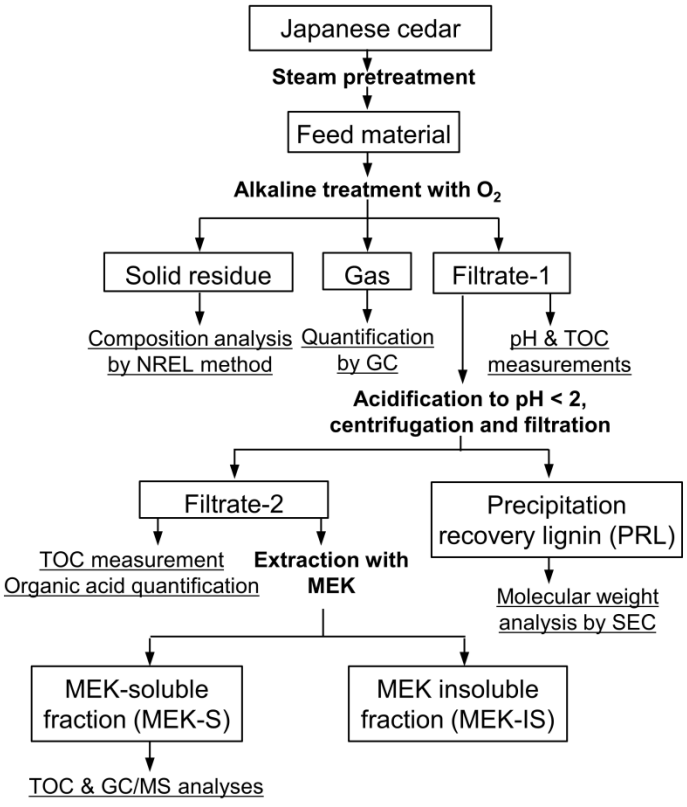

Figure 2.1. Workflow of product separation, collection, and analysis.

The pH of the liquid (filtrate-1) was measured with a pH meter (D-71; Horiba Ltd., Japan). Inorganic and organic carbons in filtrate-1 were quantified using a total organic carbon (TOC) analyzer (Shimadzu, TOC-5000A). A portion of filtrate-1 was acidified to

pH <2 to precipitate light brown-colored lignin (precipitation recovery lignin, PRL). PRL was isolated by centrifugation, filtration, washing with water, and vacuum drying at 60 ℃. Size exclusion chromatography (SEC) was applied for measurement of the apparent molecular weight (MW) distribution of PRL. To improve the solubility of the acid-insoluble lignin (PRL) in tetrahydrofuran (THF) and minimize molecular association issues, PRL was acetylated in pyridine-acetic anhydride mixture (1:1, volume fraction) at 30 ℃ in the dark for 48 h. The mixture was poured into cold acidic water to get precipitate (acetylated lignin). The acetylated lignin was washed and vacuum-dried before re-dissolved in THF. A series of TSKgel G2000HXL, G3000HXL, and G4000HXL columns (Tosoh, Japan) was used at 30℃. Eluent was THF with a flow rate of 1.0 mL/min. The absorbance at 280 nm wavelength was recorded with an ultraviolet detector (Shimadzu, SPD-20AD). A set of polystyrene (Sigma-Aldrich) was used as the molecular weight standards. Formic, acetic, oxalic, glycolic, lactic, malonic, succinic, and 3-hydroxypropionic acids dissolved in filtrate-2 were quantified by high-performance liquid chromatography (HPLC) using an Aminex HPX-87H column (300 × 7.8 mm^2, Bio-Rad). A 4 mM H_2SO_4 aqueous solution was used as the mobile phase. Filtrates 1 and 2 were also subjected to another HPLC for quantification of monosaccharides, but none of these was detected. The organic compounds in filtrate-2 were recovered by liquid–liquid extraction with methyl ethyl ketone (MEK). The residue after evaporation of MEK was defined as the MEK-soluble fraction (MEK-S). Its yield was quantified by TOC analysis. The yields of oxalic acid, glycolic acid, malonic acid, succinic, and 3-hydroxypropionic acid, which had already been determined by the previous HPLC analysis, were subtracted from the carbon-based yield of MEK-S. It was assumed that lactic acid, acetic acid, and formic acid had been evaporated together with MEK. No further analysis was performed for the MEK-insoluble material (MEK-IS) left in the aqueous phase. It was speculated that the MEK-IS consisted mainly of derivatives of hemicellulose and cellulose. [25]

The lignin after the treatment was classified into unconverted lignin in the residue (RL), PRL, and NPL in solution. Their yields, on the basis of the mass of lignin in the original cedar, were calculated using the following equations:

$$RL = \frac{\text{mass of lignin in residue}}{\text{mass of lignin in initial feed}},\ PRL = \frac{\text{mass of precipitated lignin}}{\text{mass of lignin in initial feed}},\ NPL = 1 - RL - PRL,$$

delignification rate = 1 – RL.

NPL was believed to consist of low-molecular-mass aromatic compounds; however, yields of lower organic acids and CO_2 originating from lignin were included in that of NPL inevitably.

2.3. Results and Discussion

2.3.1. Delignification and decomposition of carbohydrates

Table 2.2 summarizes the results of alkaline water treatments with or without O_2. The chemical compositions of the resulting solids are listed in **Table 2.3**. A positive effect of O_2 on the delignification is evident by comparing run 1 (R1) with O_2 and run 2 (R2) without O_2. R1 and R2 gave delignification rates of 0.536 and 0.084, respectively. The O_2 oxidation of R1 also caused loss of cellulose but leaving 84.2% in the solid. The pH after R1, 9.0, was much lower than that after R2, and this was due to the formation of organic acids and CO_2. **Figure 2.2** presents a more detailed comparison of the product distribution between R1 and R2. The lignin dissolved into the solution was classified into precipitation recovery lignin (PRL) and nonprecipitated lignin (NPL). As shown in **Figure 2.2a**, the introduction of O_2 increased the overall rate of dissolution from 0.06 to 0.36 on the cedar carbon basis. The dissolved matter consisted of PRL, organic acids, CO_2, methyl ethyl ketone-soluble fraction (MEK-S), and MEK-insoluble material (MEK-IS). The organic acids and CO_2 were contributed by not only the oxidative degradation of lignin but also that of carbohydrates. This will be demonstrated later. Some organic acids were also formed in the absence of O_2, probably due to reactions preferred in alkaline water such as deacylation and base-catalyzed hydrolysis. [25,26] The MEK-S was characterized by gas chromatography/mass spectrometry (GC/MS), and the results are shown in **Figure S2.2**. The GC/MS detected over 30 types of aliphatic acids, ethers, and esters in MEK-S, but these were not quantified due to very low yields, or the commercial unavailability of the pure standard samples.

Table 2.2. Results of alkaline treatment.

run ID	conditions	delignification rate	NPL yield	PRL yield	cellulose retention	hemicellulose retention			pH of suspension
						xylan	galactan	mannan	
R1	standard conditions, O_2–8 h	0.536	0.425	0.111	0.842	0.379	0.264	0.746	9.0
R2	N_2 2 MPa	0.084	0.013	0.071	0.963	0.851	0.978	0.883	14.0
R3	O_2 0.5 MPa	0.476	0.408	0.069	0.847	0.399	0.294	0.789	12.9
R4	O_2 3 MPa	0.559	0.464	0.095	0.846	0.333	0.249	0.722	9.0
R5	2 h	0.425	0.340	0.085	0.843	0.428	0.313	0.841	13.5
R6	4 h	0.486	0.387	0.099	0.847	0.402	0.295	0.809	10.1
R7	12 h	0.591	0.454	0.138	0.831	0.349	0.237	0.702	9.0
R8	16 h	0.630	0.462	0.168	0.829	0.332	0.219	0.682	8.9
R9	20 h	0.666	0.481	0.185	0.833	0.317	0.217	0.65	8.7
R10	0.5 mol/L	0.375	0.312	0.064	0.896	0.438	0.328	0.874	7.9
R11	1.0 mol/L	0.657	0.499	0.158	0.800	0.316	0.209	0.636	10.6
R12	L/S = 5 mL/g	0.353	0.320	0.034	0.946	0.463	0.361	0.933	8.2
R13	L/S = 20 mL/g	0.656	0.476	0.181	0.757	0.323	0.21	0.601	13.8
R14	70 ℃	0.396	0.345	0.051	0.956	0.464	0.311	0.909	13.1
R15	130 ℃	0.879	0.774	0.106	0.659	0.149	0.032	0.312	7.1
R16	repetitive treatment with solution renewal, 2 ×2-h	0.701	0.472	0.229	0.736	0.152	0.105	0.364	13.9
R17	3×2-h	0.906	0.574	0.332	0.71	0.112	0.044	0.19	13.9
R18	4×2-h	0.959	0.596	0.363	0.665	0.088	0.032	0.11	13.9
R19	2×12-h	0.941	0.677	0.264	0.677	0.077	0.001	0.171	13.2
R20	3×12-h	0.978	0.702	0.276	0.504	0.056	0.001	0.128	13.4

Table 2.3 Composition of residues after alkaline treatment[a].

run ID	conditions	residue composition					ash
		lignin	cellulose	hemicellulose			
				xylan	galactan	mannan	
R1	Standard conditions, O_2–8 h	0.264	0.548	0.038	0.012	0.07	0.033
R2	N_2 2 MPa	0.393	0.46	0.063	0.022	0.062	0.016
R3	O_2 0.5 MPa	0.29	0.538	0.039	0.013	0.072	0.033
R4	O_2 3 MPa	0.25	0.557	0.035	0.011	0.068	0.031
R5	2 h	0.302	0.508	0.04	0.013	0.073	0.032
R6	4 h	0.279	0.527	0.039	0.012	0.072	0.037
R7	12 h	0.243	0.566	0.037	0.011	0.069	0.027
R8	16 h	0.227	0.583	0.036	0.01	0.069	0.031
R9	20 h	0.21	0.602	0.036	0.011	0.068	0.025
R10	0.5 mol/L	0.313	0.515	0.039	0.013	0.072	0.023
R11	1.0 mol/L	0.221	0.59	0.036	0.01	0.068	0.029
R12	L/S = 5 mL/g	0.307	0.514	0.039	0.013	0.073	0.025
R13	L/S = 20 mL/g	0.233	0.586	0.039	0.011	0.067	0.032
R14	70 ℃	0.284	0.526	0.039	0.011	0.07	0.033
R15	130 ℃	0.12	0.746	0.026	0.002	0.051	0.006
R16	Repetitive treatment with solution renewal 2 h × 2	0.211	0.632	0.02	0.006	0.045	0.036
R17	2 h × 3	0.084	0.727	0.018	0.003	0.028	0.016
R18	2 h × 4	0.044	0.821	0.017	0.003	0.02	0.014
R19	12 h × 2	0.064	0.793	0.014	0.002	0.029	0.014
R20	12 h × 3	0.032	0.818	0.01	0.002	0.022	0.013

[a]Standard conditions in the autoclave were as follows: O_2 2 MPa, 8 h, NaOH 0.8 mol/L, L/S = 10 mL/g, and 90 ℃.

Figure 2.2b shows the lignin conversions. The presence of O_2 substantially increased the lignin conversion from 0.1 to 0.53. The major part of this increase was explained by the formation of NPL. The MW distributions of PRL are compared between R1 and R2 in **Figure 2.2c**. The PRL from R1 had a broad MW distribution up to 30000 Da, unlike that from R2. The following two hypotheses were developed from the presence of greater MW component in PRL from R1.

(1) MW of PRL from the oxidative lignin extraction was greater than that from the nonoxidative one.

(2) The oxidative and nonoxidative extractions yielded PRL with the same or very similar MW. However, the PRL from the former underwent particular secondary reactions, i.e., chemical condensation (repolymerization) that caused MW increase.

The above hypotheses will be examined later. **Figure 2.2d** shows the yields of major organic acids ranging from formic acid to succinic acid. It seemed that the oxalic acid was formed only by the oxidation. It was difficult to exactly determine the contributions of the carbohydrates and lignin to the individual acids.

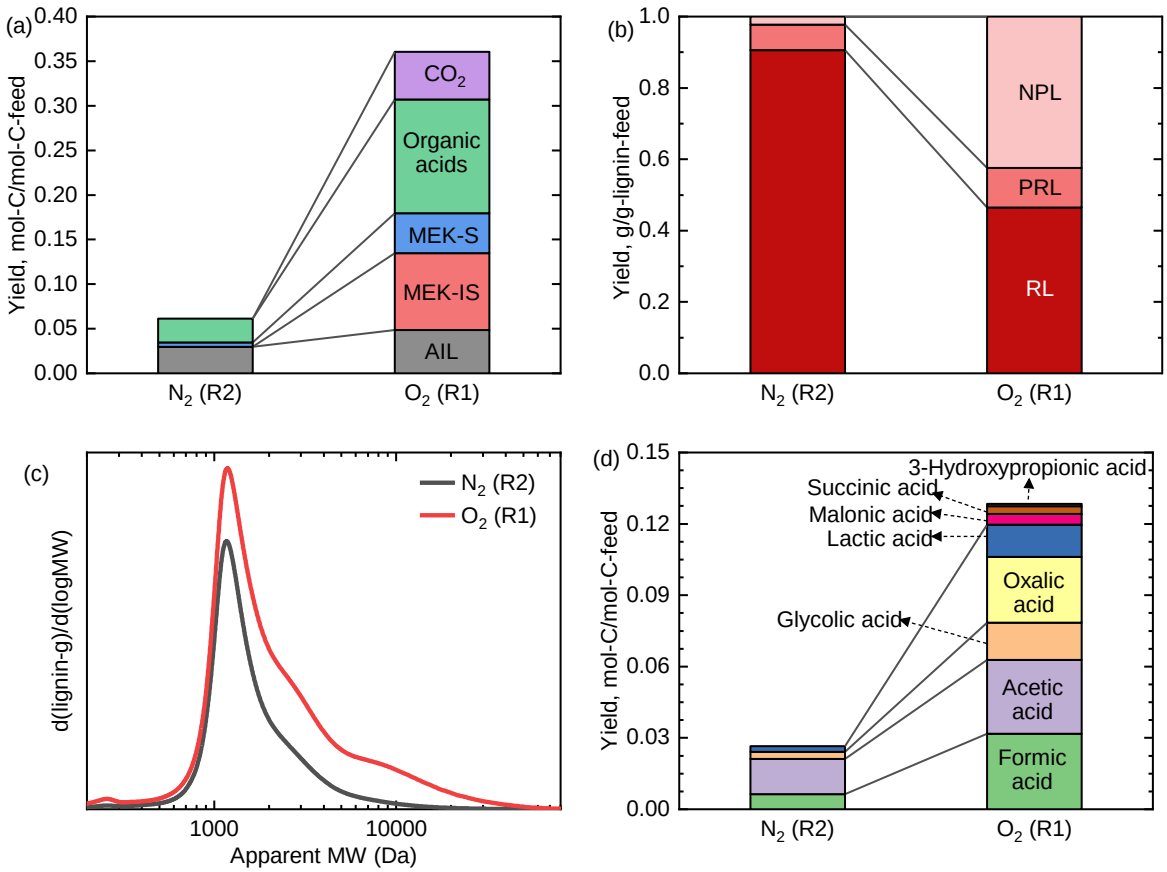

Figure 2.2. Comparison between R1 and R2 in (a) carbon-based product distribution, (b) conversion of lignin, (c) molecular weight (MW) distribution of PRL, and (d) yields of organic acids. The vertical axis of (c) is based on the absorbance at 280 nm that has been normalized by the concentration of PRL in the mobile phase of tetrahydrofuran (THF) and mass of PRL per that of lignin.

Understanding of carbohydrate degradation is important to achieve high cellulose yield along with extensive delignification. The oxidation of reagent cellulose, xylan, and five monosaccharides was therefore investigated. The results of 12-h oxidation are summarized in **Figure 2.3**. Both the polysaccharides and monosaccharides were oxidized

to organic acids, CO_2, MEK-S, and MEK-IS, in apparently similar ways to that of the cedar (see **Figure 2.2**). Xylan and all the monosaccharides were degraded completely into alkaline-water-soluble matter, while the conversion of the cellulose was limited to less than 40%. The major products from the monosaccharides were organic acids. The GC/MS detected and identified up to 20 minor compounds in MEK-S, but these were not quantified due to very low yields, or the commercial unavailability of the pure standard samples. The GC/MS result is shown in **Figures S2.4–S2.10**. The monosaccharides and polysaccharides showed different product distributions, as seen in **Figure 2.3b**.

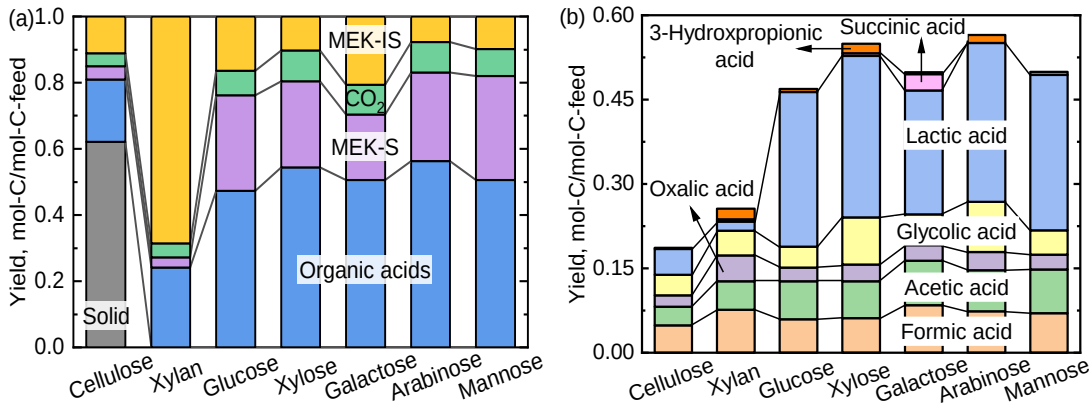

Figure 2.3. Product distribution from oxidative degradation of cellulose, xylan, and monosaccharides under the same temperature and O_2 pressure as in R1: (a) carbon-based product distribution and (b) carbon-based yields of organic acids. Approximately 1 g carbohydrate was oxidized in 20 mL of 0.8 mol/L NaOH solution for 12 h.

For every monosaccharide, lactic acid yield accounted for more than half of the total yields of the major organic acids. On the other hand, the degradation of cellulose and xylan resulted in much lower lactic acid yield and selectivity than those of the monosaccharides. This difference strongly suggests that the polysaccharides underwent direct oxidative decomposition of sugar units rather than a sequence of formation and decomposition of monomers. For the polysaccharides, rupturing of C_{-1}–C_{-2} (α-scission) and C_{-2}–C_{-3} (β-scission) forming C_1 and C_2 organic acids (formic, acetic, glycolic, and oxalic acid) was likely the main degradation pathway. [27] On the other hand, for monosaccharides, the rupture of C_{-3}–C_{-4} seemed to be important for generating C_3 organic acids such as lactic acid. [27] The organic acids formed in R1 (see **Figure 2.2d)** showed a small amount of lactic acid. This result was consistent with the above-mentioned direct oxidation of polysaccharides. It is also noted that the lignin was the other important source of formic,

acetic, oxalic, and glycolic acids.[28] Morone et al. [29] investigated alkaline treatment of rice straw at 161–204 ℃ with pressurized air and found lower organic acids with substantial yields. They speculated that the polysaccharides were first hydrolyzed into monosaccharides, and then the monosaccharides were further oxidized and degraded into organic acids. However, this was not the case the present alkaline treatment with O_2. In other words, at temperatures as low as 90 ℃, the oxidative decomposition of cellulose/hemicellulose was initiated by the direct oxidation of sugar units rather than hydrolytic monomerization or oligomerization.

2.3.2 Remarkable effects of solution renewal

The 54% delignification in R1 suggested that the alkaline treatment with O_2 worked well even at 90 ℃. However, optimization of treatment conditions was required to achieve deeper delignification. The delignification was hence investigated under various treatment conditions with different combinations of O_2 pressure, treatment time, alkali concentration, liquid/solid ratio (L/S), and temperature, and operation modes (single-batch treatment and repeated one with renewal of alkaline solution). The results are summarized in **Tables 2.2** and **2.3**. **Figure 2.4** plots the cellulose retention against the delignification rate. Interestingly, a general trend was found despite a wide variety of conditions. This trend suggested that the process of delignification and cellulose degradation consisted of three stages (i.e., early, mid, and late stages). It also suggested that the delignification selectivity was determined mainly by the chemical structures of lignin and cellulose and more importantly, their chemical interactions, i.e., chemical bonding. The characteristics of each stage are discussed later.

The results of R2–R13 show combined effects of O_2 pressure, treatment time, alkali concentration, and L/S on the delignification rate. It was, however, limited to around 0.65 even by applying 20-h treatment time (R9), and twice amount of L/S (R13). The treatment at 130 ℃ (R15) greatly promoted delignification, but its rate was less than 0.9. The cellulose retention of R15 was 0.66, which was below the trendline at 90 ℃ (**Figure 2.4**). In contrast, the repeated treatments with solution renewal (R16–R20) successfully yielded deep delignification. The 3×12-h treatments (R20) showed almost complete delignification. The 4×2-h treatments (R18) gave a delignification rate of 0.96, with cellulose retention of 0.67. The solution renewal thus enabled deeper delignification than the single treatment at 130 ℃ with the same treatment time and cellulose retention. In other words, the alkaline treatment with O_2 at lower temperatures was more favored for near-complete delignification with less

cellulose degradation. Lower temperatures are expected to slow down undesirable reactions such as degradation of crystalline cellulose that takes place in parallel with the delignification but with higher activation energy than the delignification.

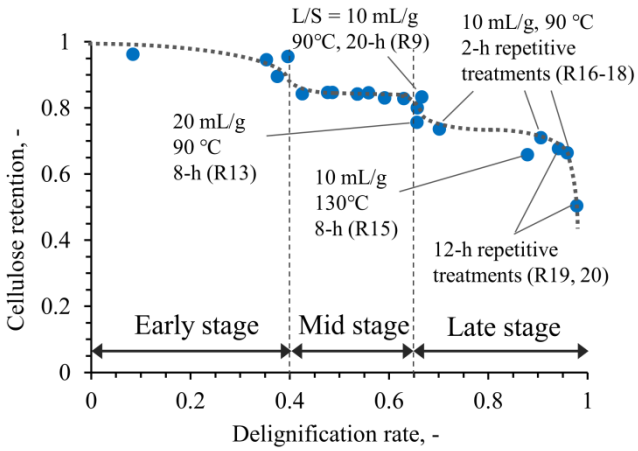

Figure 2.4. Cellulose retention against delignification rate for all the runs. The dotted line illustrates the general trend.

The pH after the 2×2-h repetitive treatments with L/S of 10 mL/g (R16) gave a higher delignification rate than that by the single 8-h treatment with a doubled L/S of 20 mL/g (R13). The pH after the treatment was approximately 14 for both R13 and R16. The pH after the treatment was approximately 14 for both R13 and R16. Thus, neither alkali amount nor pH was a major factor intensified by the solution renewal. It was therefore implied that the dissolved lignin-derived matter, in particular, PRL, hampered the primary reactions between the solid and active oxidative species in the liquid phase by consuming such species, or otherwise, suppressing their formation. **Figure 2.5a** displays the apparent MW distributions of the PRLs from runs with single and repeated 2-h treatments or doubled L/S (R5, R16–R18, and R13) on lignin-weight basis. In contrast to the MW distribution for the 8-h treatment (R1) and the doubled L/S (R13), those for R5 and R16 had no shoulder peaks at the higher MW side. **Figure 2.5b** shows the height-standardized chromatograms. Two-hour repetitive treatments (R5, R16-R18) resulted in almost completely identical MW distributions. It was implied that MW distributions of dissolving lignin were constant when undesirable secondary reactions were inhibited. On the other hand, runs with longer treatment times resulted in a larger shoulder peak. This is explained by the progress of chemical condensation of PRL to form that with MW > 2000. Thus, short-time residence of the lignin fragments in the liquid phase suppressed their chemical condensation therein. From the

comparison of R13 with poorer delignification performance even with doubled L/S of 20 mL/g, and R16 with better delignification performance with the same liquid input of 10 mL/g × 2, it is concluded that the undesirable condensation of dissolved lignin fragments consumed O_2-derived active species, inhibiting the delignification from the solid.

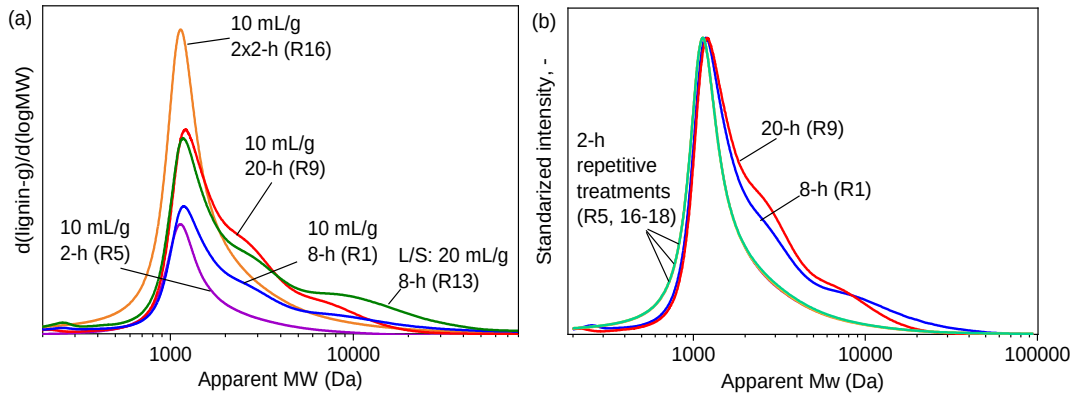

Figure 2.5. Size exclusion chromatography (SEC) chromatograms for selected PRL samples: (a) weight-based representation and (b) height-standardized representation.

2.3.3 Three stages of delignification

As illustrated in **Figure 2.4** the delignification process consists of three stages in terms of cellulose retention. In the early stage (delignification rate <0.4), the loss of cellulose is 0.1 or even smaller. This small loss is attributed to that of noncrystalline cellulose. [30] In the mid stage (delignification rate 0.4–0.65), the delignification is associated with little loss of cellulose, for which retention is in a narrow range of 0.80–0.85 (entries 1, 3–9). This trend indicates the progress of selective delignification. However, the delignification in the late stage (delignification rate >0.65) accompanies significant loss of cellulose. The lignin remaining in the late stage is likely to exist in the deeper regions of the organic matrix of the cedar. Due to poor accessibility of this lignin to oxidizing species, these have to oxidize the cellulose simultaneously with the lignin.

To investigate the characteristics of the three stages from other viewpoints, the relationship between lignin and hemicellulose retentions was analyzed. **Figure 2.6a–c** illustrates the relationships of the delignification rate with xylan, galactan, and mannan retentions, respectively. By comparing the xylan retentions in **Figure 2.6a** and the product yields from the treatment of the isolated xylan shown in **Figure 2.3** it is clear that xylan units in the cedar were much more refractory than the isolated xylan. For example, R7 (12-h oxidation) gave xylan retention as high as 0.35, while the isolated xylan was

completely decomposed. It is also noted that the retentions of xylan as well as the other hemicellulose components are linearly related to the lignin retention in the mid and late stages. Such refractoriness and the linear relationship are explained reasonably by the presence of so-called lignin–carbohydrate complexes (LCC). Hemicellulose components free from LCC are decomposed rapidly in the early stage of the delignification. On the other hand, LCC is gradually decomposed and then its fragments are dissolved into the aqueous phase. The higher refractoriness of mannan, which decomposes only about 10% in the early stage, is attributed to its bonding to the lignin. [19,31] Glucomannan-linked lignin is more difficult to remove than xylan-linked lignin. [19] Thus, less refractory portions of carbohydrates and lignin easily decompose and dissolve in the early stage. Then, the degradation and dissolution of the refractory LCC occur in the mid and late stages. Simultaneous decomposition and dissolution of lignin and hemicellulose were assumed in previous studies. [30,32] However, the linear relationships shown in **Figure 2.6** are first demonstrated in the present study.

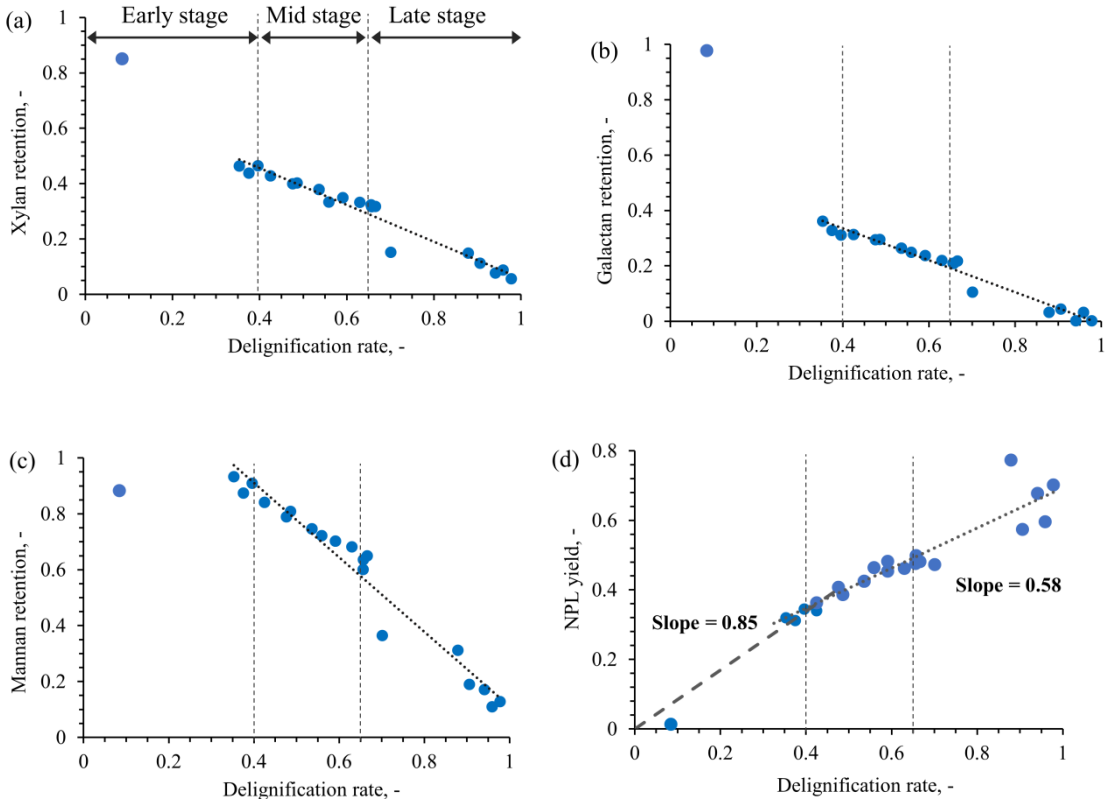

Figure 2.6. Profiles of degradation of hemicellulose and lignin during the treatment: (a–c) retentions of chemical units of hemicellulose and (d) NPL yield. Dotted lines were obtained by least-squares fitting excluding the datum from R2. Dashed lines in (d) were obtained by least-squares fitting to data from R5, R10, R12, and R14.

As shown in **Figure 2.2**, the presence of O_2 greatly increases the NPL yield. **Figure 2.6d** presents the relationship between the NPL yield and the delignification rate. Two master curves fitted for the early stage and the other stages are drawn by a dashed line and a dotted line, respectively. The slope for the early stage is clearly larger than that for the mid and late stages, indicating that the selectivity to NPL is higher at the early stage. In the early-stage delignification, the lignin is likely to be decomposed into small molecules (categorized into NPL for convenience) and thereby dissolved into the alkaline solution. Such rapid lignin removal in the early stage was reported by Shi et al. [33] However, no discussion was found in literature on the clear difference in the product distribution between the early stage and mid/late ones.

Figure 2.7 proposes reaction scheme of the delignification ranging from the early to late stages. In the early stage, the main events are degradation and dissolution of lignin and carbohydrates that are weakly bonded to each other or free from the others. More than half of the xylan, that of galactan, 15% of cellulose, and 40% of lignin are decomposed and dissolved in this stage. However, mannan units are hardly decomposed because of its tight bonding to the lignin. [19,31] The delignification continues in the mid stage but more slowly than in the early stage, while the lignin is still accessible to oxidizing species. The dissolution of lignin accompanies the hemicellulose components as they are involved in LCC. The LCC fragments undergo secondary reactions in the aqueous phase, forming heavy condensed products. The late-stage delignification requires decomposition of at least a portion of cellulose, which makes the remaining lignin accessible to oxidizing species. Lower operating temperatures can reduce the loss of cellulose, for which decomposition has higher activation energy than delignification.

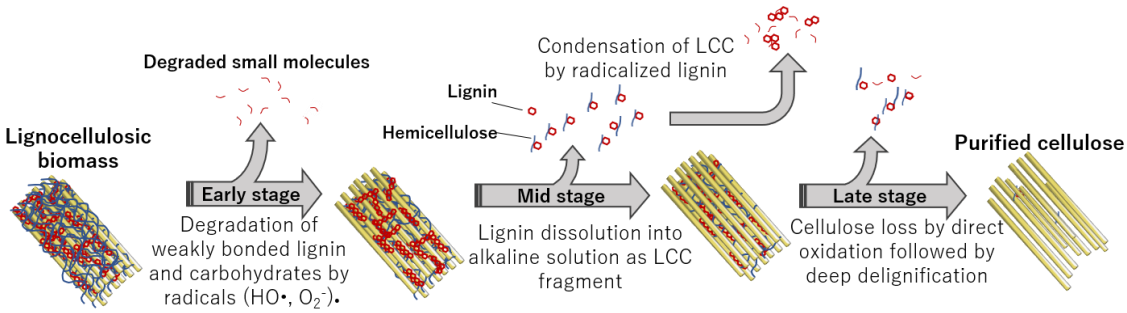

Figure 2.7. Proposed scheme of delignification and decomposition of coexisting carbohydrates in alkaline treatment with O_2.

2.4. Conclusions

This study investigated extensive delignification at low temperatures and its chemical mechanism. Even at 90 ℃, O_2 greatly promotes the lignin dissolution while decomposing carbohydrates. Polysaccharides are decomposed into small molecules without forming monosaccharides. The delignification process, in terms of the delignification rate against cellulose degradation, is mostly dominated by the chemical structure of the cedar. However, the delignification rate is greatly influenced by the operating conditions. The chemical condensation of dissolved lignin fragments, PRL, greatly impedes the delignification. With the renewal of the aqueous phase every 2 h, the undesirable chemical condensation was successfully avoided. The 4×2-h repetitive treatments achieved a delignification rate as high as 96%, which was clearly higher than that by a single treatment at 130 ℃. Use of a percolator, to which a solution is continuously fed, would be a promising approach for further research and development of the low-temperature delignification. [34,35]

Lignification consists of three stages (early, mid, and late stages). The late-stage delignification (rate >0.65) requires cellulose decomposition for making the lignin accessible to oxidizing agents. The target purity of the product cellulose should be determined in consideration of the unavoidable trade-off relationship between lignin and cellulose retentions.

2.5. References

[1] Z. Yuan, Y. Wen, evaluation of an integrated process to fully utilize bamboo biomass during the production of bioethanol. *Bioresour. Technol.* 2017, 236, 202–211.

[2] S. Kudo, N. Goto, J. Sperry, K.Norinaga, J.-I. Hayashi, Production of levoglucosenone and dihydrolevoglucosenone by catalytic reforming of volatiles from cellulose pyrolysis using supported ionic liquid phase. *ACS Sustainable Chem. Eng.* 2017, 5 (1), 1132–1140.

[3] H. Wang, Y. Pu, A.Ragauskas, B. Yang, From lignin to valuable products-strategies, challenges, and prospects. *Bioresour. Technol.* 2019, 271, 449–461.

[4] A.T.W.M. Hendriks, G. Zeeman, Pretreatments to enhance the digestibility of lignocellulosic biomass. *Bioresour. Technol.* 2009, 100 (1), 10–18.

[5] J.S. Kim, Y.Y. Lee, T.H. Kim, A review on alkaline pretreatment technology for bioconversion of lignocellulosic biomass. *Bioresour. Technol.* 2016, 199, 42–48.

[6] C. Pang, T. Xie, L. Lin, J. Zhuang, Y. Liu, J. Shi, Q. Yang, Changes of the surface structure of corn stalk in the cooking process with active oxygen and MgO-based solid alkali as a pretreatment of its biomass conversion. *Bioresour. Technol.* 2012, 103 (1), 432–439.

[7] J. Gierer, Formation and involvement of superoxide ($O_2^{\cdot-}$/$HO_2^{\cdot}$) and hydroxyl ($OH^{\cdot}$) radicals in tcf bleaching processes: a review. *Holzforschung* 1997, 51 (1), 34–46.

[8] F. Carvalheiro, L.C. Duarte, F.M. G ŕio, Hemicellulose biorefineries: a review on biomass pretreatments. *J. Sci. Ind. Res.* 2008, 67 (11), 849–864.

[9] H.B. Klinke, B.K. Ahring, A.S. Schmidt, A.B. Thomsen, Characterization of degradation products from alkaline wet oxidation of wheat straw. *Bioresour. Technol.* 2002, 82 (1), 15–26.

[10] V.S. Chang, M. Nagwani, C.H. Kim, M.T. Holtzapple, Oxidative lime pretreatment of high-lignin biomass: poplar wood and newspaper. *Appl. Biochem. Biotechnol., Part A* 2001, 94 (1), 1–28.

[11] W. Geng, T. Huang, Y. Jin, J. Song, H. Chang, H. Jameel, Comparison of sodium carbonate-oxygen and sodium hydroxide-oxygen pretreatments on the chemical composition and enzymatic saccharification of wheat straw. *Bioresour. Technol.* 2014, 161, 63–68.

[12] X. Pan, X. Zhang, D.J. Gregg, J.N. Saddler, Enhanced enzymatic hydrolysis of steam-exploded douglas fir wood by alkali-oxygen post-treatment. *Appl. Biochem.*

Biotechnol., Part A 2004, 115 (1–3), 1103–1114.

[13] H. Liu, J. Sun, S.Y. Leu, S. Chen, Toward a fundamental understanding of cellulase-lignin interactions in the whole slurry enzymatic saccharification process. *Biofuels, Bioprod. Biorefin.* 2016, 10 (5), 648–663.

[14] S. Jonasson, A. Bünder, T. Niittylä, K. Oksman, Isolation and characterization of cellulose nanofibers from aspen wood using derivatizing and non-derivatizing pretreatments. *Cellulose* 2020, 27 (1), 185–203.

[15] X. Li, Y. Zheng, Lignin-enzyme interaction: mechanism, mitigation approach, modeling, and research prospects. *Biotechnol. Adv.* 2017, 35 (4), 466–489.

[16] Y. Okahisa, K. Abe, M. Nogi, A.N. Nakagaito, T.Nakatani, H. Yano, Effects of delignification in the production of plant-based cellulose nanofibers for optically transparent nanocomposites. *Compos. Sci. Technol.* 2011, 71 (10), 1342–1347.

[17] M. Nishida, T. Tanaka, T. Miki, T. Ito, K. Kanayama, Instrumental analyses of nanostructures and interactions with bound water of superheated steam treated plant materials. *Ind. Crops Prod.* 2018, 114, 1–13.

[18] D. Tarmadi, Y. Tobimatsu, M. Yamamura, T. Miyamoto, Y.Miyagawa, T. Umezawa, T. Yoshimura, NMR studies on lignocellulose deconstructions in the digestive system of the lower termite coptotermes formosanus shiraki. *Sci. Rep.* 2018, 8 (1), 1–9.

[19] M. Lawoko, G. Henriksson, G.Gellerstedt, Structural differences between the lignin-carbohydrate complexes present in wood and in chemical pulps. *Biomacromolecules* 2005, 6 (6), 3467–3473.

[20] K. Yoshioka, Y. Kawazoe, T. Kanbayashi, T. Yamada, H. Ohno, H. Miyafuji, Reaction behavior of cryptomeria japonica treated with pyridinium chloride-water mixture. *RSC Adv.* 2016, 6 (112), 110964–110969.

[21] X. Wang, E.W. Qian, Extraction and modification of lignin from red pine using ionic liquid. *J. Jpn. Pet. Inst.* 2020, 63 (2), 102–105.

[22] M. Nishida, T. Tanaka, T. Miki, T. Ito, K. Kanayama, Instrumental analyses of nanostructures and interactions with bound water of superheated steam treated plant materials. *Ind. Crops Prod.* 2018, 114, 1–13.

[23] A. Sluiter, B. Hames, R. Ruiz, C. Scarlata, J. Sluiter, D. Templeton, D. Crocker, Determination of structural carbohydrates and lignin in biomass-laboratory analytical procedure (LAP), NREL/TP-510-42618; NREL, 2012.

[24] N. Phaiboonsilpa, K. Yamauchi, X. Lu, S. Saka, Two-step hydrolysis of japanese cedar

as treated by semi-flow hot-compressed water. *J. Wood Sci.* 2010, 56 (4), 331–338.

[25] C.J. Knill, J.F. Kennedy, Degradation of cellulose under alkaline conditions. *Carbohydr. Polym.* 2003, 51 (3), 281–300.

[26] R.C.D.A. Castro, B.G. Fonseca, H.T.L. dos Santos, I.S. Ferreira, S.I. Mussatto, I.C. Roberto, Alkaline deacetylation as a strategy to improve sugars recovery and ethanol production from rice straw hemicellulose and cellulose. *Ind. Crops Prod.* 2017, 106, 65–73.

[27] F. Jin, Z. Zhou, T. Moriya, H. Kishida, H. Higashijima, H. Enomoto, Controlling hydrothermal reaction pathways to improve acetic acid production from carbohydrate biomass. *Environ. Sci. Technol.* 2005, 39 (6), 1893–1902.

[28] W. Schutyser, J.S. Kruger, A.M. Robinson, R. Katahira, D.G. Brandner, N.S. Cleveland, A. Mittal, D.J. Peterson, R. Meilan, Y. Román-Leshkov, Revisiting alkaline aerobic lignin oxidation. *Green Chem.* 2018, 20 (16), 3828–3844.

[29] A. Morone, G. Sharma, A. Sharma, T. Chakrabarti, R.A. Pandey, Evaluation, applicability and optimization of advanced oxidation process for pretreatment of rice straw and its effect on cellulose digestibility. *Renewable Energy* 2018, 120, 88–97.

[30] M. Li, J. Wang, Y. Yang, G. Xie, Alkali-based pretreatments distinctively extract lignin and pectin for enhancing biomass saccharification by altering cellulose features in sugar-rich jerusalem artichoke stem. *Bioresour. Technol.* 2016, 208, 31–41.

[31] H. Nishimura, A. Kamiya, T. Nagata, M. Katahira, T. Watanabe, Direct evidence for α ether linkage between lignin and carbohydrates in wood cell walls. *Sci. Rep.* 2018, 8, No. 6538.

[32] S. Si, Y. Chen, C. Fan, H. Hu, Y. Li, J. Huang, H. Liao, B. Hao, Q. Li, L. Peng, Lignin extraction distinctively enhances biomass enzymatic saccharification in hemicelluloses-rich miscanthus species under various alkali and acid pretreatments. *Bioresour. Technol.* 2015, 183, 248–254.

[33] J. Shi, Q. Yang, L. Lin, The structural features of hemicelluloses dissolved out at different cooking stages of active oxygen cooking process. *Carbohydr. Polym.* 2014, 104 (1), 182–190.

[34] M. Laser, D. Schulman, S.G. Allen, J. Lichwa, M.J. Antal, L.R Lynd, A comparison of liquid hot water and steam pretreatments of sugar cane bagasse for bioconversion to ethanol. *Bioresour. Technol.* 2002, 81 (1), 33–44.

[35] W.S.L. Mok, M.J. Antal, Uncatalyzed solvolysis of whole biomass hemicellulose by

hot compressed liquid water. *Ind. Eng. Chem. Res.* 1992, 31 (4), 1157–1161.

Supporting Information

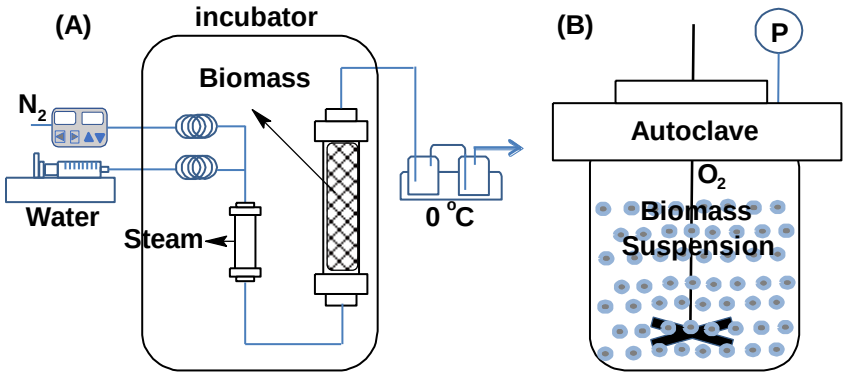

Figure S2.1. The devices of superheated steam pretreatment (A) and alkaline treatment with O_2 (B).

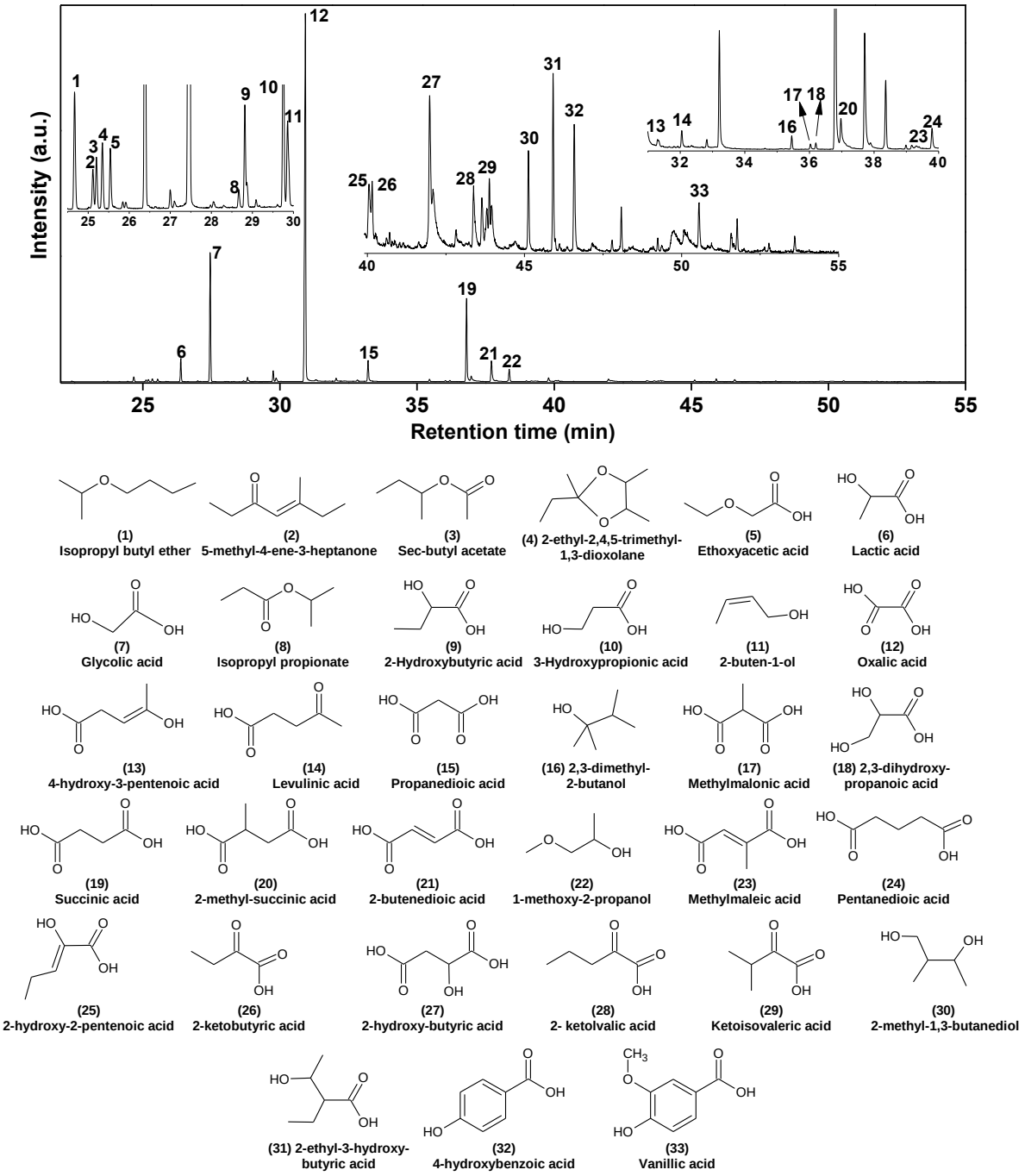

Figure S2.2. Total ion current chromatogram and detected compounds with GC-MS analysis of MEK-S under the O_2 atmosphere (R2).

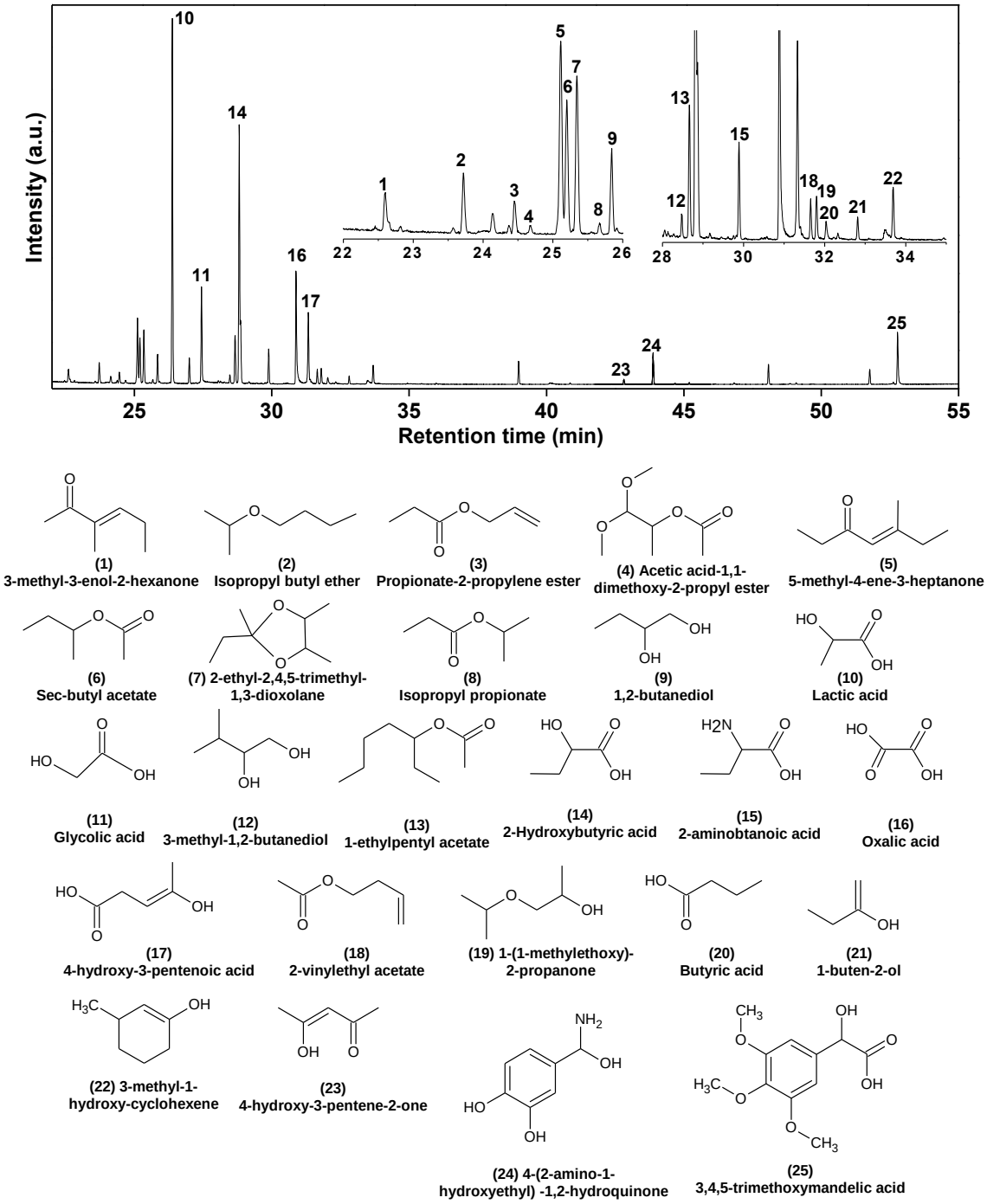

Figure S2.3. Total ion current chromatogram and detected compounds with GC-MS analysis of MEK-S under the N_2 atmosphere (R1).

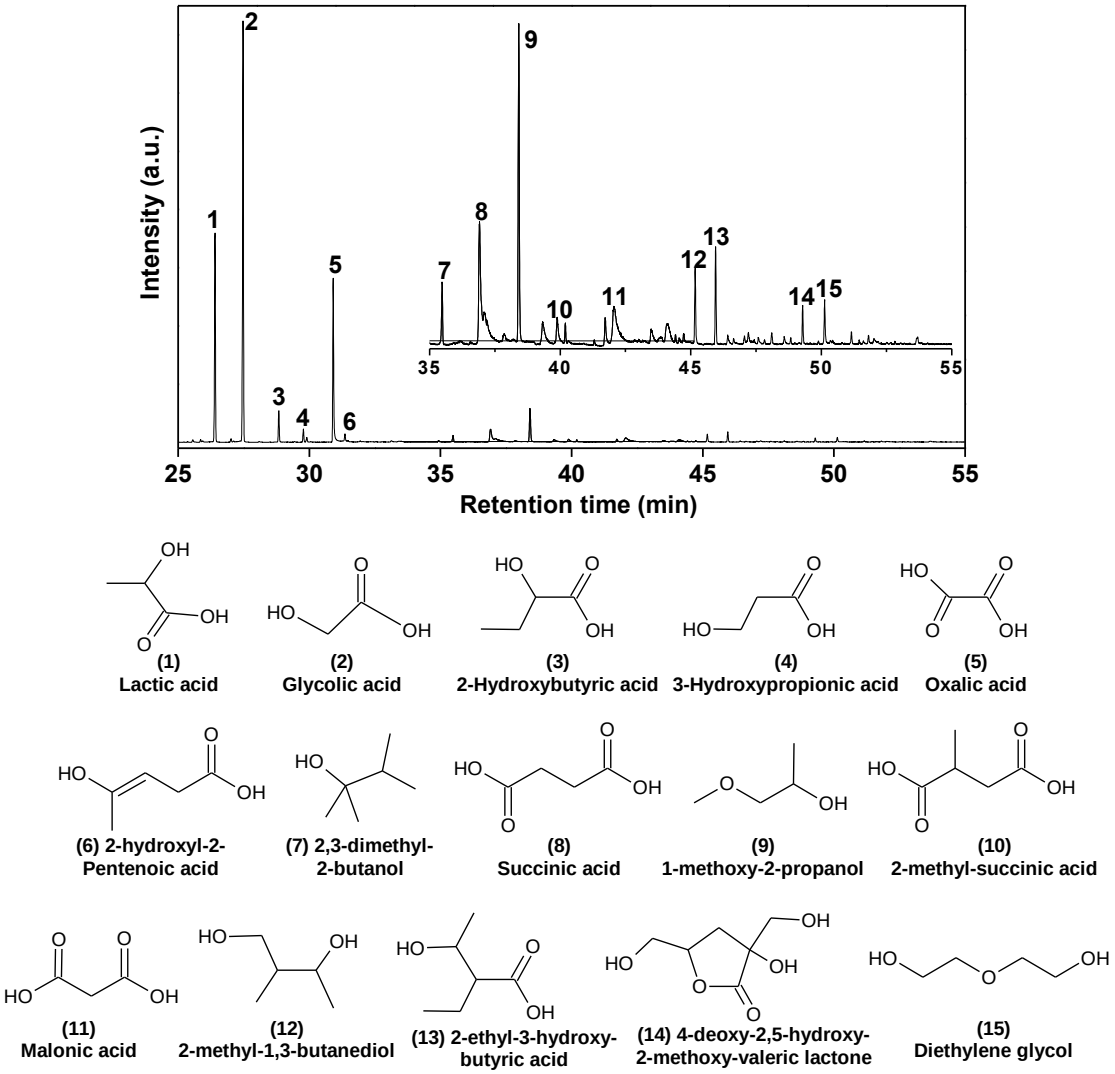

Figure S2.4. Total ion current chromatogram and detected compounds with GC-MS analysis of MEK-S from the oxidation of cellulose.

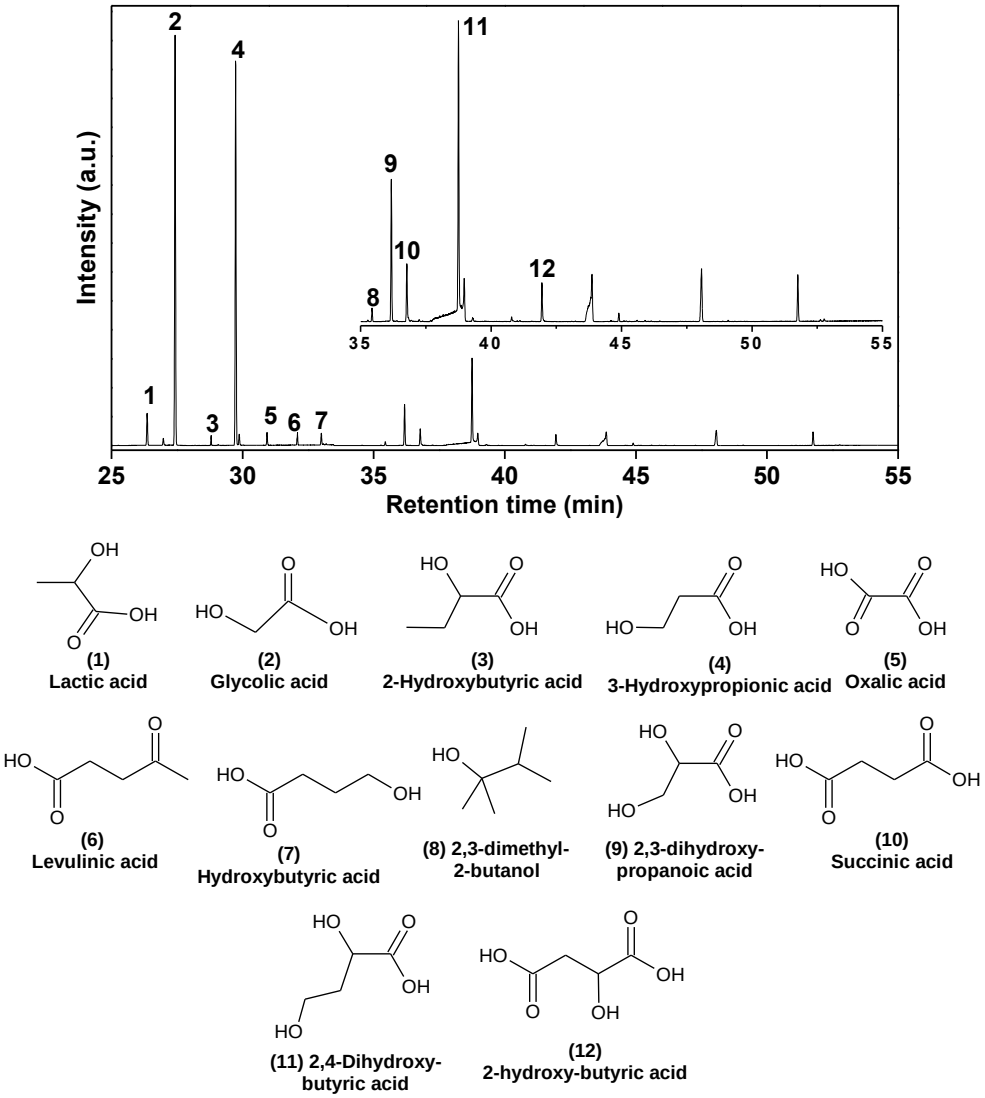

Figure S2.5. Total ion current chromatogram and detected compounds with GC-MS analysis of MEK-S from the oxidation of xylan.

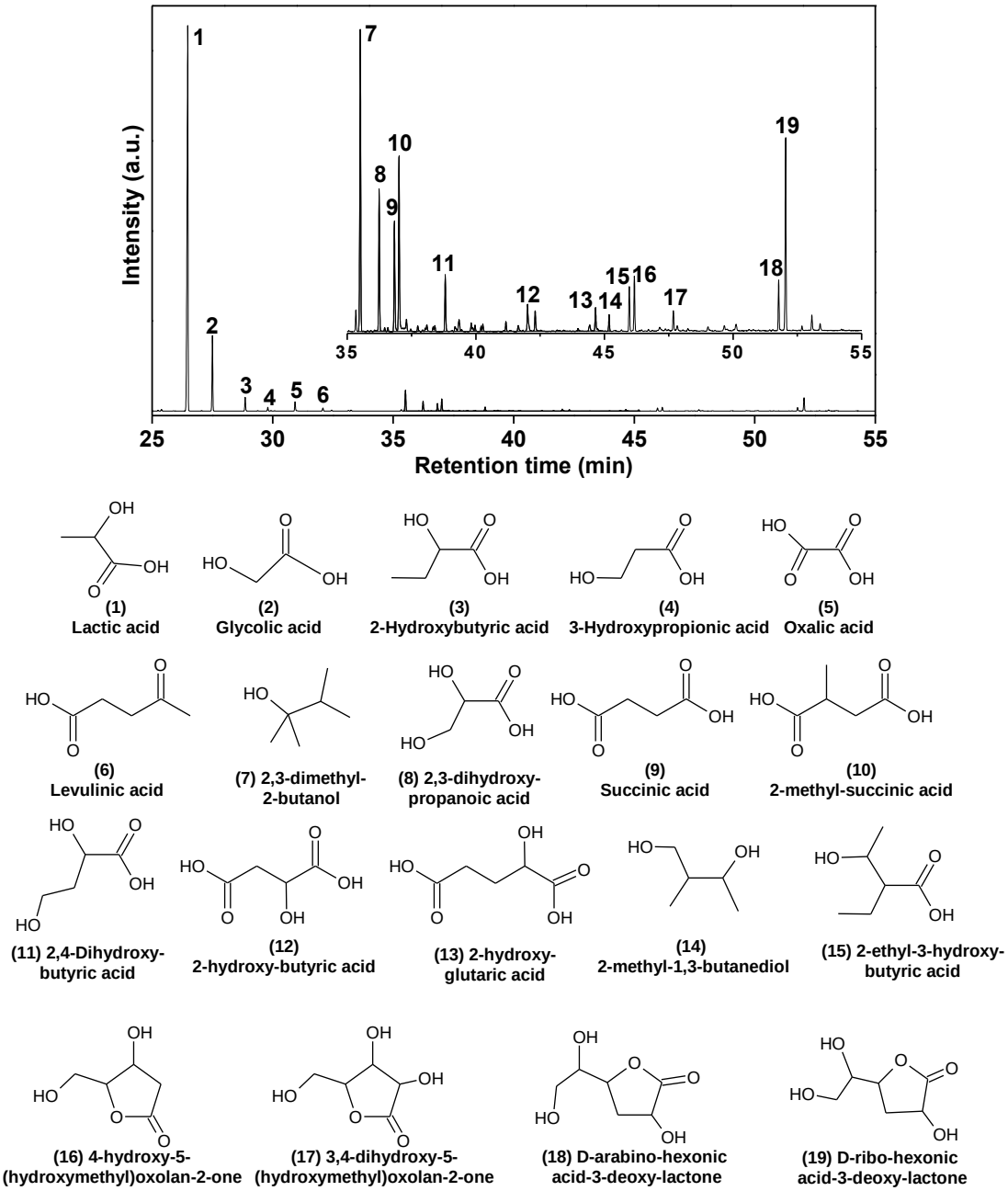

Figure S2.6. Total ion current chromatogram and detected compounds with GC-MS analysis of MEK-S from the oxidation of glucose.

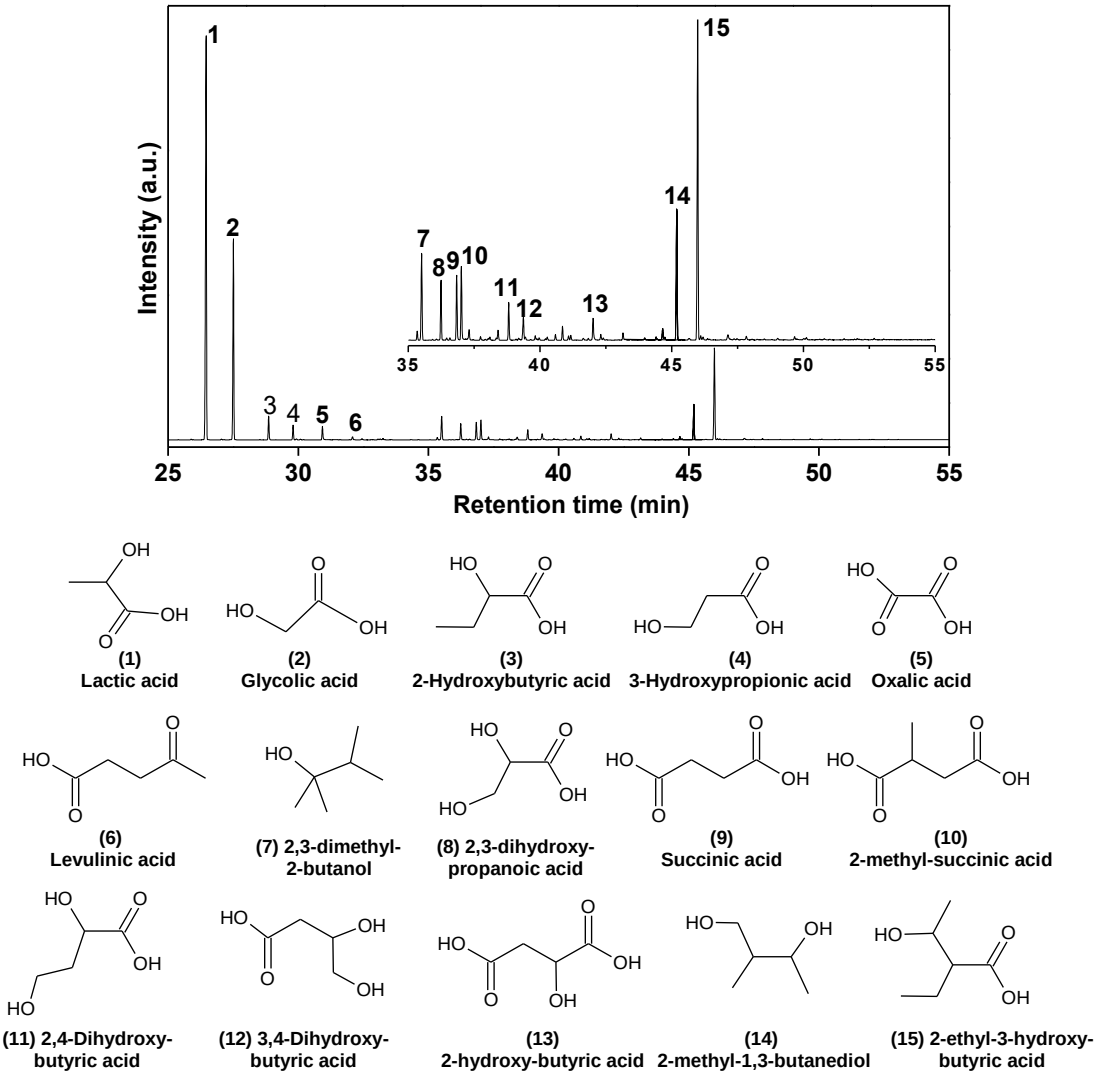

Figure S2.7. Total ion current chromatogram and detected compounds with GC-MS analysis of MEK-S from the oxidation of xylose.

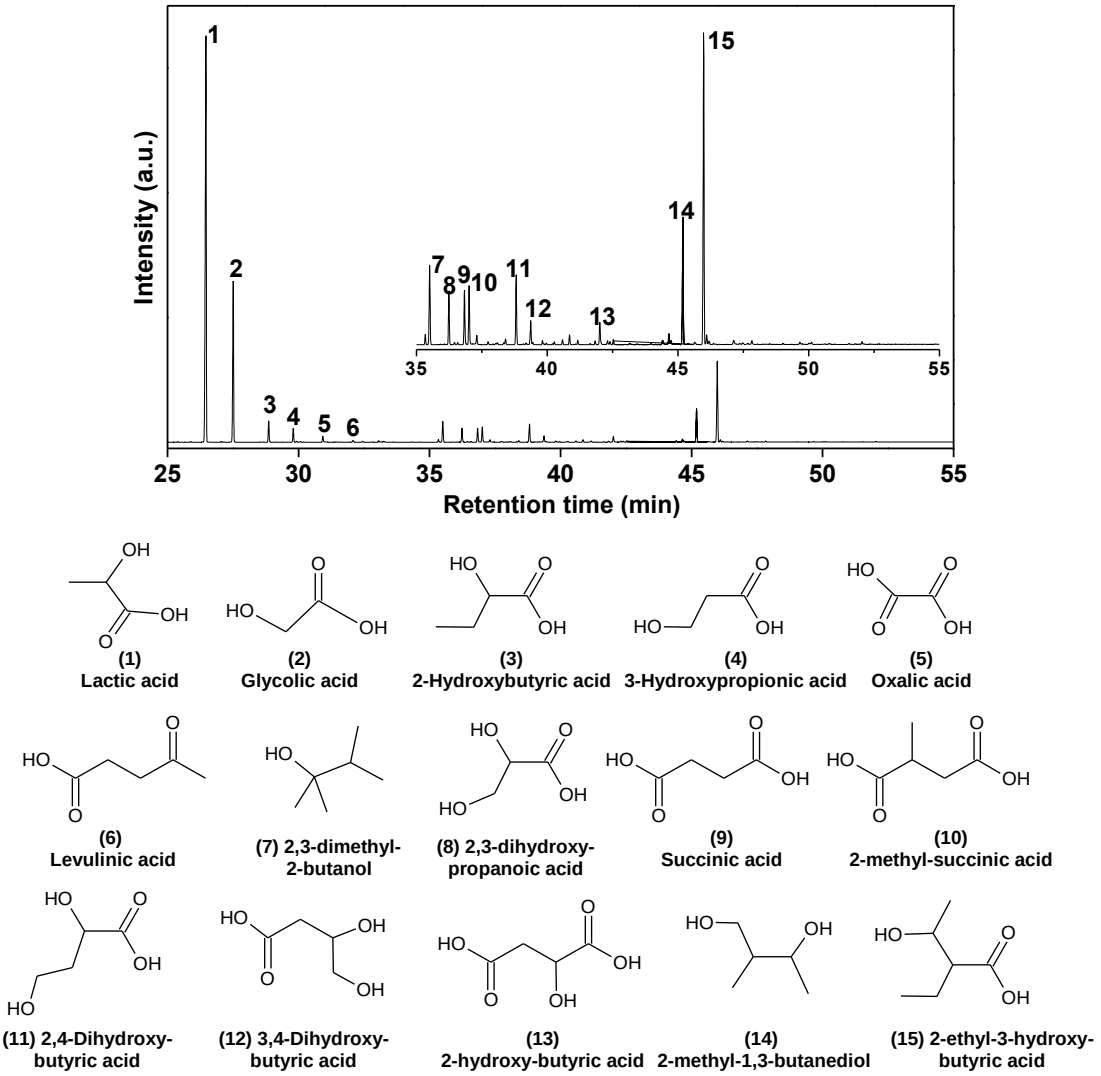

Figure S2.8. Total ion current chromatogram and detected compounds with GC-MS analysis of MEK-S from the oxidation of arabinose.

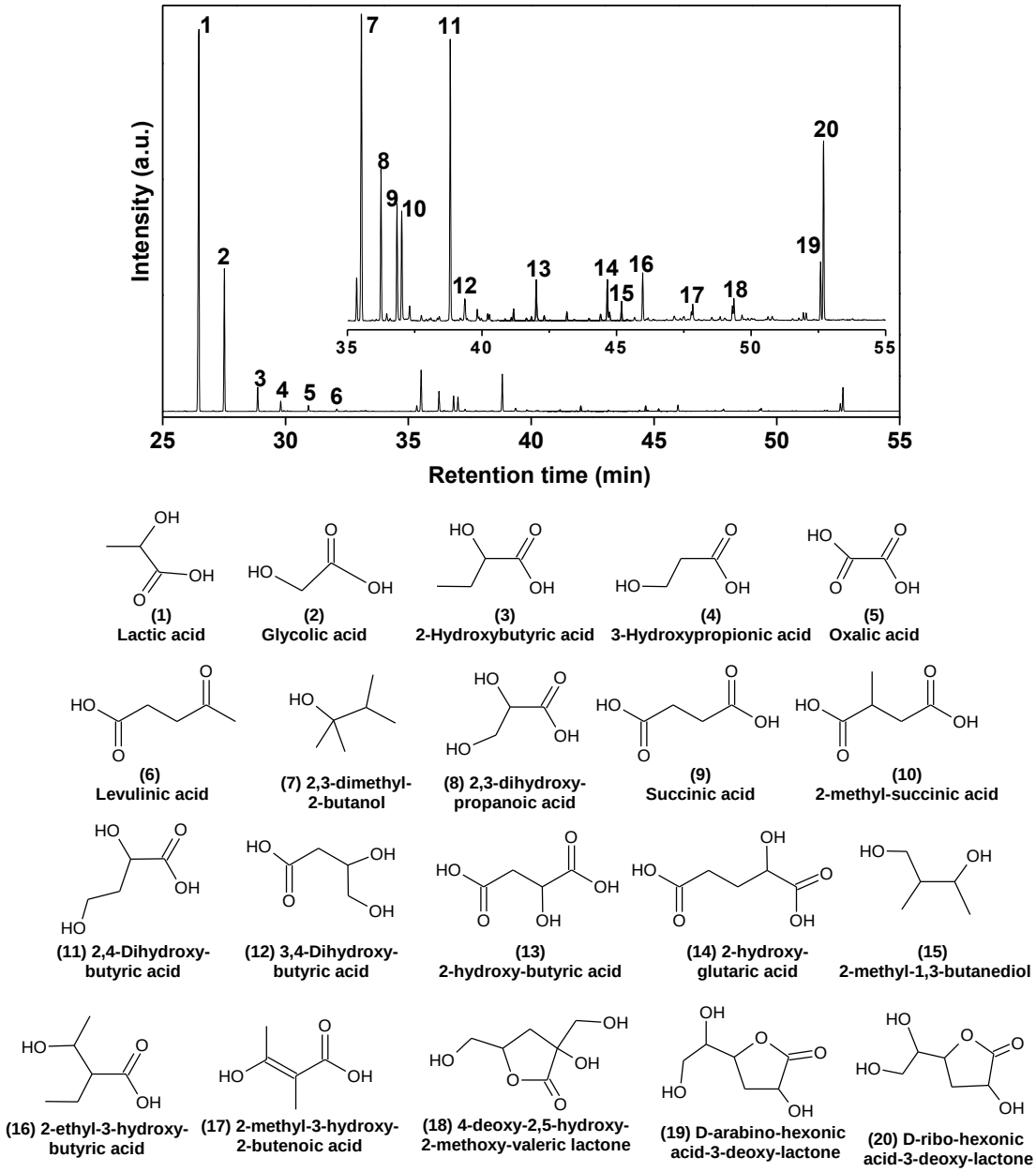

Figure S2.9. Total ion current chromatogram and detected compounds with GC-MS analysis of MEK-S from the oxidation of galactose.

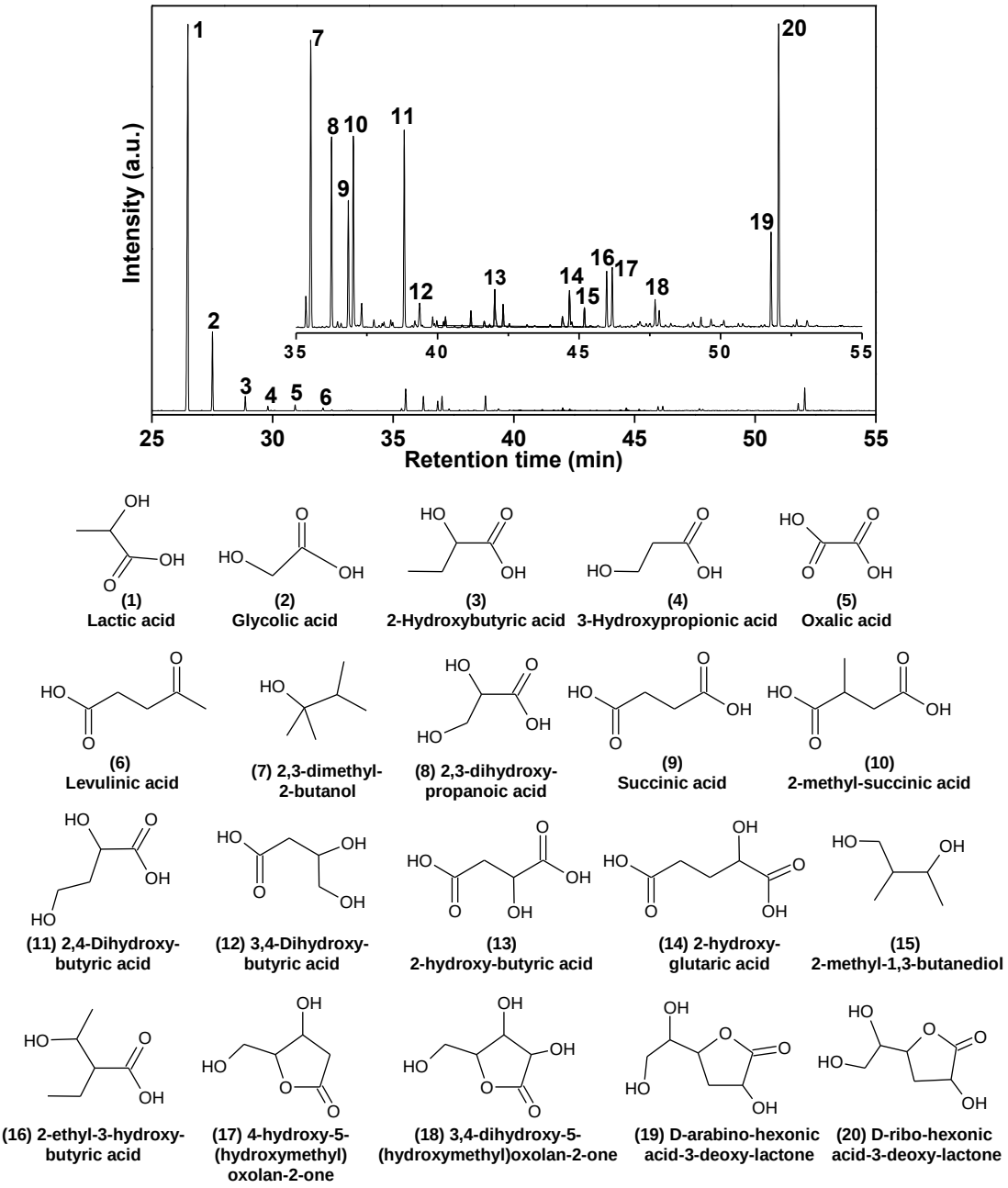

Figure S2.10. Total ion current chromatogram and detected compounds with GC-MS analysis of MEK-S from the oxidation of mannose.

CHAPTER 3

Analysis of Primary Reactions in Biomass Oxidation with O_2 in Hot Compressed Alkaline Water

3.1. Introduction

Lignocellulosic biomass is the most available and sustainable feedstock, a substantial part of that can be saccharified and transformed to biofuels and chemicals, but not readily digested because of the presence of lignin. [1-4] As a cost-effective and green oxidant, O_2 has widely been used for delignification. The electron transfer between molecular O_2 and lignin can derive active species (radicals) that attack lignin molecules, and break inter-aromatic-unit linkages and also aromatic rings, thereby increasing the solubility. [5] The oxidation of biomass with O_2 in alkaline water is promising for the delignification before production of monosaccharides or bioethanol, if the delignification is selective. [6, 7] The oxidation with O_2 removed 30–70% of the lignin and also 10–80% of hemicellulose at 160–200 ℃ under 0.6–1.4 MPa O_2, improving the accessibility of the solid to enzyme and other properties relevant to enzymatic saccharization. [8-10] In those previous studies, however, little attention was paid to the kinetics and mechanism of the oxidation and delignification.

It is believed that the oxidation consists of the primary and secondary reactions. The primary reaction is represented by intra-solid degradation. Its rate is equivalent to that of extraction unless it is limited by the solubility of the extractable matter formed. The secondary reactions consist of homogeneous reaction of the extracted matter in the aqueous phase and heterogeneous one over the solid being extracted. Understanding of the kinetics and mechanism of the oxidation requires distinguishment of those sequential reactions from each other, which can hardly be achieved by adopting conventional batch reactors. Another issue of batch reactors is accumulation of extract with time, in other words, difficulty in defining and maintaining conditions of the aqueous phase.

Kraft pulping has been investigated in detail. It is generally accepted that the pulping process consists of three stages; initial, bulk and residual stages. [11, 12] These are largely influenced by chemical nature of feedstock, in particularly, the reactivity of lignin. [13, 14] Most of the previous studies were performed by employing batch reactors with main foci on the delignification. Very little information was thus available on the primary and secondary reactions involved in the delignification. The secondary reaction of the lignin- and carbohydrate-derived extracts seemed to occur extensively during delignification. [15-17] Shi *et al.* [18] recovered hemicellulose-derived extract from the yellow liquor from a batch Kraft pulping process, and found that the recovery was as small as 1.8% of the hemicellulose

of the feedstock. This could be due to the secondary degradation of the primary extract. Moreover, the lignin-derived extract could undergo depolymerization or retrogressive condensation in the liquid phase. [19]

Jafari *et al*. [14, 20] studied the kinetics of the delignification in a Kraft pulping applying a continuous flow-through reactor, but they paid no any attention to the degradation products, of that information was essential for understanding of the mechanism of oxidative degradation and extraction of lignin and carbohydrates. It is known that the oxidative degradation of hemicellulose and that of lignin occur simultaneously. [21] To our best knowledge, no systematic information has so far been shown on the primary reaction and extraction in oxidative degradation of either woody biomass or herbaceous and other types of biomass.

The present study designed and employed a flow-through fixed-bed reactor, *i.e.*, percolator, to study the primary degradation and extraction of lignin and carbohydrates from a Japanese cedar in its treatment with hot and compressed alkaline water dissolving O_2, referencing reactor systems adopted to hydrothermal degradation of cellulose and hydrothermal degradation of lignite. [22, 23] The percolator allowed to quench the primary extract and to analyze its chemical composition. The continuous supply of O_2-saturated alkaline water to the percolator at a sufficiently high rate successfully made the conditions of the alkaline water steady, and eliminated mass transfer effects on the kinetics of extraction. [14, 24]

3.2. Experimental Section

3.2.1. Materials

Woodchips of Japanese cedar were pulverized to sizes smaller than 0.85 mm, vacuum dried at 60 ℃ for 12 h, and used as the feedstock. The particle sizes of the feedstock were well below a critical size of woodchips (as thickness, ≈ 4 mm) for eliminating the intra-solid diffusional effects on the kinetics of extraction. [25] The chemical composition of the cedar was as follows: carbohydrates; 50.2 (glucan; 36.5, xylan; 4.9, galactan; 1.6, mannan; 6.3, arabinan; 0.9), lignin; 49.8 on the carbon basis of the cedar free from ash, acetyl, extractives and ash with contents of 1.4, 0.7 and 0.9 wt% on a dry basis, respectively. The following compounds were purchased from FUJIFILM Wako Pure Chemical Co. or Tokyo Chemical Industry Co. Ltd.; glucose, xylose, arabinose, galactose, mannose, acetic acid, formic acid, oxalic acid, lactic acid, glycolic acid, ethanol, sodium hydroxide (NaOH), hydrochloric acid

(HCl), and sulfuric acid (H_2SO_4).

3.2.2. Oxidation in percolator

Figure 3.1 shows the experimental setup for the oxidative extraction. The percolator (material; SUS316, volume; 20.5 mL) was charged with prescribed mass (0.1–2.0 g) of the cedar, filled with O_2-free 0.1 mol/L NaOH aq., and connected to the tank storing 0.1 mol/L NaOH aq. (upstream side) and filter (downstream). The tank (volume; 1 L) was heated at 140 ℃ and pressurized with 2.0 MPa O_2 until saturation. The O_2 concentration in the NaOH aq. was measured and determined as 19.6 mmol-O_2 L^{-1}, which was roughly in agreement with that calculated according to a previous report, 18.1 mmol-O_2 L^{-1}. [26] The oxidative extraction was preliminarily investigated at different temperatures, and it was found that the lignin extraction was very slow at temperatures below 140 ℃. It was then chosen for operating the oxidative extraction, while minimization of the secondary reaction was considered.

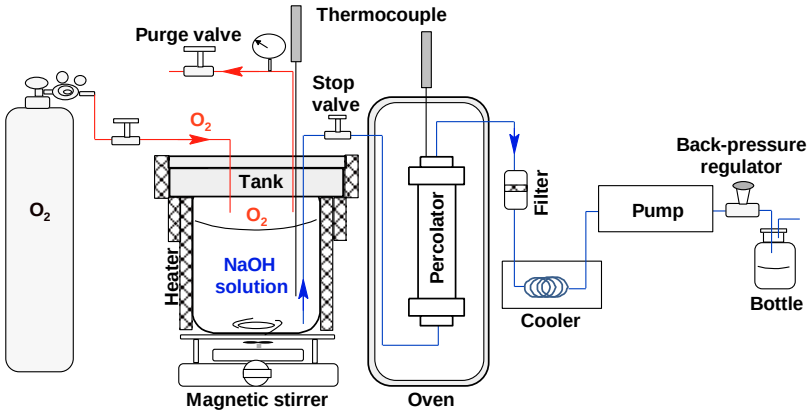

Figure 3.1. Setup of experimental system.

The percolator was heated to 140 ℃, and the temperature was held for 20 min in N_2 atmosphere. Then, the O_2-saturated NaOH aq. was fed to the percolator at a steady flow rate in a range of 1.0–7.0 mL min^{-1}. The start time of the oxidative extraction was defined as the time at which the liquid flow occurred by the pump. The effluent liquid was collected in glass bottles at downstream of the pump with fixed intervals of 10 min. The temperature and pressure inside the percolator were maintained precisely at exactly the same as those of the tank in order to avoid release of O_2 out of the NaOH aq. The liquid residence time within the cedar fixed bed (thickness; 2.5 mm in case of the initial mass of 0.10 g) was 2.5 s when a flow rate of 5.0 mL min^{-1} was applied. After the run for the prescribed time, the percolator

was cooled down to the room temperature. The solid was taken out of the percolator, washed exhaustively with pure water (electrical resistance; 18.2 MΩ), and then dried under vacuum at 60 ℃ for 12 h prior to weighing and analyses

3.2.3. Product separation and analyses

Figure 3.2 shows the flow chart of product separation and analyses. Immediately after the run, the total organic carbon (TOC) and inorganic carbon (IC) dissolved in the recovered liquid were quantified with a Shimadzu TOC-5000A analyzer. The product gas that consisted solely of CO_2 was quantified as IC. A portion of every recovered liquid was acidified to pH < 2 by adding HCl aq. for precipitating and recovering the acid-insoluble lignin (hereafter referred to as AI-L). The acidified liquid after separated from AI-L was subjected to TOC measurement and quantification of lower organic acids (LOA) with a high performance liquid chromatography (HPLC) system (Shimadzu, LC-20 Prominence Series) and a type of column (Bio-Rad Aminex HPX-87H column 300×7.8 mm).

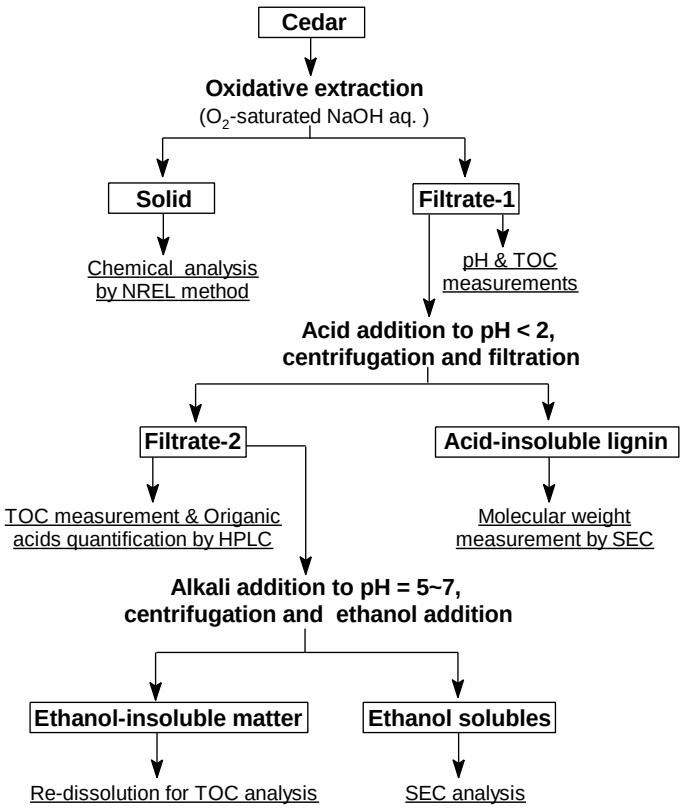

Figure 3.2. Scheme of product separation, collection and analyses. SEC; size-exclusion chromatography.

The acidified liquid was neutralized by adding an NaOH aq., concentrated by rotary evaporation and then adding ethanol. This process caused precipitation of solid consisting mainly of oligosaccharides, allowing the organic acid and acid-soluble lignin (AS-L) to remain dissolved in the acidic ethanol/water. The chemical composition of the solid residue was determined by a standard analytical procedure of NREL via a two-stage hydrolysis. [27] The above-mentioned method gave the distribution of carbon over the range from the solid residue to CO_2 quantitatively. The yields of the solid residue, AI-L, ethanol-insoluble matter (EI), AS-L, LOA, and CO_2 will be denoted by $Y_{AI\text{-}L}$, $Y_{AS\text{-}L}$, Y_{EI}, Y_{LOA}, and Y_{CO_2}, respectively. These yields were defined by

$$Y_i = m_i/m_{t,0}$$

m_i: carbon-based amount of i, $m_{t,0}$: total amount of carbon involved in the solid at time (t) = 0. The overall carbon-based conversion to extract was defined by

$$X = 1 - m_t/m_{t,0} = Y_{AI\text{-}L} + Y_{AS\text{-}L} + Y_{EI} + Y_{LOA} + Y_{CO_2}$$

3.3. Results and Discussion

3.3.1. Kinetic analysis and modeling of oxidative extraction

3.3.1.1. Rate of the primary reaction

In every run of the oxidative extraction, O_2 was fed into the percolator at a steady rate. As expected, the rate of O_2 supply was an important factor for the rate of extraction, and this will be discussed later in detail. Charging sufficiently small amount of the cedar was necessary to avoid limitation of the rate of extraction by the rate of O_2 supply.

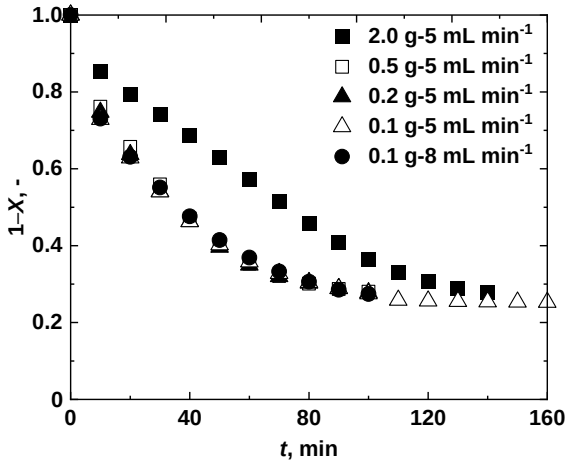

Figure 3.3. Changes in (1–X) with t for conditions with different combinations of the initial sample mass (m_0 = 0.1, 0.2, 0.5, or 2.0 g-dry) and flow rate of O_2-saturated 0.1 N NaOH aq. (v = 5.0 or 8.0 mL min^{-1})

Figure 3.3 shows changes in 1–X with t for different combinations of the initial mass of cedar (m_0) and flow rate of NaOH aq. (v). The extraction rate was maximized and independent of both m_0 and v, when $m_0 \leq 0.2$ g and $v \geq 5.0$ mL min^{-1}. It was thus demonstrated that the percolator enabled to determine the rate of the *primary* extraction as a function of t. The secondary reaction of the primary extract over the solid was, if any, unlikely to influence the 'net' rate of extraction at $m_0 \leq 0.5$ g and $v \geq 5.0$ mL min^{-1}. The secondary reaction of the primary extract in the aqueous phase will be discussed later.

Figure 3.4 shows the change in 1–X with t for $m_0 = 0.1$ g, $v = 5.0$ mL min^{-1}. 1–X by the primary extraction decreases in an exponential manner to *ca.* 0.25 in 120 min, and further decreases afterward but very slowly. This indicates the presence of at least two kinetic components in the cedar. The first focus in the kinetic analysis is put on the late stage extraction. 1–X at $t \geq 150$ min is described well by the following kinetic equation:

$$1–X = 0.26 \exp(-0.000162\, t) \qquad \text{Eq.1}$$

The amount of the solid residue after the 260 min extraction was insufficient for the analysis of chemical composition, but from a white color of the solid, it seemed that it consisted mainly of cellulose but probably also very smaller fractions of lignin and hemicellulose. This was consistent with previous studies that claimed difficulty of complete delignification and also slow delignification on the final stage. [12, 28] It is also known that complexes of lignin and cellulose are refractory, being inaccessible to oxygen-containing active species. [29] The chemical composition of the solid residue is shown and discussed quantitatively later.

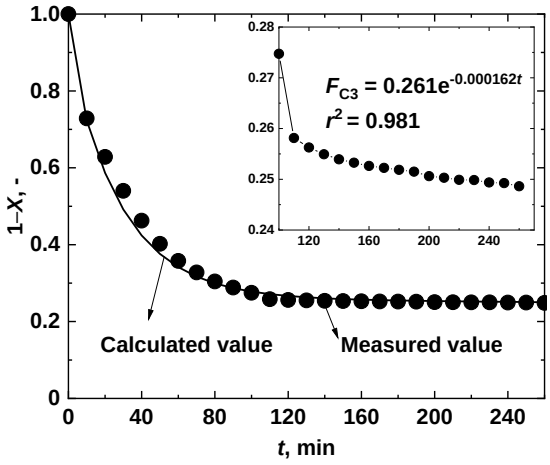

Figure 3.4. Change in 1–X with t for $m_0 = 0.1$ g, $v = 5.0$ mL min^{-1} and extended period of extraction up to $t = 260$ min.

It was assumed that the cellulose of the cedar consisted of two different types, *i.e.*, extractable (oxidatively degradable) and refractory parts, and that the later underwent the extremely slow degradation as expressed by Eq.1. The refractory cellulose was, for convenience, termed Component-3 (C3). It was also assumed that C3 underwent the extraction obeying single first-order kinetics over the range of *t*.

$$F_{C3} = F_{C3,0} \exp(-k_3 t) = 0.26 \exp(-0.000162 t) \qquad \text{Eq.2}$$

$F_{C3,0}$ and F_{C3} are the carbon-based fractions of C3 at $t = 0$ and t, respectively. k_3 is the first-order rate constant in a unit of min^{-1}. The value of k_3 is valid only within the range of conditions employed in the present study, *i.e.*, at O_2 concentration in the NaOH aq. at 19.6 mmol-O_2/L.

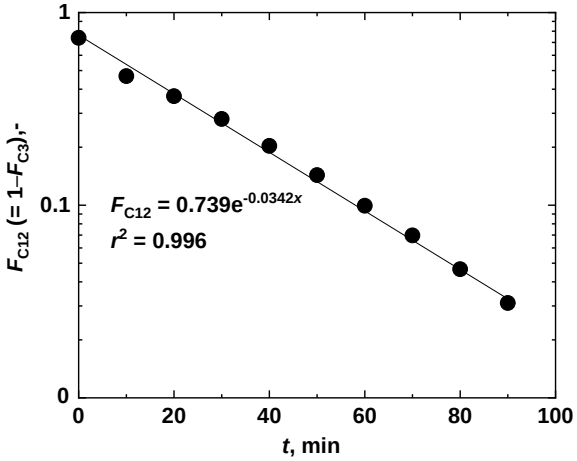

Figure 3.5. Change in the fraction of C12 (F_{C12}) with t for m_0 = 0.1 g and v = 5.0 mL min^{-1}.

It was further assumed that the cedar consisted of two kinetic components, C3 and the other (temporarily denoted by C12) that experienced the extraction simultaneously with C3.

$$F_{C12,0} + F_{C3,0} = 1 \quad (t = 0) \qquad \text{Eq.3}$$

$$F_{C12} + F_{C3} = 1 - X \quad (t = t) \qquad \text{Eq.4}$$

F_{C12}, defined as the carbon-based fraction of C12, was calculated as a function of t from the measured $1–X$ by applying Eqs. 2–4, and is shown in **Figure 3.5**. F_{C12} seems to decrease with t roughly following first-order kinetics with $F_{12,0}$ = 0.74 (= $1–F_{C3,0}$) and k_{12} = 0.034 min^{-1}. The overall rate of the primary extraction is described by

$$1–X=F_{C12,0} \exp(-k_{12} t)+F_{C3,0} \exp(-k_3 t)\approx 0.74 \exp(-0.034 t)+0.26 \exp(-0.000162 t) \qquad \text{Eq.5}$$

Kinetic analysis was performed for some other conditions with combinations of m_0/v = 0.5/5.0, 0.2/5.0, and 0.1/8.0 g/mL min^{-1}, which gave the rate of the primary extraction. The analysis was done with fixed $F_{12,0}$ and $F_{3,0}$ at 0.74 and 0.26, respectively. The result is shown

in **Table 3.1**. k_{12} falls in a narrow range of 0.034–0.035 min^{-1}, indicating validity of the kinetic analysis.

Table 3.1. k_{12} estimated for different conditions. $F_{C12,0}$, $F_{C3,0}$ and k_3 were fixed at 0.74, 0.26 and 0.000162 min^{-1}, respectively.

m_0/v, g/mL min^{-1}	k_{12}, min^{-1}	r^2 for fitting
0.5/5.0	0.0346	0.995
0.2/5.0	0.0350	0.998
0.1/5.0	0.0342	0.996
0.1/8.0	0.0347	0.985

3.3.1.2. Further consideration of kinetic components

Extraction was also carried out under conditions with m_0 = 2.0 g and v = 1.0–7.0 mL min^{-1}, where the rate of extraction was limited by that of O_2 supply due to increased m_0. Those conditions were not applicable to determination of the primary reaction rate, but found to be useful for deeper understanding of the chemical kinetics and mechanism of the conversion of C12.

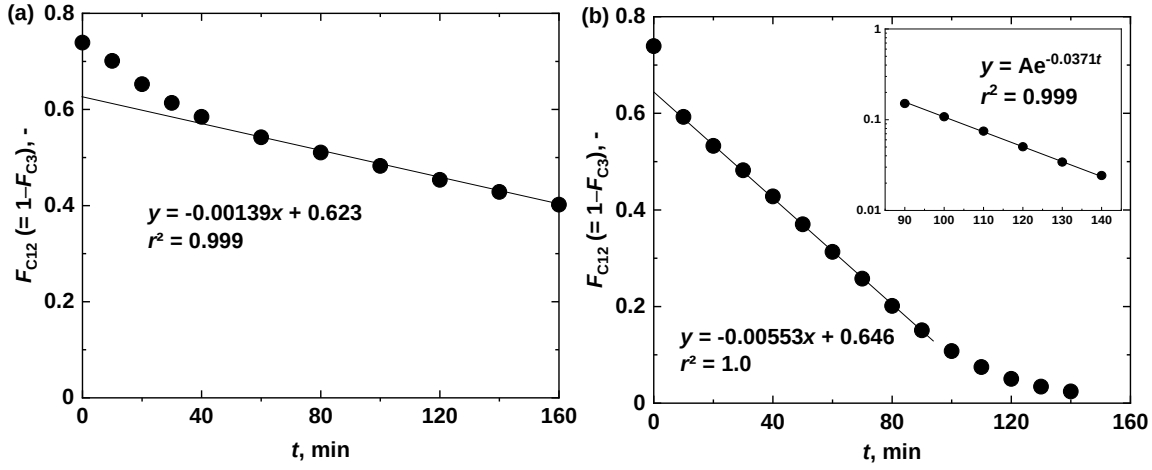

Figure 3.6. Changes in F_{C12} with t for (a) m_0 = 2.0 g. and v = 1.0 mL min^{-1} and (b) m_0 = 2.0 g and v = 5.0 mL min^{-1}. $F_{C3,0}$ was calculated by Eq.2 with k_3 of 0.26 and 0.000162 min^{-1} for calculating F_{C12}.

Figure 3.6 shows the results of kinetic analysis for two conditions as examples. Note that the vertical axes indicate F_{C12} that can be given by 1–F_{C3}. F_{C12} decreases in linear manners with t of 60–160 min or 10–90 min for v = 1.0 mL min^{-1} or 5.0 mL min^{-1},

respectively, apparently following zero-th-order kinetics. The pH of the effluent was almost steady around 13 in those periods. Such linearity is attributed to that the rate of extraction was controlled by the steady rate of O_2 supply. In case of v = 5.0 mL min^{-1} and at t > 90 min, F_{C12} decreases exponentially with t. This is reasonable because the residual amount of F_{C12} became sufficiently small that the rate of extraction was controlled chemically rather than by the rate of O_2 supply. In fact, as seen in **Figure 3.6**, the change in F_{C12} at t > 90 min was described well by first-order kinetics with respect to F_{C12} with an apparent k_2 of 0.037 min^{-1}. It was very similar to k_{12} determined for $m_0 \leq$ 0.5 g and $v \geq$ 5.0 mL min^{-1}, *i.e.*, 0.034–0.035 min^{-1} (see **Table 3.1**).

It is also noted in **Figure 3.6** that the decreases in F_{C12} for the initial 60 min (v = 1.0 mL min^{-1}) or 10 min (v = 5.0 mL min^{-1}) are clearly faster than those later. This trend indicates that F_{C12} consisted of at least two kinetic components. Then, by assuming the presence of such two components in F_{C12}, the kinetic analysis was done in more detail. The initial fractions of the two components was estimated reasonably by extrapolating the linear relationship between F_{C12} and t to t = 0. As shown in **Figure 3.7**, the Y intercept was almost independent of v over the entire range of 1.0 to 7.0 mL min^{-1}. The average value of the Y-intercepts was 0.635, and then defined as the initial fraction of a sub-component of F_{C12} (C2), *i.e.*, $F_{C2,0}$. The initial fraction of the other sub-component (C1), $F_{C1,0}$, was automatically given as 0.104 according to $F_{C12,0} = F_{C1,0} + F_{C2,0}$.

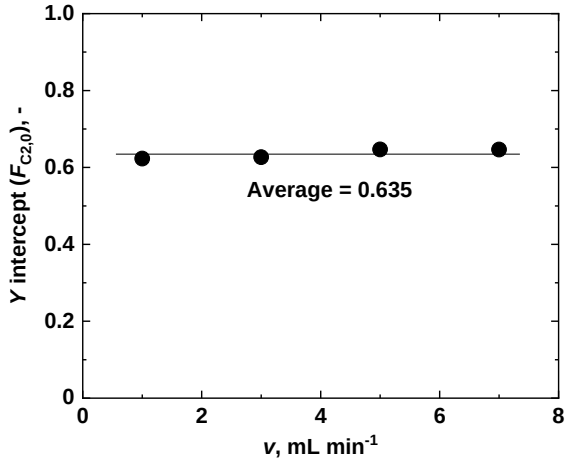

Figure 3.7. Y-intercepts of the linear relationship between F_{C12} *vs* t for different v's and fixed m_0 at 2.0 g.

Figure 3.8 plots the apparent rate of C2 extraction that was determined directly from the linear relationship between F_{C12} and t, against the rate of O_2 supply. Note that the

extraction rate is indicated in the unit of mmol-C min^{-1}. The rate of extraction is correlated linearly with each other at that of O_2 supply up to 0.1 mmol min^{-1}. This means that the O_2 dissolved in the NaOH aq. was consumed completely or near completely while passing through the fixed bed, and that the O_2 contributed to the degradation and extraction of C2 at an efficiency of 4.7 mol-C/mol-O_2, unless the liquid-phase secondary reaction occurred to a significant degree.

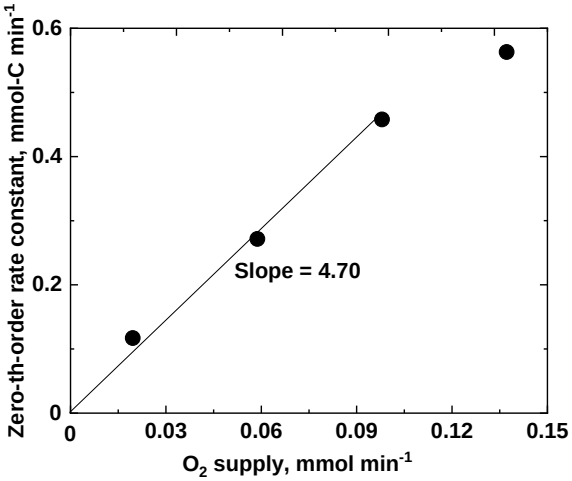

Figure 3.8. Relationship between the rate of extraction of C2 and that of O_2 supply for m_0 = 2.0 g and v = 1.0, 3.0, 5.0, or 7.0 mL min^{-1}.

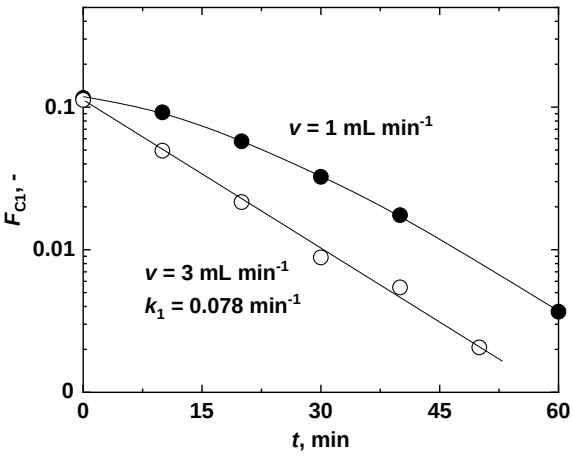

Figure 3.9. Changes with t of the fraction of C1 for m_0 = 2.0 g.

Here is considered the behavior of C1 that was extracted most rapidly and completely in the early period. It is reasonable to consider that C1 was converted and extracted by particular reactions such as ion exchange (*e.g.*, -COOH + NaOH = -COONa + H_2O) and base-catalyzed hydrolysis of ether/ester bonds, which required no O_2 supply. This idea is consistent with a previous report by Kim *et al.* [11] who compared the delignification of corn

stover under oxidative and non-oxidative conditions, and found that a portion of lignin was removed rapidly without oxidation in the initial stage of delignification. In another report, Kataria *et al.* [30] removed part of lignin and hemicellulose from a grass biomass using 0.5-2.0% NaOH without oxidation.

Figure 3.9 shows changes in F_{C1} with t. For v = 3.0 mL min^{-1}, F_{C1} is described well by assuming first-order kinetics with an apparent rate constant (k_1) of 0.078 min^{-1}. This is consistent with that the pH of the effluent was roughly steady (see **Figure 3.10**). On the other hand, for v = 1.0 mL min^{-1}, the apparent rate constant (*i.e.*, the slope of the line) increased with t. This was explained by significant change in the pH for t = 0–60 min. The chemical reactions as suggested above consumed hydroxide ions extensively lowering the pH of the aqueous solution particularly in the early period. The kinetic analysis of F_{C1} was not easy for $v \geq 5.0$ mL min^{-1} due to so fast reaction that completed the extraction of C1 within 10 min, but finally, numerical simulation gave a reasonable value of the rate constant (k_1) of 0.36–0.39 min^{-1}. Thus, in order to determine k_1, it was necessary to maintain the pH that influenced the rate of C1 extraction significantly.

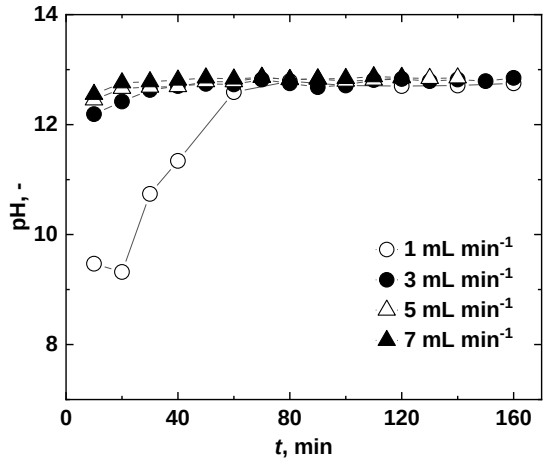

Figure 3.10. Changes in pH of effluent liquid at percolator exit for m_0 = 2.0 g.

Figure 3.10 illustrates time dependent changes in the pH of the effluent liquid for m_0 = 2.0 g. At $v \geq 3$ mL min^{-1}, the pH was initially 12.2–12.6, and it became steady within 40–60 min at 12.8–12.9. The pH in these ranges was lower than that at the inlet of the percolator. The initial decrease in the pH was, as already mentioned, mainly due to the chemical consumption of hydroxide ion. The hydrolysis formed acidic functional groups such as -COOH and phenolic or alcoholic -OH that were involved in the ion-exchange consuming hydroxide ions. [31, 32] On the other hand, the later decrease was insignificant but cannot be

ignored. As mentioned later, the oxidative degradation of C2 formed lower carboxylic acids and CO_2, which contributed to such slight decrease in the pH.

3.3.1.3. Summary of kinetic analysis

The kinetics of the primary extraction is described by the following rate equations under the conditions of temperature; 140 ℃, O_2 concentration; 19.6 mmol-O_2/L, and NaOH concentration; 0.1 mol/L.

$$dX/dt = k_1F_{C1} + k_2F_{C2} + k_3F_{C3} \quad \text{Eq.6}$$

$$F_{C1} = F_{C1,0} \exp(-k_1 t) \approx 0.10 \exp(-0.36\, t) \quad \text{Eq.7}$$

$$F_{C2} = F_{C2,0} \exp(-k_2 t) \approx 0.64 \exp(-0.034\, t) \quad \text{Eq.8}$$

$$F_{C3} = F_{C3,0} \exp(-k_3 t) \approx 0.26 \exp(-0.000162\, t) \quad \text{Eq.2}$$

k_1 of 0.36 was obtained by the kinetic analysis of the data for m_0 = 2.0 g and v = 5.0 mL min^{-1}. k_2 is a linear function of O_2 concentration. Eq.6 claims that the three components, C1, C2 and C3, underwent the extraction obeying the first-order kinetics with respect to their individual fractions. Neither C1 nor C2 corresponded simply to a particular chemical component (*e.g.*, the amorphous part of cellulose, lignin, or hemicellulose). In other words, those were mixtures of two or even more chemical components. Nonetheless, in the kinetic sense, all the components behaved as single reactants. The lignin in cedar is composed of only G units (99.5%) [33], and such a single type of aromatic unit makes the structure of lignin relatively simple. This could be an important reason for the invariance of degradation modes.

3.3.2 Chemical composition of kinetic component

3.3.2.1. Chemical composition of C3

The chemical composition of the sold is one of the most important characteristics of the oxidative extraction. **Table 3.2** shows the compositions of the solids after the extraction with m_0 = 2.0 g and v = 3.0, 5.0 or 7.0 mL min^{-1}. The data shown in this table enabled to estimate the chemical composition of C3 as the most refractory component.

Figure 3.11 displays the contents of the individual chemical components in the solid as a function of $1–X–F_{C3}$ (= F_{C1}+F_{C2}). It is noted that every content is a linear function of $1–X–F_{C3}$. This means that extrapolating the straight line to $1–X–F_{C3}$ = 0 gives the content of the chemical component in C3 as the Y-intercept, assuming that its chemical composition was steady over the range of conversion. The contents of glucan, xylan+mannan, galactan, arabinan, and lignin were 93.9%, 2.5%, 0.55%, 0.66%, and 2.41%, respectively. It was thus possible to prepare a pulp with residual lignin content as

small as 2.4% on the carbon basis. However, the complete extraction of C1 and C2 resulted in the yield of solid (as C3) with a cellulose recovery as low as $F_{C3,0}$/(glucan content in the cedar) ≈ 65%.

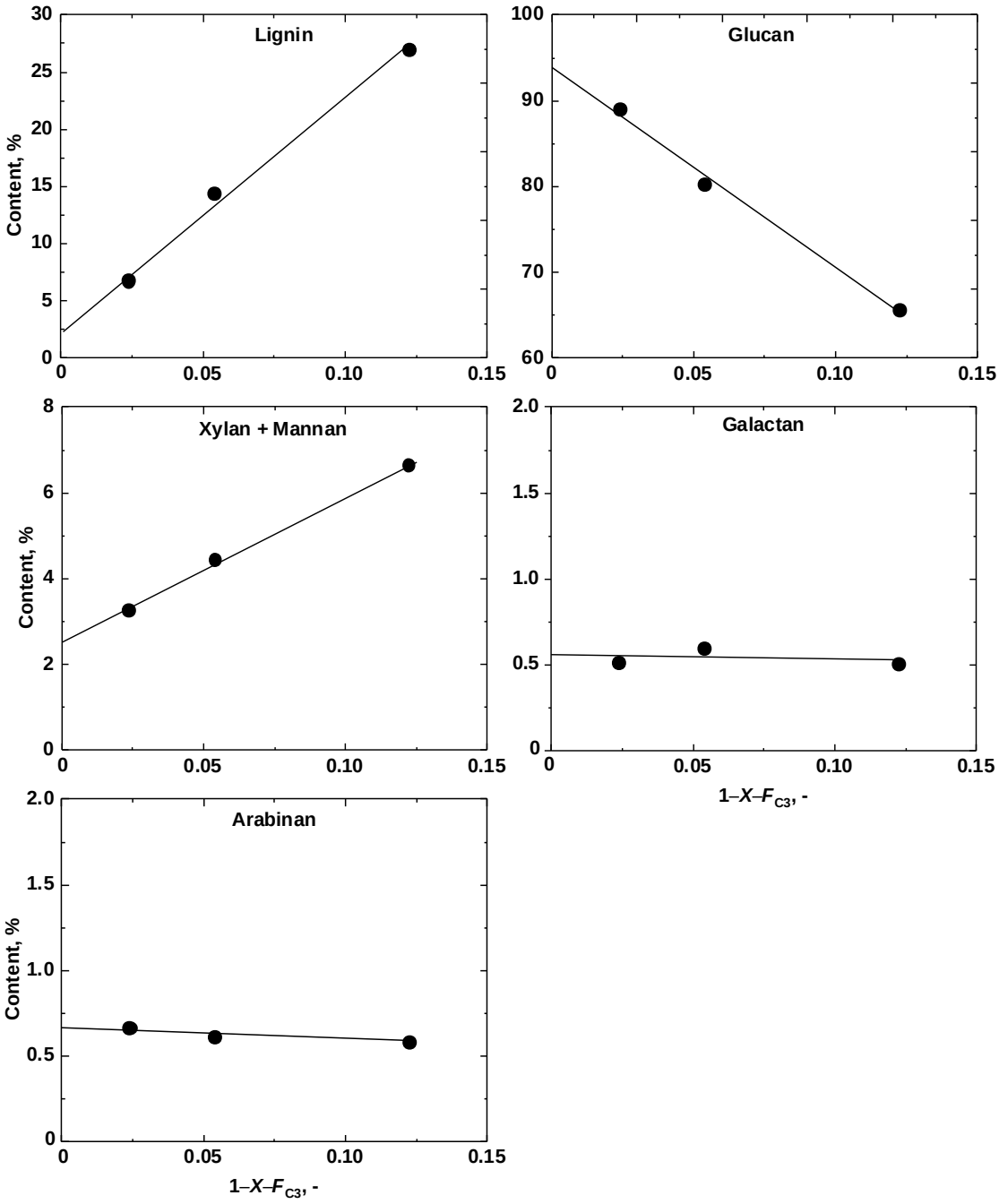

Figure 3.11. Contents of chemical components in solid as a function of $1–X–F_{C3}$ (= $F_{C1}+F_{C2}$).

Table 3.2. Chemical composition of solid after oxidative extraction with m_0 = 2.0 g. The fractions of chemical components were normalized on the carbon-bases of the solid.

Experiment	*t*, min	Lignin	Carbohydrates				
			Glucan	Xylan	Galactan	Mannan	Arabinan
Cedar		49.8	36.5	4.9	1.6	6.3	0.9
3 mL min^{-1}	160	26.9	65.5	3.4	0.5	3.3	0.6
5 mL min^{-1}	140	6.6	88.9	2.5	0.5	0.7	0.7
7 mL min^{-1}	90	14.3	80.1	3.4	0.6	1.0	0.6

3.3.2.2. Chemical compositions of C1 and C2

The quantitative knowledge of the chemical composition of C3 enabled to determine that of C2. The solids after the extraction under the conditions of m_0 = 2.0 g, v = 1.0–7.0 mL min^{-1} and sufficiently long t consisted of C3 and C2 but no C1.

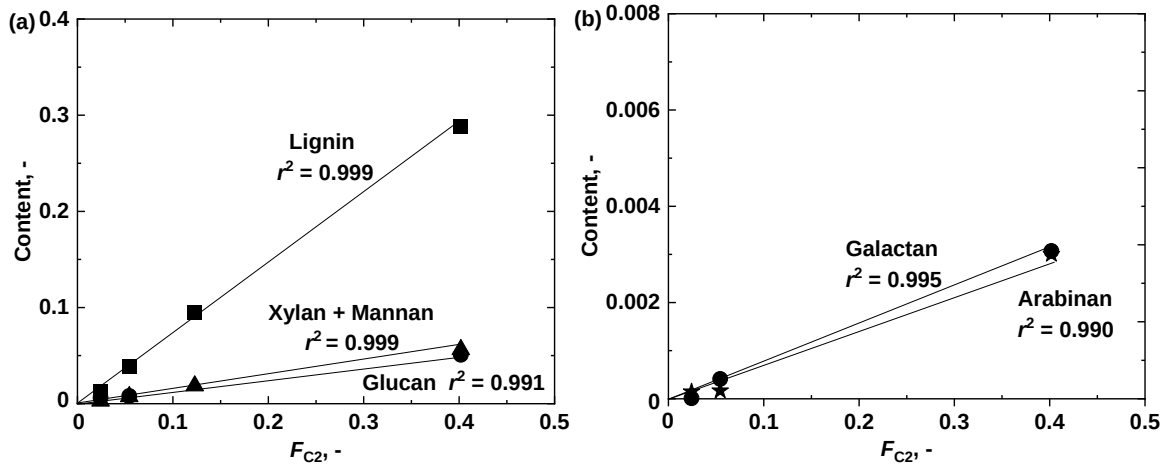

Figure 3. 12. Content of chemical component on the basis of cedar carbon as a function of F_{C2}.

Figure 3.12 shows the contents of the chemical components as functions of F_{C2}. Each content was calculated straightforwardly as the difference in that between the solid and C3 (of the solid). The content of every chemical component of C2 is a linear function of F_{C2}. This demonstrates that the chemical composition of F_{C2} was steady during the oxidative extraction, and also agrees with the behavior of C3 as a single reactant. The initial contents (at t = 0) determined were as follows: Lignin; 0.36 on the cedar carbon basis (56.7% of C2), glucan; 0.16 (24.7%), xylan + mannan; 0.11 (16.7%), galactan; 0.006 (1.0%), and arabinan; 0.006 (0.9%). The initial chemical composition of C1 was determined from those of the

cedar, C2 and C3. **Table 3.3** shows the compositions of C1 together with those of C2 and C3. C1 consisted mainly of lignin, glucan, xylan/mannan, and galactan. More importantly, the carbohydrates accounted for 2/3 of C1 on the carbon basis. Thus, hot compressed alkaline water extracted more carbohydrates than lignin in the absence of O_2. The total fraction of the carbohydrates in C2 was lower than that in C1, but still more than 40%. On the other hand, the major portion of lignin, 90%, was involved in C2, indicating that the oxidation was mandatory for extracting the lignin extensively.

Table 3.3. Chemical compositions of C1, C2, and C3. The fraction is based on the total carbon involved in cedar. The numbers in parentheses (%) are the carbon-based fractions in C1, C2, or C3.

Kinetic component	Lignin	Glucan	Xylan + Mannan	Galactan	Arabinan	Total
C1	0.032 (30.6)	0.036 (34.3)	0.022 (20.9)	0.011 (10.9)	0.003 (3.3)	0.104 (100)
C2	0.360 (56.7)	0.157 (24.7)	0.106 (16.7)	0.006 (1.0)	0.006 (0.9)	0.635 (100)
C3	0.006 (2.4)	0.245 (93.9)	0.006 (2.5)	0.001 (0.6)	0.002 (0.7)	0.261 (100)

3.3.3. Analysis of composition of extracts

3.3.3.1 Selectivities to products from C2

The products from the extraction were lumped into CO_2, LOA, AS-L, AI-L, and EI. Among these, AI-L and AS-L were characterized by SEC. The molecular mass of AS-L ranged 100–2,000 Da (calibrated with polystyrene standards), and clearly differed from that of AI-L over a range up to 100,000 (see **Figure S3.2**). AS-L consisted of monomers, dimers, and small amounts of oligomers. [34] LOA was represented by formic, acetic, lactic, glycolic, and oxalic acids (**Figure S3.1**), the major portions of which were derived from the carbohydrates and lignin (inter-aromatic linkages and aromatic rings). [35-37]

The yields of CO_2, LOA, AS-L, AI-L and EI, were analyzed within ranges of t after complete conversion of C1. Such ranges of t were, ≥60, ≥50, ≥30, and ≥20 min for the conditions of v = 1.0, 3.0, 5.0 and 7.0 mL min^{-1}, respectively, with the fixed m_0 of 2.0 g. In other words, $(1–X–F_{C3}) = F_{C1}+F_{C2} \approx F_{C2}$. **Figure 3.13** plots the yields of CO_2, LOA, AS-L,

AI-L, and EI against Y_{C2}, which is defined by $Y_{C2} = F_{C2,0}–F_{C2}≈0.635–F_{C2}$. All the yields increase linearly with Y_{C2} but with different slopes, which correspond directly to the selectivities to the corresponding products from C2. This trend reveals no or very little change in the product selectivity, and agrees well with the steady chemical composition of C2, strongly supporting the behavior of C2 as a single reactant. It is known that O_2-derived active species can directly attack electron-rich aromatic and olefinic moieties, and also aliphatic chains connected to aromatic ring systems. [38, 39] It is therefore hypothesized that such active species indiscriminately attacked the lignin as well as associated carbohydrates (hemicellulose and cellulose), and this resulted in simultaneous and synchronized extraction from the different chemical components of C2. This hypothesis is supported by Yokoyama *et al*. [40] who found that the O_2 active species generated by a phenolic compound (2,4,6-trimethylphenol) attacked a carbohydrate (a model compound; methyl *p*-D-glucopyranoside) in an alkaline environment.

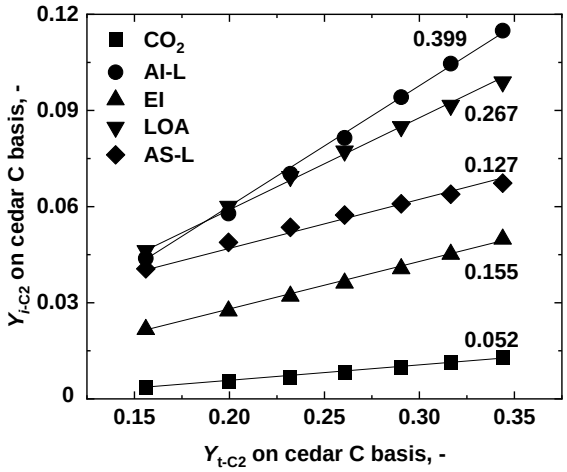

Figure 3.13. The yields of CO_2, LOA, AI-L, AS-L, and EI from C2 as functions of $F_{C2,0}–F_{C2}$ for m_0 = 2.0 g and v = 1.0 mL min^{-1}. The numbers indicated in the frame are slopes of the corresponding straight lines, *i.e.*, selectivities to the products.

The product selectivities were also determined for v = 3.0, 5.0 and 7.0 mL min^{-1}. The result is shown in **Figure 3.14**. The selectivities are almost steady at $v \geq 3.0$ mL min^{-1}, while those to AS-L and EI decreases and increases at v = 1.0–3.0 mL min^{-1}, respectively. In addition to this, the selectivity to LOA slightly decreases at v = 1.0–3.0 mL min^{-1}. Such influences of v on the selectivities to AS-L, EI and LOA can be explained by chemical bonding between fragments of lignin and carbohydrates. EI at $v \geq 3.0$ mL min^{-1} carried lignin fragments (as AS-L precursor), but it was partly decomposed to EI, AS-L and LOA by

decreasing v below 3.0 mL min^{-1} (*i.e.*, by extending the residence time of the primary product). Such the aqueous-phase secondary reaction decreased the selectivity to EI while increasing those AS-L and LOA. In fact, the decrease in the selectivity to EI seems to be compensated by the increases in those to AS-L and LOA at v = 3.0 – 1.0 mL min^{-1}. The O_2 consumption was complete under the conditions of m_0 = 2.0 g, regardless of v. Aqueous-phase base-catalyzed hydrolysis of carbohydrates [32, 41], which did not require O_2, would be an important secondary reaction to change the product distribution.

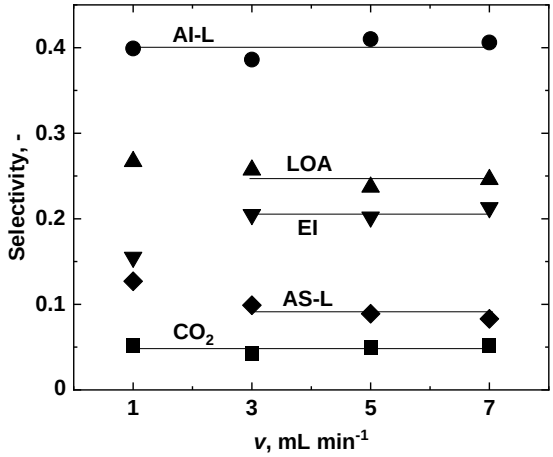

Figure 3.14. Effects of v on selectivities to AI-L, AS-L, LOA, EI, and CO_2 for conversion of C_2. m_0: 2.0 g.

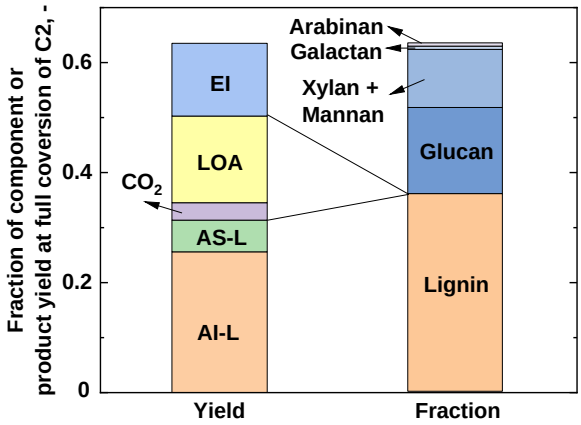

Figure 3.15. Contrast between the chemical composition of C2 and product yields from C2.

Figure 3.15 contrasts the chemical composition of C2 and primary product distribution. The sum of the AI-L and AS-L yields, 0.314, is smaller than, but close to the lignin content in C2. Considering that EI contains lignin fragments to be released by the secondary reaction, the total yields of AI-L and AS-L is even closer to the lignin content. Their yields for m_0 =

2.0 g and v = 1.0 mL min^{-1} were an example. The relationship between AI-L plus AS-L yields and lignin content thus shows that the lignin was converted mainly into AI-L and AS-L but minimally into LOA and CO_2, even though the degradation of C2 was caused by the oxidation. LOA and CO_2 were rather formed from the degradation of the carbohydrates. It is then hypothesized that the oxidative extraction was caused by the oxidation of the lignin-carbohydrate complex (LCC) and resultant release of lignin fragments together with LOA and CO_2 mainly from the carbohydrate part. [42] It was also estimated that LCC of EI was carbohydrate-rich and therefore insoluble in ethanol.

3.3.3.2 Selectivities to products from C1

Quantitative knowledge of the product selectivities for the C2 conversion enabled to derive those for C1. F_{C2} is expressed as a function of t.

$$F_{C2} = F_{C2,0} - k_2\, t \qquad \text{Eq.9}$$

As shown in **Figure 3.13**, the individual products from C2 are expressed as follows.

$$Y_{i\text{-}C2} = (F_{C2,0} - F_{C2})S_{i\text{-}C2} = F_{t\text{-}C2}\, S_{i\text{-}C2} \qquad \text{Eq.10}$$

$Y_{i\text{-}C2}$, $Y_{t\text{-}C2}$ and $S_{i\text{-}C2}$ are the yield of product i, the total product yield from C2 and selectivity to i from C2, respectively. The yield of product i from C1 is then given by

$$Y_{i\text{-}C1} = Y_i - Y_{i\text{-}C2} = Y_{t\text{-}C1}\, S_{i\text{-}C1} \qquad \text{Eq.11}$$

$Y_{i\text{-}C1}$ and Y_i are the yield of i from C1 and total yield of i (from C1 and C2), respectively. Strictly saying, it is necessary to consider the products from not only from C2 but also those from C3. But, the latters can be ignored due to extremely slow degradation of C3.

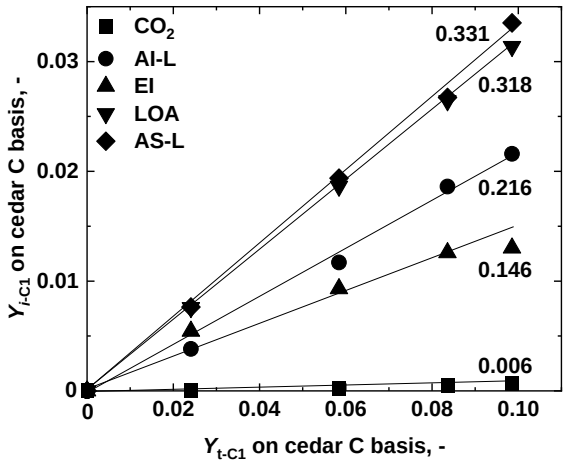

Figure 3.16. The yields of CO_2, LOA, AI-L, AS-L, and EI from C1 as functions of $F_{C1,0}$– F_{C1} for m_0 = 2.0 g and v = 1.0 mL min^{-1}. The numbers indicated in the graphs are slopes of the straight lines, *i.e.*, selectivities to the individual products.

Figure 3.16 shows the calculated $Y_{i\text{-}C1}$ as a function of $Y_{t\text{-}C1}$. Every $Y_{i\text{-}C1}$ increases in a linear manner with $Y_{t\text{-}C1}$. It is thus reasonable to determine the selectivity, $S_{i\text{-}C1}$. **Table 3.4** lists the selectivities for different v's, showing no or little influences of v on the selectivities, *i.e.*, no or little progress of the aqueous-phase secondary reaction of the primary extract from C1. The selectivity to CO_2 was below 0.01, and this was consistent with that C1 underwent non-oxidative degradation (or just dissolution).

Table 3.4. Selectivities to products from C1.

v, mL min^{-1}	CO_2	LOA	AS-L	AI-L	EI
1.0	0.0060	0.32	0.33	0.22	0.15
3.0	0.0077	0.31	0.30	0.25	0.16
5.0	0.0053	0.33	0.32	0.20	0.18
Average $S_{i\text{-}C1}$	0.0063	0.32	0.32	0.22	0.16

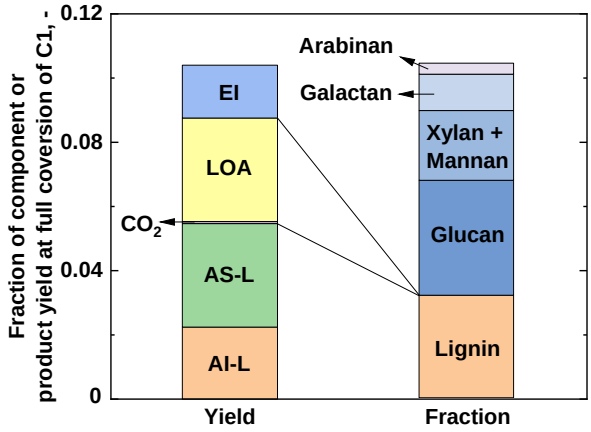

Figure 3.17. Contrast between the chemical composition of C1 and product yields from C1.

Figure 3.17 compares the product yields from C1 with its chemical composition. It is believed that LOA as well as EI was derived from the carbohydrates, according to previous studies, which showed hydrolytic degradation of hemicellulose and cellulose produced oligosaccharides and LOA. [43, 44] More importantly, the sum of AS-L and AI-L yield is clearly greater than the lignin content of C1. This can be explained only by that AS-L and/or AI-L chemically incorporated carbohydrates forming LCC. It was also believed that the LCC was lignin-rich, and then recovered as a portion of AS-L, or otherwise, AI-L. Baptista *et al*. [17] reported that the pine lignin obtained by the conventional kraft cook (NaOH and Na_2S) at 170 ℃ contains about 4 wt% carbohydrates, and shortening the residence time can increase the carbohydrate content. More detailed chemical analysis of

AS-L and AI-L is necessary for clarifying the abundance and chemical structure of LCC and deeper understanding of the mechanism of C1 degradation in the future work. On the other hand, for the C2 degradation, more analysis of EI is needed for characterization of LCC that would be abundant in carbohydrate-rich LCC.

3.4. Conclusions

The oxidative extraction of the cedar in the flow-through percolator, and combined analysis of the kinetics of extraction and chemical compositions of the products have demonstrated the followings within the ranges of experimental conditions.

(1) Sufficiently small mass of the cedar and large liquid flow rate (*i.e.*, O_2 feeding rate) enable to determine the rate of the primary extraction, eliminating the rate-limiting physical processes. The primary extract can be recovered by eliminating its secondary reactions in the aqueous phase and over the surface of solid being extracted.

(2) Limiting the rate of O_2 supply enables to derive three kinetic components, C1, C2 and C3, quantitatively.

(3) All of C1, C2 and C3 undergo degradation following first-order kinetics with respect to their carbon-based fractions, F_{C1}, F_{C2} and F_{C3}, respectively. C1 is converted by non-oxidative reaction such as ion-exchange and base-catalyzed hydrolysis, while C2 and C3 are converted by oxidation. C3 is much more refractory than C2 as well as C1.

(4) The chemical analysis of solids at different conversions enables to clarify the chemical compositions of the individual kinetic components.

(5) The individual kinetic components are chemical mixtures of lignin and carbohydrates, but they behave as single reactants while maintaining their chemical compositions. The product selectivities are therefore steady over the ranges of their conversions. LCC is abundant in C1 and C2, playing important roles in the product selectivities.

(6) C3 as the refractory component consists of glucan and other carbohydrates with the total content as high as 98% on the carbon basis, but C3 accounts for only 26% of the cedar.

3.5. References

[1] S.N. Sun, S.L. Sun, X.F. Cao, R.C. Sun, The role of pretreatment in improving the enzymatic hydrolysis of lignocellulosic materials, *Bioresource Technol.*, 199 (2016) 49-58.

[2] A.T.W.M. Hendriks, G. Zeeman, Pretreatments to enhance the digestibility of lignocellulosic biomass, *Bioresource Technol.*, 100 (2009) 10-18.

[3] Y. Kawamata, T. Yoshikawa, H. Aoki, Y. Koyama, Y. Nakasaka, M. Yoshida, T. Masuda, Kinetic analysis of delignification of cedar wood during organosolv treatment with a two-phase solvent using the unreacted-core model, *Chem. Eng. J.*, 368 (2019) 71-78.

[4] D.L. Huang, R.J. Li, P. Xu, T. Li, R. Deng, S. Chen, Q. Zhang, The cornerstone of realizing lignin value-addition: Exploiting the native structure and properties of lignin by extraction methods, *Chem. Eng. J.*, 402 (2020) 126237.

[5] P. Posoknistakul, T. Akiyama, T. Yokoyama, Y. Matsumoto, Stereo-preference in the degradation of the erythro and threo isomers of *β*-O-4-type lignin model compounds in oxidation processes: Part 1: In the reaction with active oxygen species under oxygen delignification conditions, *J. Wood Chem. Technol.*, 36 (2016) 288-303.

[6] A. Mittal, R. Katahira, B.S. Donohoe, B.A. Black, S. Pattathil, J.M. Stringer, G.T. Beckham, Alkaline peroxide delignification of corn stover, *ACS Sustainable Chem. Eng.*, 5 (2017) 6310-6321.

[7] E. Arvaniti, A.B. Bjerre, J.E. Schmidt, Wet oxidation pretreatment of rape straw for ethanol production, *Biomass Bioenerg.*, 39 (2012) 94-105.

[8] C. Mart ń, H.B. Klinke, A.B. Thomsen, Wet oxidation as a pretreatment method for enhancing the enzymatic convertibility of sugarcane bagasse, *Enzyme Microb. Tech.*, 40 (2007) 426-432.

[9] J.S. Kim, Y.Y. Lee, T.H. Kim, A review on alkaline pretreatment technology for bioconversion of lignocellulosic biomass, *Bioresource Technol.*, 199 (2016) 42-48.

[10] A. Morone, G. Sharma, A. Sharma, T. Chakrabarti, R.A. Pandey, Evaluation, applicability and optimization of advanced oxidation process for pretreatment of rice straw and its effect on cellulose digestibility, *Renew. Energ.*, 120 (2018) 88-97.

[11] S. Kim, M.T. Holtzapple, Delignification kinetics of corn stover in lime pretreatment, *Bioresource Technol.*, 97 (2006) 778-785.

[12] V.L. Chiang, J. Yu, R.C. Eckert, Isothermal reaction kinetics of kraft delignification of

douglas-fir, *J. Wood Chem. Technol.*, 10 (1990) 293-310.

[13] A. Lourenco, J. Gominho, A.V. Marques, H. Pereira, Reactivity of syringyl and guaiacyl lignin units and delignification kinetics in the kraft pulping of Eucalyptus globulus wood using Py-GC-MS/FID, *Bioresource Technol.*, 123 (2012) 296-302.

[14] V. Jafari, K. Nieminen, H. Sixta, A.V. Heiningen, Delignification and cellulose degradation kinetics models for high lignin content softwood Kraft pulp during flow-through oxygen delignification, *Cellulose*, 22 (2015) 2055-2066.

[15] H.B. Klinke, B.K. Ahring, A.S. Schmidt, A.B. Thomsen, Characterization of degradation products from alkaline wet oxidation of wheat straw, *Bioresource Technol.*, 82 (2002) 15-26.

[16] N. Ding, X.Q. Song, Y.T. Jiang, B. Luo, X.H. Zeng, Y. Sun, X. Tang, T.Z. Lei, L. Lin, Cooking with active oxygen and solid alkali facilitates lignin degradation in bamboo pretreatment, *Sustain. Energ. Fuels*, 2 (2018) 2206-2214.

[17] C. Baptista, D. Robert, A.P. Duarte, Effect of pulping conditions on lignin structure from maritime pine kraft pulps, *Chem. Eng. J.*, 121 (2006) 153-158.

[18] J.B. Shi, Q.L. Yang, L. Lin, Structural features and thermal characterization of bagasse hemicelluloses obtained from the yellow liquor of active oxygen cooking process, *Polym. Degrad. Stabil.*, 98 (2013) 550-556.

[19] F.D.C. Oliveira, K. Srinivas, G.L. Helms, N.G. Isern, J.R. Cort, A.R. Goncalves, B.K. Ahring, Characterization of coffee (Coffea arabica) husk lignin and degradation products obtained after oxygen and alkali addition, *Bioresource Technol.*, 257 (2018) 172-180.

[20] V. Jafari, H. Sixta, A.V. Heiningen, Kinetics of oxygen delignification of high-kappa pulp in a continuous flow-through reactor, *Ind. Eng. Chem. Res.*, 53 (2014) 8385-8394.

[21] R. Yang, L. Lucia, A.J. Ragauskas, H. Jameel, Oxygen delignification chemistry and its impact on pulp fibers, *J. Wood Chem. Technol.*, 23 (2003) 13-29.

[22] N. Kashimura, J. Hayashi, T. Chiba, Degradation of a Victorian brown coal in sub-critical water, *Fuel*, 83 (2004) 353-358.

[23] Y. Yu, H.W. Wu, Characteristics and precipitation of glucose oligomers in the fresh liquid products obtained from the hydrolysis of cellulose in hot-compressed water, *Ind. Eng. Chem. Res.*, 48 (2009) 10682–10690.

[24] Y. Ji, M.C. Wheeler, A.V. Heiningen, Oxygen delignification kinetics: CSTR and batch reactor comparison, *AIChE J.*, 53 (2007) 2681-2687.

[25] V.Q. Dang, K.L. Nguyen, A universal kinetic model for characterisation of the effect of chip thickness on kraft pulping, *Bioresource Technol.*, 99 (2008) 1486-1490.

[26] D. Tromans, Modeling oxygen solubility in water and electrolyte solutions, *Ind. Eng. Chem. Res.*, 39 (2000) 805–812.

[27] B.H. A. Sluiter, R. Ruiz, C. Scarlata, J. Sluiter, D. Templeton, and D. Crocker, Determination of structural carbohydrates and lignin in biomass. Laboratory Analytical Procedure, *National Renewable Energy Laboratory Golden*, CO. (2012).

[28] R. Sierra-Ramirez, L.A. Garcia, M.T. Holtzapple, Selectivity and delignification kinetics for oxidative short-term lime pretreatment of poplar wood, Part I: Constant-pressure, *Biotechnol. Prog.*, 27 (2011) 976-985.

[29] S.Y. Fu, L.A. Lucia, Investigation of the Chemical basis for inefficient lignin removal in softwood kraft pulp during oxygen delignification, *Ind. Eng. Chem. Res.*, 42 (2003) 4269–4276.

[30] R. Kataria, R. Ruhal, R. Babu, S. Ghosh, Saccharification of alkali treated biomass of Kans grass contributes higher sugar in contrast to acid treated biomass, *Chem. Eng. J.*, 230 (2013) 36-47.

[31] S.L. Walton, D. Hutto, J.M. Genco, G.P.V. Walsum, A.R.P.V. Heiningen, Pre-extraction of hemicelluloses from hardwood chips using an alkaline wood pulping solution followed by kraft pulping of the extracted wood chips, *Ind. Eng. Chem. Res.*, 49 (2010) 12638–12645.

[32] R.C.D.A. Castro, B.G. Fonseca, H.T.L.D. Santos, I.S. Ferreira, S.I. Mussatto, I.C. Roberto, Alkaline deacetylation as a strategy to improve sugars recovery and ethanol production from rice straw hemicellulose and cellulose, *Ind. Crop. Prod.*, 106 (2017) 65-73.

[33] D. Tarmadi, Y. Tobimatsu, M. Yamamura, T. Miyamoto, Y. Miyagawa, T. Umezawa, T. Yoshimura, NMR studies on lignocellulose deconstructions in the digestive system of the lower termite Coptotermes formosanus Shiraki, *Sci. Rep.*, 8 (2018) 1290.

[34] R. Katahira, A. Mittal, K. McKinney, X.W. Chen, M.P. Tucker, D.K. Johnson, G.T. Beckham, Base-catalyzed depolymerization of biorefinery lignins, *ACS Sustainable Chem. Eng.*, 4 (2016) 1474-1486.

[35] D.C. Zhang, X.S. Chai, Q.X. Hou, A. Ragauskas, Characterization of fiber carboxylic acid development during one-stage oxygen delignification, *Ind. Eng. Chem. Res.*, 44 (2005) 9279–9285.

[36] V. Jafari, S.R. Labafzadeh, A. King, I. Kilpeläinen, H. Sixta, A.V. Heiningen, Oxygen delignification of conventional and high alkali cooked softwood Kraft pulps, and study of the residual lignin structure, *RSC Adv.*, 4 (2014) 17469-17477.

[37] L. Pola, S. Collado, P. Oulego, P.Á. Calvo, M. Díaz, Characterisation of the wet oxidation of black liquor for its integration in Kraft paper mills, *Chem. Eng. J.*, 405 (2021) 126610.

[38] B.J. Gierer, E. Yang, T. Reitberger, On the significance of the superoxide radical (O_2•$^-$/HO_2•) in oxidative delignification, dtudied with 4-*t*-butylsyringol and 4-*t*-butylguaiacol. Part I. The mechanisrn of aromatic ring opening, *Holzforschung*, 48 (1994) 405-414.

[39] J. Gierer, Formation and involvement of superoxide (O_2•$^-$/HO_2•) and hydroxyl (OH•) radicals in TCP bleaching processes: a review, *Holzforschung*, 51 (1997) 34-46.

[40] T. Yokoyama, Y. Matsumoto, G. Meshitsuka, Reaction selectivity of active oxygen species in oxygen-alkali bleaching, *J. Wood Chem. Technol.*, 19 (1999) 187-202.

[41] W. Farhat, R. Venditti, A. Quick, M. Taha, N. Mignard, F. Becquart, A. Ayoub, Hemicellulose extraction and characterization for applications in paper coatings and adhesives, *Ind. Crop. Prod.*, 107 (2017) 370-377.

[42] M. Lawoko, G. Henriksson, G. Gellerstedt, Structural differences between the lignin-carbohydrate complexes present in wood and in chemical pulps, *Biomacromolecules*, 6 (2005) 3467–3473.

[43] C.J. Knill, J.F. Kennedy, Degradation of cellulose under alkaline conditions, *Carbohyd. Polym.*, 51 (2003) 281-300.

[44] F.M. Jin, Z.Y. Zhou, T. Moriya, H. Kishida, H. Higashijima, H. Enomoyo, Controlling hydrothermal reaction pathways to improve acetic acid production from carbohydrate biomass, *Environ. Sci. Technol.*, 39 (2005) 1893–1902.

Supporting information

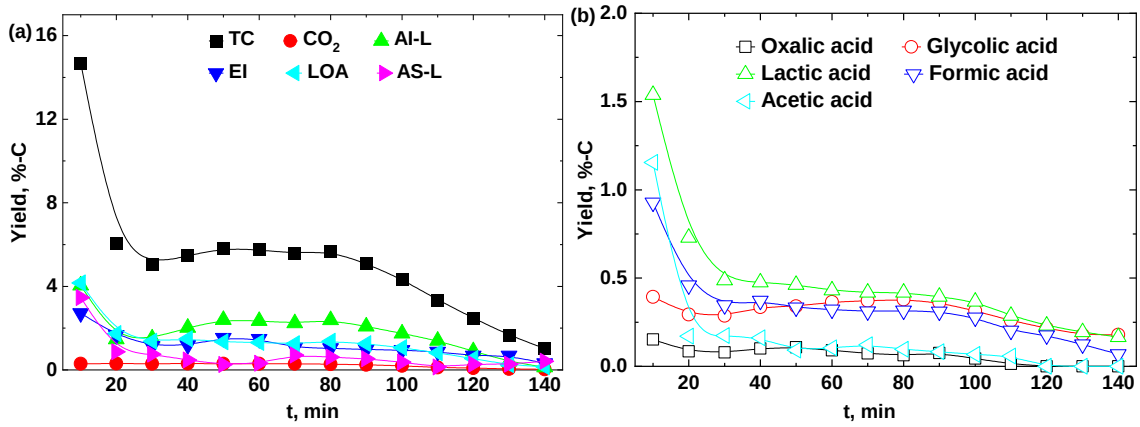

Figure S3.1. Cedar-Carbon-based product distribution (a) yields of CO_2, LOA, EI, AS-L and AI-L, and their sum (TC), (b) yields of lower organic acids as representatives of LOA. Conditions; m_0 = 2.0 g, v = 5.0 mL min^{-1}. The yield of each product is defined as its carbon-based amount formed in time intervals (0–10 min, 10–20 min, 20–30 min, ……) that has been normalized by that of the cedar charged in the percolator.

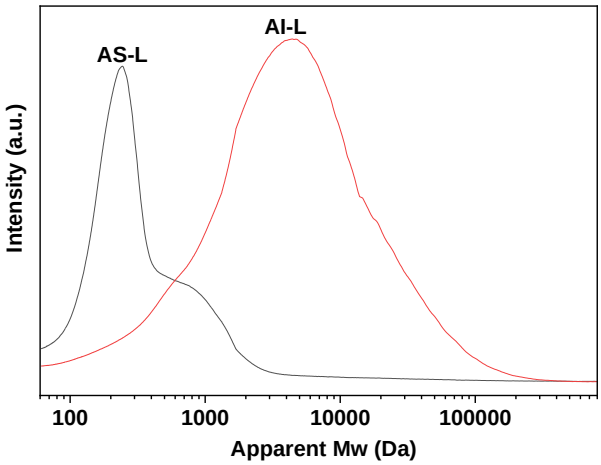

Figure S3.2. SEC chromatograms for AI-L and AS-L recovered after the oxidation under the conditions of m_0 = 2.0 g and v = 5.0 mL min^{-1}. The AS-L and AI-L are the entire portions of the corresponding extracts that are collected for t = 0–140 min.

Table S3.1. Selectivity to product from C2 for the four different conditions.

v, mL min^{-1}	CO_2	LOA	AS-L	AI-L	EI	Total
1.0	0.052	0.267	0.127	0.399	0.155	1.000
3.0	0.043	0.257	0.099	0.386	0.205	0.990
5.0	0.050	0.237	0.089	0.410	0.202	0.988
7.0	0.052	0.246	0.083	0.406	0.213	1.000
Average [a]	0.049	0.247	0.090	0.400	0.207	0.933
Normalized [b]	0.050	0.248	0.091	0.403	0.208	1.000

[a] In averaging the selectivities to LOA, AS-L, and EI, those at v = 1.0 mL min^{-1} was not employed.

[b] The average selectivities were normalized so that their sum agreed with unity.

CHAPTER 4

Hydrothermal Extraction and Alkaline Wet Oxidation of Cedar for Hemicellulose Recovery and Cellulose Purification

4.1. Introduction

Lignocellulosic biomass as the only abundant renewable carbon resources on earth that can be converted into fuels, platform chemicals, and related materials to replace fossil-based resources. However, its intricate structure (cellulose-hemicellulose-lignin matrix) and natural recalcitrance lead to low productivity and complex unstable products, seriously restricting its effective utilization in biochemical and biofuel technologies. [1] Therefore, an integrated pretreatment process to destroy its original structure or fractionate lignocellulose into its main components that improve the conversion efficiency is considered to be the foundation step for the establishment of an economical and sustainable lignocellulosic biorefinery. [2, 3] Cellulose is a homogeneous polymer composed of glucose, and hemicelluloses are heterogeneous polymers consisting of pyranoses and furanoses units including xylose, mannose, arabinose, glucose, and galacturonic acid. Generally, they can be fed into already-developed biorefinery product streams for pulp, monosaccharide products or bioethanol. [4, 5] High-purity cellulose also was used to viscose rayon, cellulose nitrate, cellulose acetate, and nanocrystalline cellulose for getting higher utilization value. [6] Lignin is the most abundant renewable resource containing aromatic rings, which can be depolymerized into phenolic compounds as the precursors for chemicals and biofuels. [7, 8]

The alkaline wet oxidation is a promising method for delignification of lignocellulose and providing cellulose-rich residue and a liquid stream of lignin. [9] The functionalization and partial depolymerization of lignin occurred during oxidation which is helpful for its further catalytic conversion. [7, 10, 11] As the most attractive oxidant (low cost, nontoxicity, and environment-friendly), molecular oxygen (O_2) has been applied to delignify for enhancing the digestibility of biomass and to depolymerize lignin for aromatics. [9, 12, 13] Although high temperatures (>150 ℃) are usually used, the removal rate of lignin is less than 70% due to the weak oxidability of O_2. [3, 14] Effective and near-complete removal of lignin using O_2 under mild conditions for producing high-purity cellulose is rarely reported. Mild conditions are conducive to reducing energy requirements, safety problems, and capital costs of equipment. [15] Oxidative delignification is always accompanied by the serious degradation of hemicellulose making it difficult to recover hemicellulose and its degradation products from black liquor. [3, 16] The loss of hemicellulose is mainly caused by alkaline hydrolysis, peeling of end-groups, and oxidative degradation reactions. [17] Although hemicelluloses can be converted into organic acids during alkaline wet oxidation, they are more valuable if recovered as monosaccharides or oligosaccharides. [18] Therefore, the

recovery of hemicellulose before alkaline wet oxidation is beneficial to the economics of the entire process. Hemicellulose can be isolated as monomeric or oligomeric sugars using appropriate separation techniques. Among various hemicellulose extraction methods, the hydrothermal extraction (HE) in a flow-through reactor using hot pressurized water is an advantageous method, which mainly produces hemicellulose oligomers. [19, 20] Hemicelluloses are closely associated with cellulose and lignin by hydrogen and covalent (mainly α-benzyl ether linkages) bonds. [21] The extraction of hemicellulose inevitably leads to the collapse of cell wall structure, which is conducive to the further removal of lignin.

In this study, the HE and alkaline wet oxidation were combined as an attractive method to recover hemicellulose as oligosaccharides and completely remove lignin for high-purity cellulose. The HE of cedar was performed under both non-isothermal and isothermal mode using a flow-through percolator for investigating the extraction process of hemicellulose. The hemicellulose-depleted cedar was then treated by NaOH or Na_2CO_3 using green oxidant O_2 under mild conditions for deep delignification. Furthermore, as the typical strong base (NaOH) and milder base (Na_2CO_3), their effects on the oxidative degradation of biomass were compared for the first time by analyzing the degradation products.

4.2. Experimental Section

4.2.1. Experimental materials

The Japanese cedar (850 μm-2 mm) was used as raw material. The compositional analysis of cedar showed that it is composed of 43.11% glucose, 6.23% xylose, 1.88% galactose, 6.35% mannose, 1.86% arabinose, 36.69% lignin, and 0.32% ash (based on the dry base). The five monosaccharides (glucose, xylose, arabinose, galactose, mannose), organic acids, model compounds, NaOH and Na_2CO_3 were obtained from Wako Pure Chemical Industries, Ltd or Tokyo Chemical Industry.

4.2.2. Hydrothermal extraction and alkaline wet oxidation

Cedar was hydrothermally treated in a flow-through percolator (**Figure 4.1A**) using water flow of 5 mL/min under 5 MPa. The temperature was increased stepwise from 80 to 260 °C with a holding time of 30 min at each temperature in non-isothermal operation. The outlet samples of each temperature were collected separately. In isothermal operation, the reaction temperature was constant throughout the operation at 180 °C and the extracted

solution was collected every 10 min.

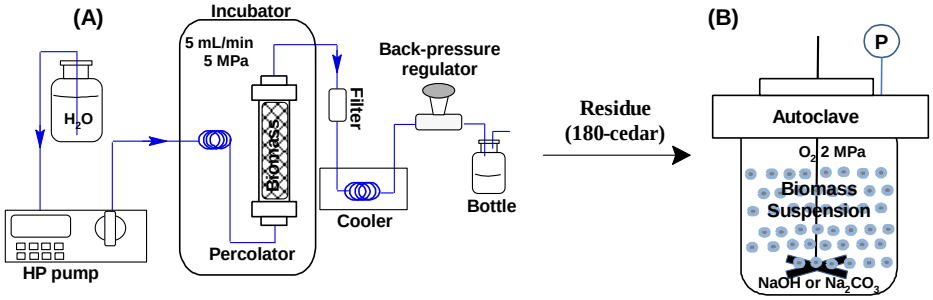

Figure 4.1. The devices of hydrothermal extraction (A) and alkaline wet oxidation (B).

After hydrothermal extraction at 180 ℃ for 60 min, the solid residues (180-cedar) were collected and dried as the feed for downstream alkaline wet oxidation. Specifically, 2 ±0.1 g 180-cedar was treated in an autoclave (**Figure 4.1B**) using 0.8 mol/L NaOH or Na_2CO_3 solution at 90 or 120 ℃ under 2 MPa O_2 for 8 h. The liquid-solid ratio was varied from 10-20 mL/g. The specific experimental conditions are shown in **Table 4.1**.

4.2.3. Characterization of products

For the hydrothermal extraction, monosaccharides in effluent were quantitatively analyzed by high-performance liquid chromatography (HPLC, Shimadzu LC-20 prominence series, Shodex SUGAR SP0810) after filtration with 0.45 μm PTFE membrane filter. The yield of oligosaccharides was calculated by the difference of monosaccharides in effluent before and after hydrolysis (4% H_2SO_4 at 121.0 ℃ for 1 h). The molecular weight distribution of oligosaccharides was determined by size exclusion chromatography (SEC) equipped with series columns of Shodex KS-801, KS-802, and KS-803. Monosaccharides (150–180 Da), cellobiosan (342 Da), cellotriosan (504 Da), and a series of pullulan (1080–47100 Da) were used as standards. The effluent pH was recorded by pH meter D-71 (Horiba Ltd., Japan). The total amount of organic carbon in the effluent was quantified by a total organic carbon analyzer (TOC, Shimadzu, TOC-5000A).

After alkaline wet oxidation, the suspension was filtered to get filtrate which was further adjusted to pH < 2 to precipitate acid-insoluble lignin (AI-L). The AI-L was washed by HCl solution (pH < 2), dried in vacuum (60 ℃, 24 h), weighed, and finally characterized by SEC (TSKgel G3000H + G2000H + G1000H)XL columns). The organic acids in the acidic filtrate were quantified by HPLC equipped with Aminex HPX-87H Ion Exchange column 300 × 7.8 mm (Bio-Rad, United States). Other small molecule degradation products

(such as pentacyclic compounds and aromatic aldehydes) and acid-soluble lignin (AS-L) fragments in acidic solution were sufficiently extracted by ethyl acetate. The volatile small molecule products were quantified by gas chromatography (GC, Shimadzu, GC-2030) and the AS-L fragments were characterized by SEC. The residue was thoroughly washed with hot ultrapure water until neutralization for further drying and compositional analysis. The morphological feature of residues was characterized by a scanning electron microscope (SEM, Keyence model VE-9800).

Chemical compositions (glucan, xylan, arabinan, galactan, mannan, and lignin) of the solid residues were determined by the National Renewable Energy Laboratory (NREL) method. The yields of monosaccharides, cellulose, hemicellulose, and lignin in the residue were calculated by Eqs. (1)-(4). In particular, all contents are based on a dry ash-free basis.

$$\text{Cellulose in residue(wt\%)} = \frac{\text{mass of glucose} \times 0.9}{\text{mass of the initial feed}} \times 100\% \quad (1)$$

$$\text{Lignin in residue(wt\%)} = \frac{\text{mass of the total lignin}}{\text{mass of the initial feed}} \times 100\% \quad (2)$$

$$\text{Monosaccharide(wt\%)} = \frac{\text{mass of monosaccharide (xylose/arabinose} \times 0.88 \text{ or mannose/galactose} \times 0.9)}{\text{mass of the residues}} \times 100 \quad (3)$$

$$\text{Hemicellulose in residue(wt\%)} = \text{xylose} + \text{arabinose} + \text{mannose} + \text{galactose} \quad (4)$$

4.3. Results and Discussion

4.3.1. The hydrothermal extraction

4.3.1.1 Hemicellulose dissolution process

The non-isothermal experiment was performed to check the temperature dependency and choose an appropriate temperature for the isothermal mode. The extraction of hemicellulose can be associated with the yield of its main component of mannan, arabinan, and xylan. As shown in **Figure 4.2c**, these oligosaccharides yields are obviously affected by temperature. The hydrothermal extraction of hemicellulose began at 140 ℃ and then peaked at 160 ℃, and eventually solubilized completely at 200 ℃. Among the hemicellulose-constituting sugars, arabinose and galactose were mainly dissolved as monosaccharides. The xylose and mannose were mainly isolated in oligomeric form between 150 to 180 ℃ indicating that they were mainly present in the backbone of hemicellulose. Cellulose started to be severely hydrolyzed to glucose above 200 ℃. It is, therefore, necessary to select an appropriate operating temperature for recovering hemicellulose and avoiding loss of cellulose, such as 180 ℃.

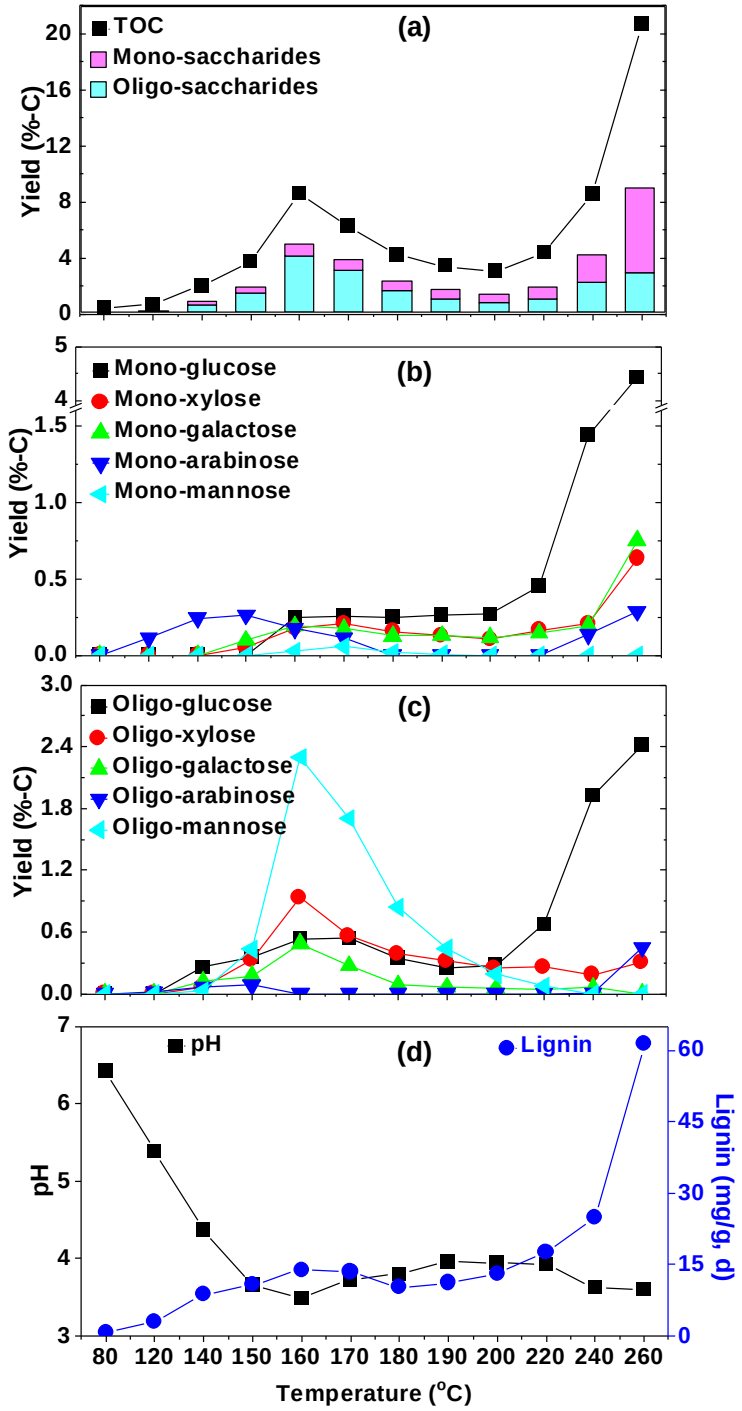

Figure 4.2. The non-isothermal mode of hydrothermal extraction. (a) Total carbon yield of mono- or oligosaccharides; (b) Carbon yields of monosaccharides; (c) Carbon yields of oligosaccharides; (d) The pH of effluent and the lignin yield (mg/g raw cedar).

The pH of effluent decreased rapidly with increasing temperature with a minimum of 3.6 at 160 ℃ and then increased slowly with temperature, eventually reached a lower value at the end of the experiment. The reduction of pH is directly related to the deacylation of hemicellulose and the degradation of sugars at elevated temperatures. [19] As shown in

Figure 4.2d, the dissolution of lignin is consistent with that of carbohydrates indicating that they are in the form of lignin-carbohydrates combinations.

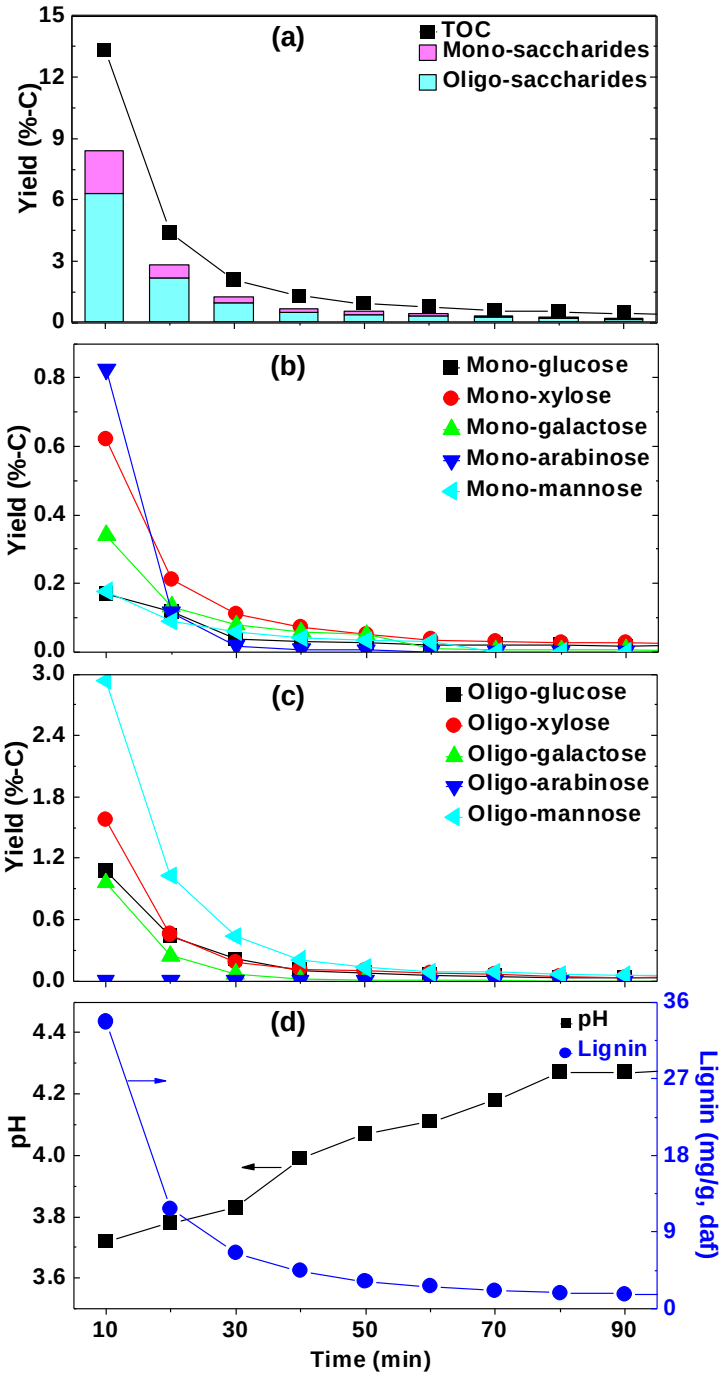

Figure 4.3. The isothermal mode of hydrothermal extraction. (a) Total carbon yield of mono- or oligosaccharides; (b) Carbon yields of monosaccharides; (c) Carbon yields of oligosaccharides; (d) The pH of effluent and the lignin yield (mg/g raw cedar).

The results of isothermal mode (**Figure 4.3**) show that the hemicellulose can be effectively recovered in 60 min at 180 ℃. Hemicellulose was primarily recovered as

oligosaccharides, and more than 90% of glucan was preserved in residues. In detail, 86.0% of mannose was mainly recovered as oligosaccharides, while all arabinose was recovered as monosaccharides. The dissolved glucose is mainly attributed to the hydrolysis of hemicellulose and the amorphous regions of cellulose. Generally, the amorphous regions of the cellulose are degraded at considerably lower temperatures compared to the polymorphic parts. [22] 15.7% lignin was simultaneously dissolved due to the covalent cross-linkages to hemicellulose. [22]

4.3.1.2 Molecular weight of extracted hemicelluloses

The molecular weight of extracted oligosaccharides is very important because this affects its further utilization and also is conducive to reveal its degradation behaviors.

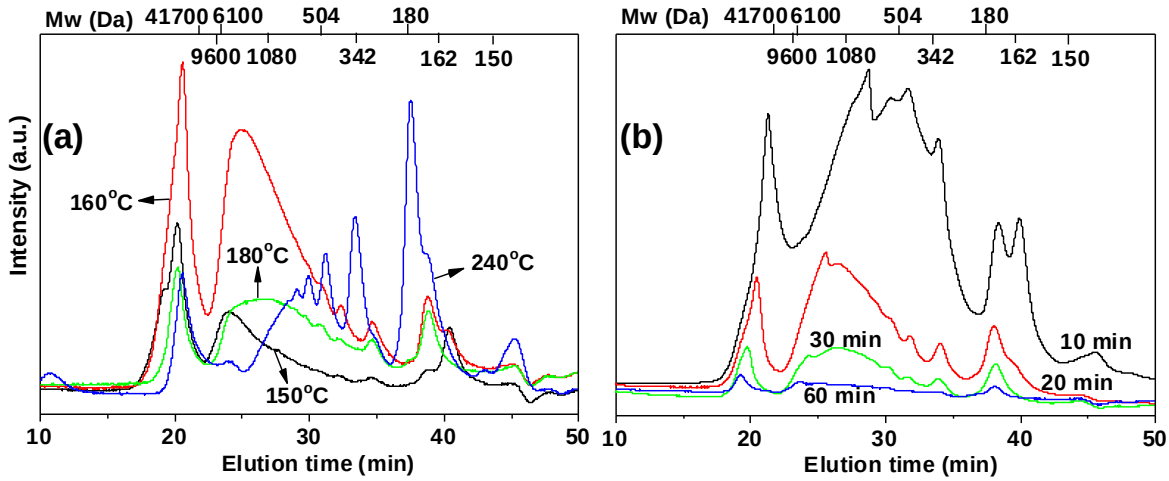

Figure 4.4. The molecular weight of extracted hemicelluloses. (a) Hemicellulose was extracted by non-isothermal mode; (b) Hemicellulose was extracted by isothermal mode.

The molecular weight of extracted hemicelluloses gradually decreased with the increase of temperature due to the intense rupture of glycosidic ether linkages in oligosaccharides. [23] As shown in **Figure 4.4**, a large part of hemicelluloses has molecular weight of more than 10,000 Da at 150 °C. The proportion of oligosaccharides with molecular weight < 1000 Da was significantly increased when temperature increased to 180 °C. The monosaccharides with molecular weight <180 Da mainly are xylose and arabinose. The discharge of hemicelluloses with relatively high molecular weight can be explained by the severe interruption of the holocellulose macrostructure. [24] According to the results of **Figure 4.2** and **Figure 4.4**, it is can be concluded that the main product was glucose oligomers with a degree of polymerization less than 10 when cellulose was

hydrolyzed at 240 ℃. The molecular weight of hemicellulose isothermally extracted at 180 ℃ was mostly between 200 to 10000 Da. These hemicellulose polysaccharides were generally considered to have high industrial value as manufacturing of food additives, emulsifiers, plastic film for foods, or superabsorbent hydrogels. [19] A large amount of relatively small oligosaccharides (molecular weight <1080 Da) were extracted at beginning 10 min indicating that some hemicellulose fragments having small molecular weight are easily extracted. Mannose is the dominant sugar in polysaccharides illustrating that cedar is a good source of mannan-oligosaccharides. Studies found that mannan-oligosaccharides have excellent performance in the biomedical field, such as, as a dietary supplement of glyconutrient for human health, as raw material for the synthesis of drug delivery systems, as bioactive material conjugated to the vaccine for cancer immunotherapy, as antiadhesion coating against fungal growth, etc. [20, 25] It also has been widely used as a supplement for increasing the quality of pets and livestock. [26]

4.3.2. Alkaline wet oxidation

4.3.2.1 Residues composition

The composition of residues and pH of suspension after alkaline wet oxidation are illustrated in **Table 4.1**. Cellulose was well enriched in residues due to the removal of lignin and hemicellulose. Increasing the amount of alkaline and treatment time significantly increased the lignin removal, but caused more loss of cellulose. For NaOH, the lignin removal increased from 72.5 to 86.8%, whereas cellulose retention decreased from 76.2 to 55.6% after the liquid-solid ratio increased from 10 to 15 mL/g. However, there was no significant difference in the pH (8.6−8.9) of suspensions, indicating that NaOH in the reaction system was consumed. Using the liquid-solid ratio of 20 mL/g resulted in further lignin removal without a further loss of cellulose and the pH of the suspensions rose to 12.9. It is indicated that sufficient alkalinity (pH >12) is necessary for efficient removal of lignin and the remaining cellulose in the residue is extremely recalcitrant. Finally, 91.3% lignin and all hemicellulose were removed, as well as a residue containing 85.5% glucose was obtained using 0.8 mol/L of NaOH at 90 ℃ for 8h.

Table 4.1. Residues composition (wt.%, daf) and pH of suspension.

Samples	Lignin [a]	Sugar [b]			pH
	TL	Glucan	Xylan	Mannan	
Hydrothermal extraction- 180 ℃, H_2O, 5 mL/min, 40 min, 5 Mpa					
180-Cedar	41.27 (15.7)	53.46 (92.9)	2.84 (34.1)	1.18 (14.0)	4.11
Alkaline wet oxidation - NaOH, 90 ℃, 0.8 mol/L, 20 mL/g, 2 Mpa, 8 h, O_2					
10 mL/g	22.47 (72.5)	73.20 (76.2)	1.34 (9.6)	0.49 (3.5)	8.64
15 mL/g	16.95 (86.8)	83.78 (55.6)	-	-	8.91
4 h	23.04 (76.4)	77.09 (67.1)	-	-	13.05
8 h	11.50 (91.3)	85.45 (55.2)	-	-	12.97
Alkaline wet oxidation - Na_2CO_3, 90 ℃, 0.8 mol/L, 20 mL/g, 2 Mpa, 8 h, O_2					
10 mL/g	33.65 (49.4)	64.53 (82.6)	1.93 (17.1)	0.51 (4.4)	9.85
20 mL/g	32.42 (52.8)	63.89 (79.1)	1.43 (12.3)	0.39 (3.3)	9.56
1.5 mol/L	31.04 (57.5)	66.59 (77.6)	1.03 (8.3)	0.27 (2.1)	9.97
120°C-4 h	14.63 (89.5)	69.72 (50.1)	-	-	8.80
120°C-8 h	1.99 (98.9)	98.88 (49.1)	-	-	8.71

[a]The data in parentheses show the removal rate of lignin (based on the lignin in cedar); [b]The data in parentheses show the retention rates of carbohydrates (based on the carbohydrates in cedar); - Not detected; TL is the total lignin.

For Na_2CO_3, the removal efficiency of lignin was not significantly improved either by increasing Na_2CO_3 concentration or liquid-solid ratio at 90 ℃, but it was significantly improved by increasing temperature to 120 ℃. Increasing Na_2CO_3 concentration (0.8 to 1.5 mol/L) and liquid-solid ratio (10 to 20 mL/g) at 90 ℃ increased the lignin removal by 4.7% and 3.4%, respectively. The lignin removal reached 98.9% generating a high-cellulose content residue (98.9%) after temperature increased to 120 ℃. The pH of suspensions was always below 10 with no significant change probably because a large amount of HCO_3^- was generated in the solution due to the generation of CO_2 and organic acids. The carbonates and bicarbonates in solution played a buffer role in stabilizing the pH value. The Na_2CO_3 can be recycled as long as the organic substances in solution are utilized by catalytic hydrothermal reforming. [27] The carbonates recovery without causticization and calcination is much simpler than that of NaOH. [28] Na_2CO_3 preserved more cellulose than NaOH at 90 ℃. Although the use of Na_2CO_3 greatly reduced the alkalinity of the reaction system, it did not prevent a large loss of glucan at 120 ℃. The glucan retention in residue decreased from 79.1% at 90 ℃ to 49.1% at 120 ℃. High-purity cellulose contenting 98.9% glucan was obtained

using Na_2CO_3 solution at 120 ℃. Yang et al. [29] treated cornstalk with ionic liquid at 100 ℃ and then washed the residue with acetone and water for high-purity cellulose (99.1%). Roselli et al. [30] reported that a high purity pulp (98%) was obtained by upgrading the eucalyptus kraft pulp using endoxylanase and ionic liquid. In another paper, Liu et al. [31] isolated the high-purity cellulose (94.2%) from wheat straw through a multistep treatment process including steam explosion, acid prehydrolysis, microwave-assisted hydrolysis, and microfluidization. Therefore, this study used water, oxygen, and Na_2CO_3 under mild conditions (120 ℃) to recover high-purity cellulose, which is much more environmental and economical than previous reports.

4.3.2.2 Morphology analysis of representative solids

The morphological features (**Figure 4.5**) show that the cedar macrostructure hardly changed after hydrothermal treatment, but the color changed to dark brown. After further alkaline wet oxidation by NaOH at 90 ℃ for 8 h, a light brown and rigid solid residue was obtained after drying.

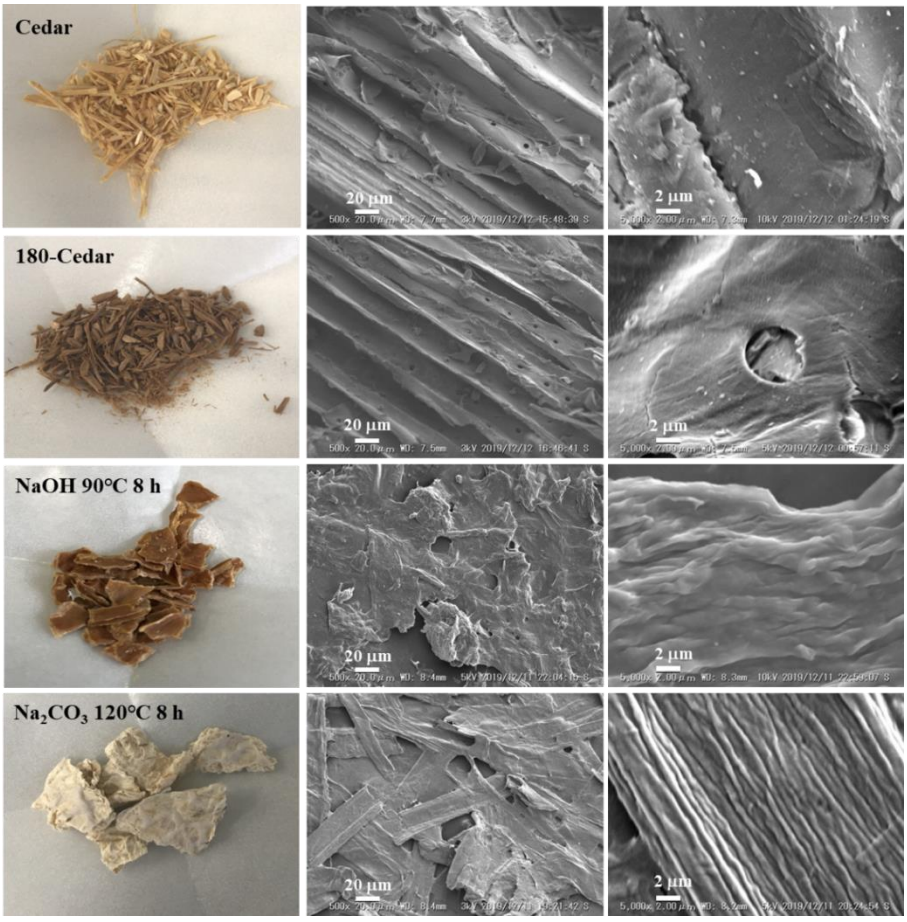

Figure 4.5. Photographs and SEM images of cedar, 180-cedar and representative residues.

The residue obtained by Na_2CO_3 at 120 ℃ for 8 h is a relatively fluffy and soft cellulose cake with a bright white color. SEM images show that the surface structure of raw cedar is compact and regular with some flakes of channels wall. Hydrothermal extraction hardly caused destruction on its regular mechanical structure and surface. Alkaline wet oxidation completely damaged its mechanical structure after substantial removal of lignin, resulting in thin flakes of debris. NaOH produced small and flaky debris with an irregular fibrous surface, while Na_2CO_3 obtained relatively large regular fiber ribbons with regular fiber bundles surface. NaOH caused severe etching and fiber breakage, while the Na_2CO_3 preserved long fibers. These regular fiber ribbons came from the peeling of channels wall with a width of about 25 μm. These regular fiber ribbons are completely different from the fiber bundles obtained from corn stover by Karp [2] and Pang [32].

4.3.2.3 The degradation products analysis

About 65 wt% of 180-cedar were degraded by NaOH at 90 ℃ in 8 h (**Figure 4.6**). Na_2CO_3 dissolved about 30 wt% of feed at 90 ℃ and it reached more than 70 wt% at 120 ℃. It shows that Na_2CO_3 requires higher temperature to achieve a similar performance as NaOH. More AI-L was precipitated from NaOH solution than that of Na_2CO_3. The water soluble substances (as water soluble part in **Figure 4.6**) after acidification are small molecular products produced by oxidative degradation, mainly including organic acids and small lignin fragments. [33]

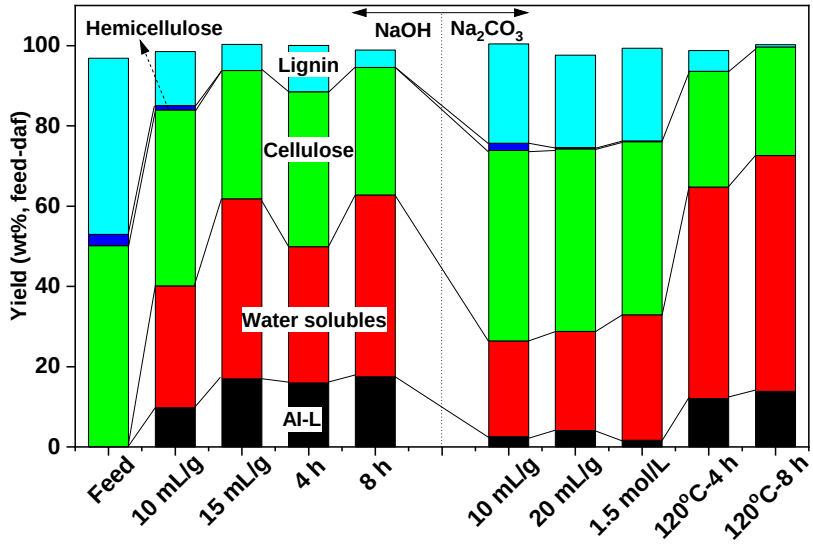

Figure 4.6. The components composition of products. (Reference condition: The 180-cedar was oxidative alkaline treated by 0.8 mol/L NaOH or Na_2CO_3 at 90 ℃ for 8 h with a solid-liquid ratio of 20 mL/g; Components composition is based on the dry ash-free feed.)

For better understanding, lignin was divided into three parts after dissolution and oxidative degradation: the lignin in the residue (R-L), the AI-L, and severely degraded lignin (SD-L, products of severe lignin degradation including AS-L fragments and small molecule degradation products). The yield of SD-L was obtained by the difference method. According to the distribution of lignin (**Figure 4.7**), most of the lignin dissolved in alkaline solution was severely degraded into small molecular fragments, organic acids, and aromatic aldehydes which are soluble in an acidic environment, and the other part is AI-L which is considered as the large molecular fragments of lignin. The degradation ratio (DR) of dissolved lignin was defined as DR(%)=100%-(AI-L)/(the total dissolved lignin)×100%, which was used to evaluate the degradation of lignin during alkaline wet oxidation. A high DR indicates that more dissolved lignin was oxidatively degraded.

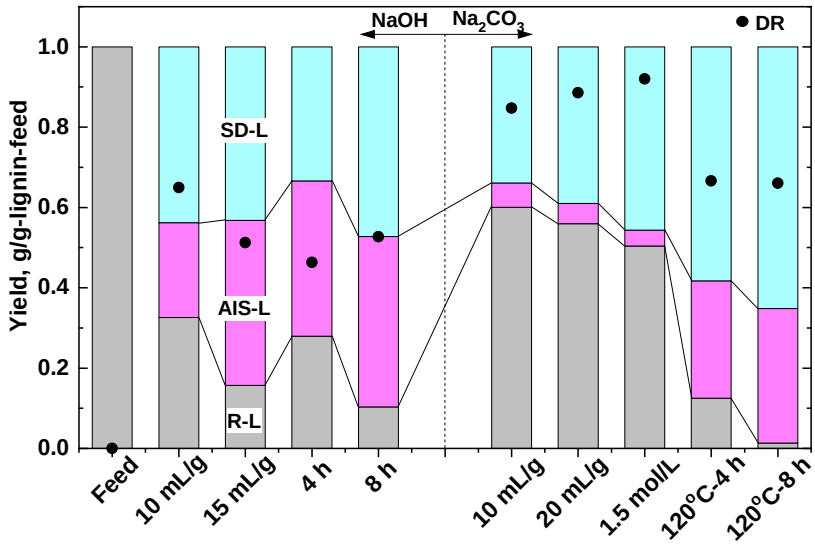

Figure 4.7. The conversion of lignin. (Reference condition: The 180-cedar was oxidative alkaline treated by 0.8 mol/L NaOH or Na_2CO_3 at 90 ℃ for 8 h with a solid-liquid ratio of 20 mL/g; Lignin distribution is based on the total amount of lignin in the feed.)

The DR of lignin dissolved in NaOH slightly decreased from 65.0% to 51.3% after the liquid-solid ratio increased from 10 to 20 mL/g, indicating that the lignin dissolved first is more easily depolymerized and degraded than the dissolved after that. Another possible reason is that the depolymerization of lignin is always accompanied by its repolymerization and condensation. [34] More than 80% lignin dissolved by Na_2CO_3 at 90 ℃ was degraded. The DR of lignin reached 92.0% when 1.5 mol/L Na_2CO_3 was used at 90 ℃. Obviously, the depolymerization and oxidation of lignin are dominant reactions during the lignin removal, although it is still unclear whether the reactions mainly occurred before or after lignin

removal from the matrix. It is, anyway, an attractive strategy to directly depolymerize lignin in the solid-state from biomass, which can avoid serious condensation and passivation of lignin during the separation process. The DR of lignin decreased to about 66% due to the dissolution of more refractory lignin at 120 ℃. Although prolonging treatment time resulted in more lignin dissolution, the DR of lignin did not significantly reduce due to the further degradation of lignin. From these results, it can be concluded that the use of Na_2CO_3 is more conducive to the depolymerization of lignin during the removal process than NaOH. As a biodegradable polymer material, small lignin fragments have great potential application in the manufacture of various chemicals and functional materials. [35]

A typical product of alkaline wet oxidation is organic acid, such as formic, acetic, lactic, oxalic, glycolic, malonic, and succinic acids, and their yields are shown in **Figure 4.8.** Carbohydrates (monosaccharides and polysaccharides) and their derivatives (5-hydroxymethyl-2-furaldehyde and 2-furaldehyde) can be oxidized to produce organic acids. [14, 36] The oxidation of lignin also produces a large amount of organic acids. [37] Hasegawa et al. [35] proposed that the succinic acid was derived from the rupturing of the aromatic ring, whereas formic and acetic acids were formed from the oxidative degradation of aliphatic side chains.

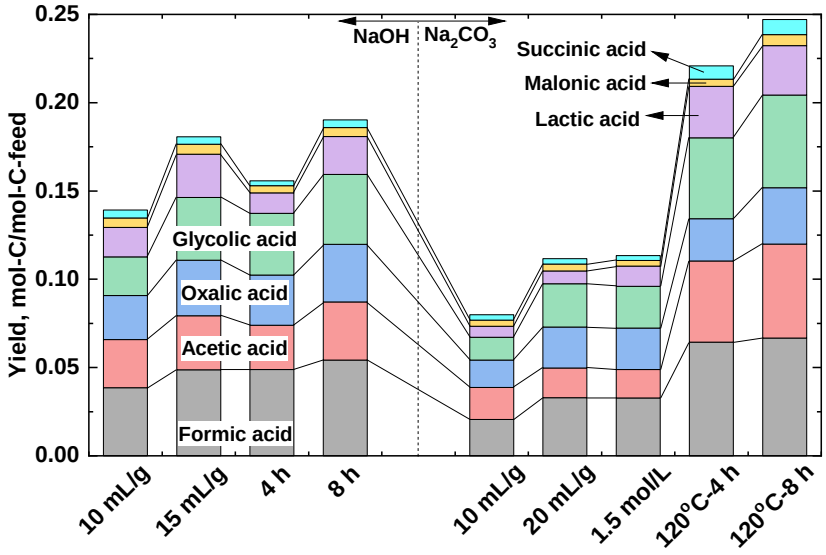

Figure 4.8. The organic acids yields. (Reference condition: The 180-cedar was oxidative alkaline treated by 0.8 mol/L NaOH or Na_2CO_3 at 90 ℃ for 8 h with a solid-liquid ratio of 20 mL/g; Organic acid yield is based on the total carbon in the feed.)

The similar distribution of organic acids indicates that organic acids are formed in the

same way in NaOH and Na_2CO_3 solutions. The hydroxyl radicals and hydroperoxide anions formed by oxygen electron-transfer in alkaline solution are considered as the direct oxidant. [38] The yield of organic acids reached 19.0%-C using NaOH which is much higher than that (11.2%-C) of using Na_2CO_3 at 90 ℃ in 8 h. The yield of organic acids increased to 24.7%-C when the temperature increased to 120 ℃. These organic acids obtained by direct oxidation of biomass with molecular O_2 are valuable chemicals and they are one of the potential target products to achieve high value-added utilization of biomass.

4.3.2.4 Molecular weight distribution of AI-L and AS-L

As described above, a part of dissolved lignin was depolymerized into AS-L fragments. In order to further understand the depolymerization behaviors of lignin, their molecular weight was characterized and the results are shown in **Figure 4.9**.

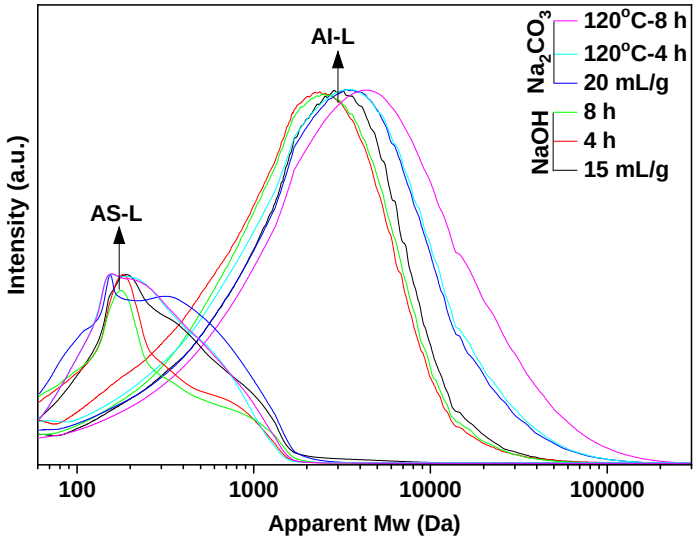

Figure 4.9. Molecular weight distribution of AI-L and AS-L obtained under different experimental conditions. (Reference condition: The 180-cedar was oxidative alkaline treated by 0.8 mol/L NaOH or Na_2CO_3 at 90 ℃ for 8 h with a solid-liquid ratio of 20 mL/g.)

The molecular weight of AI-L is mainly between 1000 to 100000 Da which is much larger than that of the AS-L fragments (< 2000 Da). The AI-L and AS-L fragments obtained by Na_2CO_3 solution was significantly larger than that produced by NaOH solution. The possible reason is that the alkalinity of NaOH is stronger than that of Na_2CO_3 causing more severe fracture of the linkages between lignin units. AS-L fragments outputted by NaOH solution have a distinct peak between 100-200 Da due to the formation of monophenolic compounds, such as the aromatic aldehydes mentioned later. However, the AS-L fragments

yielded by Na_2CO_3 have a relatively broad molecular weight distribution. The AS-L fragments > 300 Da were significantly reduced due to further depolymerization at a high temperature (120 °C). For NaOH solution, the molecular weight of AI-L increased slightly when reaction time extended from 4 h to 8 h, indicating that the re-polymerization between lignin fragments was very weak under the milder condition at 90 °C. For the Na_2CO_3 solution, the molecular weight of AI-L increased significantly with increasing temperature and prolonging treatment time, indicating that the re-polymerization between lignin fragments intensely occurred at 120 °C.

4.3.2.5 Pentacyclic compounds and aromatic aldehydes

Trace amounts of small molecular compounds (**Figure 4.10**) were produced during oxidative degradation, such as pentacyclic compounds from carbohydrates and aromatic aldehydes from lignin. [14, 33] Such low yields of these compounds indicate that the conversion of biomass to organic acids under such conditions has a high selectivity.

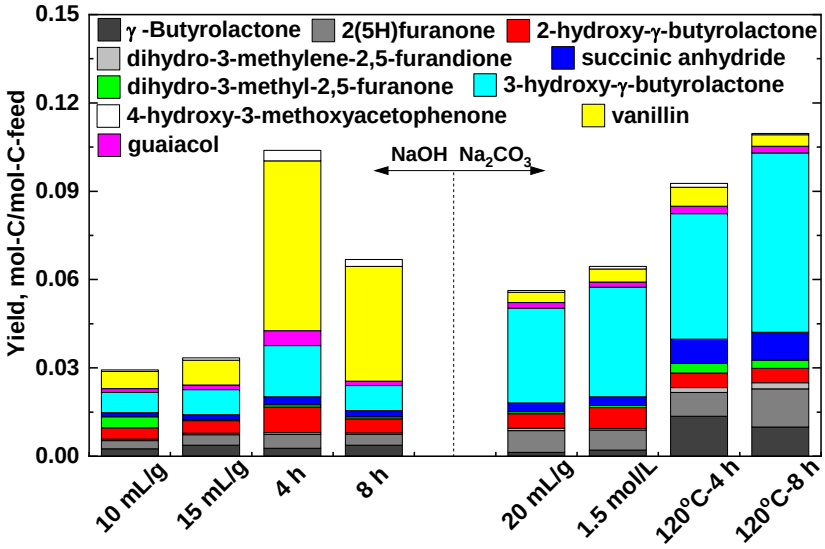

Figure 4.10. The yields of pentacyclic compounds and aromatic aldehydes obtained under different experimental conditions. (Reference condition: The 180-cedar was oxidative alkaline treated by 0.8 mol/L NaOH or Na_2CO_3 at 90 °C for 8 h with a solid-liquid ratio of 20 mL/g.)

More 3-hydroxy-γ-butyrolactone was produced using Na_2CO_3, while more aromatic aldehydes (especially vanillin) were generated using NaOH. Most compounds decreased with time in NaOH solution but increased in Na_2CO_3 solution indicating that NaOH promoted the further degradation of these compounds more than that of Na_2CO_3. A

reduction trend was clearly observed in the yield of these lignin monomers with time in both solutions, indicating that they are easy to be further degraded. Both the formation and degradation of lignin monomers simultaneously happened. [33, 37] It is the main reason why the lignin monomers yield was very low despite a large amount of lignin was depolymerized during alkaline wet oxidation.

4.4. Conclusions

The integrated approach combining hydrothermal extraction for recovering hemicellulose as oligosaccharides and alkaline wet oxidation for lignin removal and depolymerization, is a promising strategy for the high-purity cellulose. Most hemicelluloses in cedar were recovered as mannose-oligosaccharides before the subsequent alkaline wet oxidation which removed 98.9% lignin using Na_2CO_3 at 120 ℃. Although NaOH effectively removed lignin at lower temperatures (90 ℃), the Na_2CO_3 was more conducive to depolymerize lignin and preserve the longer fibers than NaOH. Large amounts of organic acids were generated from lignin and carbohydrates degradation. Ultimately, the high-purity cellulose contenting 98.8% glucose was recovered.

4.5. References

[1] J.S. Kim, Y.Y. Lee, T.H. Kim, A review on alkaline pretreatment technology for bioconversion of lignocellulosic biomass, *Bioresource Technol.*, 199 (2016) 42-48.

[2] E.M. Karp, B.S. Donohoe, M.H. O'Brien, P.N. Ciesielski, A. Mittal, M.J. Biddy, G.T. Beckham, Alkaline pretreatment of Corn stover: Bench-scale fractionation and stream characterization, *ACS Sustainable Chem. Eng.*, 2 (2014) 1481-1491.

[3] J. Shi, Q. Yang, L. Lin, The structural features of hemicelluloses dissolved out at different cooking stages of active oxygen cooking process, *Carbohydr. Polym.*, 104 (2014) 182-190.

[4] Q. Zheng, T. Zhou, Y. Wang, X. Cao, S. Wu, M. Zhao, H. Wang, M. Xu, B. Zheng, J. Zheng, X. Guan, Pretreatment of wheat straw leads to structural changes and improved enzymatic hydrolysis, *Sci. Rep.*, 8 (2018) 1321.

[5] Z. Yuan, Y. Wen, Evaluation of an integrated process to fully utilize bamboo biomass during the production of bioethanol, *Bioresource Technol.*, 236 (2017) 202-211.

[6] Q. Wang, S. Xiao, S.Q. Shi, L. Cai, Microwave-assisted formic acid extraction for high-purity cellulose production, *Cellulose*, 26 (2019) 5913-5924.

[7] S.C. Qi, L. Zhang, S. Kudo, J.-i. Hayashi, Catalytic hydrogenolysis of Kraft lignin to

monomers at high yield in alkaline water, Green Chemistry, 19 (2017) 11.

[8] N. Li, Y. Li, C.G. Yoo, X. Yang, X. Lin, J. Ralph, X. Pan, An uncondensed lignin depolymerized in the solid state and isolated from lignocellulosic biomass: a mechanistic study, *Green Chem.*, 20 (2018) 4224-4235.

[9] F.C. Oliveira, K. Srinivas, G.L. Helms, N.G. Isern, J.R. Cort, A.R. Goncalves, B.K. Ahring, Characterization of coffee (Coffea arabica) husk lignin and degradation products obtained after oxygen and alkali addition, *Bioresource Technol.*, 257 (2018) 172-180.

[10] C. Zhang, H. Li, J. Lu, X. Zhang, K.E. MacArthur, M. Heggen, F. Wang, Promoting lignin depolymerization and restraining the condensation via an oxidation−hydrogenation strategy, *ACS Catal.*, 7 (2017) 3419-3429.

[11] R. Ma, M. Guo, X. Zhang, Recent advances in oxidative valorization of lignin, *Catal. Today*, 302 (2018) 50-60.

[12] G. Lyu, C.G. Yoo, X. Pan, Alkaline oxidative cracking for effective depolymerization of biorefining lignin to mono-aromatic compounds and organic acids with molecular oxygen, *Biomass Bioenerg.*, 108 (2018) 7-14.

[13] S. An, W. Li, Q. Liu, Y. Xia, T. Zhang, F. Huang, Q. Lin, L. Chen, Combined dilute hydrochloric acid and alkaline wet oxidation pretreatment to improve sugar recovery of corn stover, *Bioresource Technol.*, 271 (2019) 283-288.

[14] H.B. Klinke, B.K. Ahring, A.S. Schmidt, A.B. Thomsen, Characterization of degradation products from alkaline wet oxidation of wheat straw, *Bioresource Technol.*, 82 (2002) 12.

[15] H.R. Lee, R.J. Kazlauskas, T.H. Park, One-step pretreatment of yellow poplar biomass using peracetic acid to enhance enzymatic digestibility, *Sci. Rep.*, 7 (2017) 12216.

[16] X. Chen, R. Katahira, Z. Ge, L. Lu, D. Hou, D.J. Peterson, M.P. Tucker, X. Chen, Z.J. Ren, Microbial electrochemical treatment of biorefinery black liquor and resource recovery, *Green Chem.*, 21 (2019) 1258-1266.

[17] A.T. Hendriks, G. Zeeman, Pretreatments to enhance the digestibility of lignocellulosic biomass, *Bioresource Technol.*, 100 (2009) 10-18.

[18] A.C. Ruthes, A. Mart ńez-Abad, H.T. Tan, V. Bulone, F. Vilaplana, Sequential fractionation of feruloylated hemicelluloses and oligosaccharides from wheat bran using subcritical water and xylanolytic enzymes, *Green Chem.*, 19 (2017) 1919-1931.

[19] G. Gallina, E.R. Alfageme, P. Biasi, J. Garcia-Serna, Hydrothermal extraction of

hemicellulose: from lab to pilot scale, *Bioresource Technol.*, 247 (2018) 980-991.

[20] W. Farhat, R.A. Venditti, M. Hubbe, M. Taha, F. Becquart, A. Ayoub, A review of water-resistant hemicellulose-based materials: Processing and applications, *ChemSusChem*, 10 (2017) 305-323.

[21] M.G. Ma, N. Jia, J.F. Zhu, S.M. Li, F. Peng, R.C. Sun, Isolation and characterization of hemicelluloses extracted by hydrothermal pretreatment, *Bioresource Technol.*, 114 (2012) 677-683.

[22] T. Ingram, T. Rogalinski, V. Bockemühl, G. Antranikian, G. Brunner, Semi-continuous liquid hot water pretreatment of rye straw, *J. Supercrit. Fluid.*, 48 (2009) 238-246.

[23] C. Wang, J. Yang, J. Wen, J. Bian, M. Li, F. Peng, R. Sun, Structure and distribution changes of Eucalyptus hemicelluloses during hydrothermal and alkaline pretreatments, *Int. J. Biol. Macromol.*, 133 (2019) 514-521.

[24] W. Farhat, R. Venditti, A. Quick, M. Taha, N. Mignard, F. Becquart, A. Ayoub, Hemicellulose extraction and characterization for applications in paper coatings and adhesives, *Ind. Crop. Prod.*, 107 (2017) 370-377.

[25] X. Hu, Y. Shi, P. Zhang, M. Miao, T. Zhang, B. Jiang, d-Mannose: Properties, production, and applications: An overview, *Compr. Rev. Food Sci. F.*, 15 (2016) 773-785.

[26] C. Nopvichai, T. Charoenwongpaiboon, N. Luengluepunya, K. Ito, C. Muanprasat, R. Pichyangkura, Production and purification of mannan oligosaccharide with epithelial tight junction enhancing activity, *PeerJ*, 7 (2019) e7206.

[27] S. Kudo, Y. Hachiyama, Y. Takashima, J. Tahara, S. Idesh, K. Norinaga, J.-i. Hayashi, Catalytic hydrothermal reforming of lignin in aqueous alkaline medium, *Energ. Fuel*, 28 (2013) 76-85.

[28] W. Geng, T. Huang, Y. Jin, J. Song, H.M. Chang, H. Jameel, Comparison of sodium carbonate-oxygen and sodium hydroxide-oxygen pretreatments on the chemical composition and enzymatic saccharification of wheat straw, *Bioresource Technol.*, 161 (2014) 63-68.

[29] J. Yang, X. Lu, X. Liu, J. Xu, Q. Zhou, S. Zhang, Rapid and productive extraction of high purity cellulose material via selective depolymerization of the lignin-carbohydrate complex at mild conditions, *Green Chem.*, 19 (2017) 2234-2243.

[30] A. Roselli, M. Hummel, A. Monshizadeh, T. Maloney, H. Sixta, Ionic liquid extraction method for upgrading eucalyptus kraft pulp to high purity dissolving pulp, *Cellulose*,

21 (2014) 3655-3666.

[31] Q. Liu, Y. Lu, M. Aguedo, N. Jacquet, C. Ouyang, W. He, C. Yan, W. Bai, R. Guo, D. Goffin, J. Song, A. Richel, Isolation of High-purity cellulose nanofibers from wheat straw through the combined environmentally friendly methods of steam explosion, microwave-assisted hydrolysis, and microfluidization, *ACS Sustainable Chem. Eng.*, 5 (2017) 6183-6191.

[32] C. Pang, T. Xie, L. Lin, J. Zhuang, Y. Liu, J. Shi, Q. Yang, Changes of the surface structure of corn stalk in the cooking process with active oxygen and MgO-based solid alkali as a pretreatment of its biomass conversion, *Bioresource Technol.*, 103 (2012) 432-439.

[33] W. Schutyser, J.S. Kruger, A.M. Robinson, R. Katahira, D.G. Brandner, N.S. Cleveland, A. Mittal, D.J. Peterson, R. Meilan, Y. Román-Leshkov, G.T. Beckham, Revisiting alkaline aerobic lignin oxidation, *Green Chem.*, (2018).

[34] A. Toledano, L. Serrano, J. Labidi, Improving base catalyzed lignin depolymerization by avoiding lignin repolymerization, *Fuel*, 116 (2014) 617-624.

[35] I. Hasegawa, Y. Inoue, Y. Muranaka, T. Yasukawa, K. Mae, Selective production of organic acids and depolymerization of lignin by hydrothermal oxidation with diluted hydrogen peroxide, *Energ. Fuel*, 25 (2011) 791-796.

[36] F. Jin, H. Enomoto, Rapid and highly selective conversion of biomass into value-added products in hydrothermal conditions: chemistry of acid/base-catalysed and oxidation reactions, *Energy Environ. Sci.*, 4 (2011) 382-397.

[37] K. Srinivas, F. de Carvalho Oliveira, P.J. Teller, A.R. Gonalves, G.L. Helms, B.K. Ahring, Oxidative degradation of biorefinery lignin obtained after pretreatment of forest residues of Douglas Fir, *Bioresource Technol.*, 221 (2016) 394-404.

[38] Y. Jiang, X. Zeng, R. Luque, X. Tang, Y. Sun, T. Lei, S. Liu, L. Lin, Cooking with active oxygen and solid alkali: A promising alternative approach for lignocellulosic biorefineries, *ChemSusChem*, 10 (2017) 3982-3993.

CHAPTER 5

Mild Oxygen Oxidation of Rice Husk to Remove Lignin and Ash (Si) for Producing High-purity Pulp

5.1. Introduction

Rice husk (RH) is one of the main agricultural wastes by-produced from the rice production, and most of it is either burnt or dumped as waste. The annual production of rice husk in the world is about 1.2 billion tons, which is an attractive renewable resource for production of biofuels and biochemical as it can be collected easily from the rice production plant. [1] RH is mainly composed of ~35% cellulose, ~20% hemicellulose, ~28% lignin, ~15% ash with other substances. The silica in RH is mainly bonded to the hemicellulose molecules forming the silicon oxygen tetrahedral frameworks [$*Si(OSi)_4$], silanol groups ([$(OH)*Si(OSi)_3$]), and silanediol groups [$(OH)_2*Si(OSi)_2$]. [2] Its disposal is limited in many conversion technologies due to its hard shell, low digestibility, abrasiveness, low apparent density, and high ash contents. Combustion for energy supply and ash (SiO_2) collection is the traditional way of utilizing RH, however it generates a large amount of harmful gases and carcinogenic dust. [3]

Direct conversion of RH often leads to low yield of target products. Appropriate pretreatment of RH is necessary for delignification or deashing to partially disrupt its recalcitrant structure before further transformation. Some pretreatments of rice husk, including acid/alkaline, alkaline peroxide, hydrothermal, enzyme, and ionic liquid pretreatment, etc., promote its subsequent conversion for saccharification or bioethanol. [4] Hydrothermal treatment of biomass is an excellent technology to recover most of the hemicellulose using hot water. [5] The alkaline wet oxidation achieves effective removal of lignin from biomass. [6] It has been reported that the amorphous silica in rice husk ash has good solubility in alkaline solutions with pH > 10, which provide an inspiration for the removal of silicon from RH by alkaline solution. [7]

Cellulose is the most prevalent and abundant natural polymer on earth and is widely used in ropes, sails, paper, building materials, and many other applications. [8] It currently comes mainly from woody biomass that is not consistently available at reasonable prices in the future. Therefore, the preparation of cellulose from agricultural byproducts will become increasingly attractive. [9] The isolation of cellulose fibers and even nanocrystals from RH is possible with the deep removed of other components (hemicellulose, lignin, and ash). Jeetah et al. [10] produced pulp for cardboard by treating RH using hydrogen peroxide and glacial acetic acid at 29 ℃ for 6-10 days. Johar et al. [11] prepared high-purity cellulose fibers (96%) from RH by alkaline (NaOH) and bleaching (acetic acid and aqueous chlorite)

treatments. Cellulose fibers are precursors to cellulose whiskers and nanofibers which have received a remarkable interest from many researchers. [9] The preparation of high-purity cellulose from RH is promising.

Kraft and Sulfite pulping are the dominant technologies for delignification in pulp and paper processing. In the conventional kraft pulp process, biomass is cooked at about 170 ℃ for few hours in an aqueous solution of NaOH and Na_2S. In the Sulfite process, the biomass is typically cooked with an aqueous magnesium bisulfite solution at a pH of either 1.5 or 4.0. [12] Sodium sulfide has a serious negative impact on the environment and the utilization of black liquor. [13, 14] Another popular technology is the soda pulping process which usually requires the addition of redox catalysts (anthraquinone) in the NaOH solution to accelerate delignification. [15] The resulting pulp needs to be bleached with chloride for further delignification.

The present study proposed a method to prepare high-purity cellulose from hydrothermally pretreated RH using Na_2CO_3 and O_2 under mild conditions. The effect of hydrothermal pretreatment on lignin and ash removal in the subsequent alkaline wet oxidation was investigated. Two types of reactors, the batch reactor and the percolator, were employed. The repeated use of Na_2CO_3 solution for lignin and ash removal was evaluated.

5.2. Experimental Section

5.2.1. Experimental materials

The RH used as raw material was obtained from Fukuka, Japan. The RH was washed with 80 ℃ H_2O to remove impurities and then crushed to 0.85−2 mm. The detailed chemical composition was given in Table 5.1. All chemicals including Na_2CO_3, NaOH, hydrochloric acid (HCl), and model compounds were purchased from Wako Pure Chemical Industries, Ltd or Tokyo Chemical Industry.

5.2.2. Hydrothermal pretreatment and alkaline wet oxidation

Hydrothermal pretreatment of RH was performed in a flow-through percolator which was described in **Chapter 4**. RH was treated by hot H_2O at 180 ℃ for 150 min under 5 MPa. The hydrothermally pretreated RH (HTRH) was dried at 60 ℃ under vacuum for 24 h and used as the feed for the subsequent alkaline wet oxidation.

Alkaline wet oxidation in batch reactor: Specifically, 2±0.1 g HTRH was treated in an autoclave using 1.0 mol/L Na_2CO_3 solution at 120 ℃ under 2 MPa O_2 for 120 min. Different times (120 vs. 180 min), temperatures (100, 120, and 140 ℃), O_2 pressures (2 vs. 3 MPa),

atmospheres (N_2 vs. O_2), and liquid-solid ratio (20 vs. 40 mL/g) were examined. For the reuse of the alkaline solution, 1 g HTRH and 40 mL filtrate from the previous operation were used in the autoclave at 120 ℃ under 2 MPa O_2 for 120 min. The experimental setup and detailed operations were described in **Chapter 4**. The detailed experimental conditions were summarized in **Table 5.1**.

Alkaline wet oxidation in percolator: 2±0.1 g feed was loaded into percolator and then continuously feed an oxygen-saturated Na_2CO_3 solution at 120 ℃ for 120 min. The Na_2CO_3 solution saturated with 2.0 MPa O_2 in a tank (volume; 1 L) at 120 ℃ before starting the experiment. The experimental setup and detailed operations were described in **Chapter 3**.

Table 5.1. Detailed experiment conditions of alkaline wet oxidation.

Experiment	Feed	Reactor	Atmosphere	Alkaline	Liquid/solid (mL/g)	Temperature (℃)	Time (min)
RH-OT	RH	Autoclave	O_2	Na_2CO_3	20	120	120
RH-OT-P	RH	Percolator	O_2	Na_2CO_3	5 mL/min	120	120
HTRH-OT	HTRH	Batch	O_2	Na_2CO_3	20	120	120
HTRH-OT-P	HTRH	Percolator	O_2	Na_2CO_3	5 mL/min	120	120
100 ℃+3 MPa+180 min	HTRH	Batch	O_2	Na_2CO_3	20	100	180
180 min	HTRH	Batch	O_2	Na_2CO_3	20	120	180
140 ℃	HTRH	Batch	O_2	Na_2CO_3	20	140	120
40 mL/g	HTRH	Batch	O_2	Na_2CO_3	40	120	120
HTRH-NaOH	HTRH	Batch	O_2	NaOH	20	120	120
HTRH-H_2O	HTRH	Batch	O_2	H_2O	20	120	120
HTRH-N_2	HTRH	Batch	N_2	Na_2CO_3	20	120	120

5.2.3. Characterization of products

After the experiment, the filtrate and the solid product (residue) were separated by filtration. The effluent pH was recorded by pH meter D-71 (Horiba Ltd., Japan). The filtrate was acidified and then the organic acids were quantified by high performance liquid chromatography (HPLC, Shimadzu LC-20 prominence series, Aminex HPX-87H Ion Exchange column). The residue was thoroughly washed with 80 ℃ H_2O until neutral. The solid residue was then characterized by scanning electron microscopy (SEM, Keyence model VE-9800), Fourier transform infrared (FTIR) spectroscopy, and X-ray diffraction (XRD, Rigaku, TTR-III). Chemical compositions (glucan, xylan, arabinan, galactan,

mannan, lignin, and ash) of the solid residues were determined by a standard analytical procedure of NREL. The yields of monosaccharides, cellulose, hemicellulose, and lignin in the residue were calculated according to the method described in **Chapter 4.**

5.3. Results and Discussion

5.3.1. Chemical composition of residue

The chemical composition of residue was analyzed and the results are presented in **Table 5.2.** The components yield of the residue based on raw RH are shown in the **Figure 5.1**. The original RH contained 31.4 wt% cellulose, 21.4 wt% hemicelluloses, 28.0 wt% lignin, and 15.5 wt% ash. The hydrothermal treatment removed 83.3% hemicellulose, 43.4% lignin, and 66.9% ash. The alkaline wet oxidation enriched cellulose in the solid residue as expected. After alkaline wet oxidation of RH (RH-OT), xylan, lignin, and ash in the residue were as high as 19.1, 14.3 and 5.9%, respectively, indicating that it is difficult to receive high-purity cellulose from raw RH. Using HTRH (HTRH-OT) reduced the xylan, lignin, and ash to 2.4, 4.2, and 3.2%, respectively. The hemicellulose, lignin, and ash in the HTRH are more easily removed after hydrothermal pretreatment than in the original RH. The main reason is the destruction of original stubborn structure of the RH. HTRH yielded the highest purity cellulose is 98.1% using an appropriate condition which is much higher than that obtained from the original RH (73.3%).

The components yield of the residue based on raw RH are shown in the **Figure 5.1**. Almost all of the ash in HTRH was removed, while a small amount of lignin was removed under N_2 atmosphere. The lignin was effectively removed under O_2 atmosphere. The removal behaviors of lignin and ash are obviously different. Ash removal requires alkaline rather than oxidation and the lignin removal requires both alkaline and oxidation. Comparing Na_2CO_3 with NaOH, NaOH produced almost pure cellulose but caused severe cellulose loss, leaving less than 40% of the cellulose. More than 87% of the cellulose was well preserved using Na_2CO_3. Na_2CO_3 offered an enormous advantage in avoiding cellulose degradation. Na_2CO_3 offered an enormous advantage in avoiding cellulose degradation. A large amount of lignin and ash was not removed at 100 ℃ even with higher O_2 pressure (3 MPa) and longer treatment time (180 min) than at 120 ℃ (2 MPa and 120 min). Cellulose with a purity of 93% was obtained by treating HTRH at 120 ℃ using 20 mL/g for 120 min. Extending the time and increasing the temperature had limited effect on the purification of cellulose. The yield of cellulose was reduced from 87% to 72% after the temperature was

increased from 120 to 140 ℃. Increasing the amount of alkali solution from 20 to 40 mL/g significantly increased the purity of cellulose from 93.1 to 98.1 with no serious cellulose loss.

Table 5.2. Residues composition (wt%, d) and pH of suspension.

Samples	Lignin	Sugar					
	TL	Glucan	Xylan	Galactan	arabinan	Ash	pH
RH	28.00	31.37	15.76	2.26	3.35	15.45	
Hydrothermal extraction - 180 ℃, H_2O, 5 mL/min, 150 min, 5 Mpa							
HTRH	29.12	55.34	4.43	2.14	-	9.38	
Alkaline wet oxidation - Na_2CO_3, 120 ℃, 1.0 mol/L, 20 mL/g, O_2 2 Mpa, 120 min							
RH-OT	14.27	52.33	19.05	1.70	2.43	5.87	9.67
RH-OT-P	9.46	73.35	16.50	0.79	1.33	1.01	11.05
HTRH-OT	4.23	93.12	2.38	0.61	-	3.26	9.66
HTRH-OT-P	2.19	97.5	1.54	0.77	-	0.55	11.05
100 ℃	6.31	85.15	2.32	0.44	-	6.31	9.98
180 min	3.24	92.33	2.13	0.37	-	5.65	9.65
140 ℃	2.92	89.84	1.86	0.51	-	5.20	9.19
40 mL/g	2.07	98.11	1.05	0.32	-	0.32	10.26
HTRH-OT-NaOH	0.46	101.39	-	-	-	-	12.12
HTRH-H_2O	28.43	55.74	4.50	2.34	-	9.25	2.75
HTRH-N_2	24.49	67.47	2.57	1.20	-	0.88	10.42
Reuse of filtrate - Na_2CO_3, 120 ℃, filtrate, 40 mL/g, O_2 2 Mpa, 120 min,							
Run1	2.07	98.11	1.05	0.32	-	0.32	10.26
Run2	3.06	92.76	1.41	0.48	-	2.61	9.51
Run3	4.00	88.74	2.48	0.56	-	6.94	9.05
Run4	6.09	80.89	2.71	0.58	-	13.43	8.63

- Not detected; TL is the total lignin.

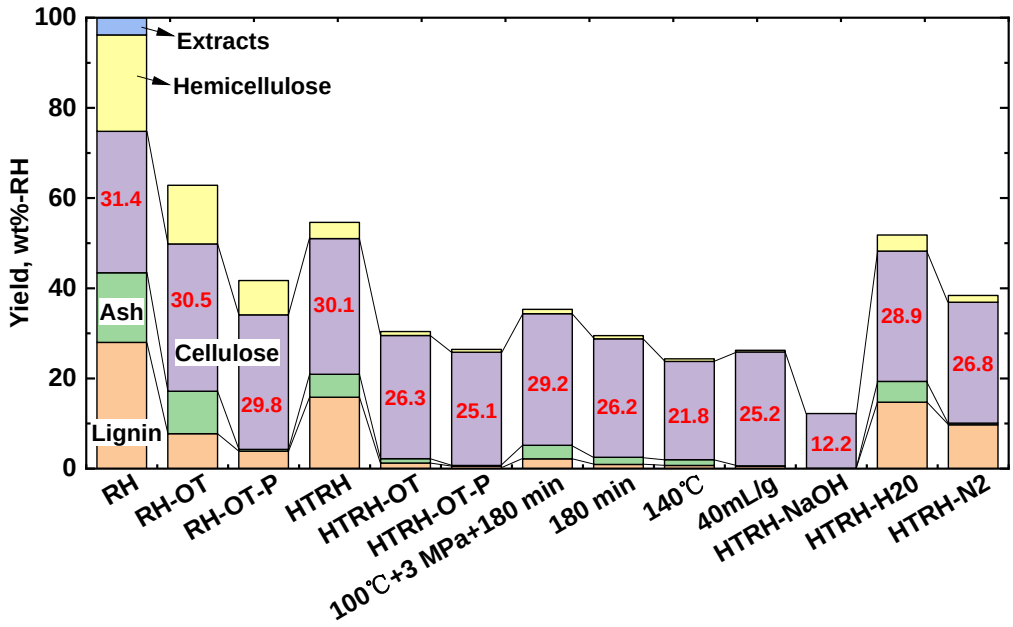

Figure 5.1. Components yield of the residue. (HTRH-OT: O_2 2 MPa, 120 min, Na_2CO_3 1 mol/L, L/S = 20 mL/g, and 120 ℃; Percolator: O_2 2 MPa, 120 min, Na_2CO_3 1 mol/L, 5 mL/min, and 120 ℃.)

To investigate the effect of the products in solution on the purification of cellulose the percolator were employed. Comparing the two reactors, the percolator promoted the removal of lignin and ash, especially the ash was almost completely removed. Although the percolator operation consumed a large amount of alkaline solution (300 mL/g), the improvement in cellulose purification was very limited (93.1 *vs.* 97.5%). The complete ash removal results from the fact that the final suspension pH is greater than 10. It is reasonable to think that the deep deashing can be achieved by keeping a sufficient alkalinity pH > 10 even in a batch reactor.

5.3.2. Reuse of liquid products

The recyclability of the Na_2CO_3 solution was examined by multiple reuses in batch reactor (**Figure 5.2**). The reuse of Na_2CO_3 solution (filtrate) allowed cellulose to be enriched in the solid residue, but the purity of cellulose was gradually reduced from 98.1% to 80.9%. Repeated use of the filtrate yielded a cellulose recovery of over 90%. The reuse of alkaline liquor maintained high lignin removal efficiency, but the ash removal efficiency decreased sharply. 84% lignin was removed while only 31% ash was removed after four repetitions.

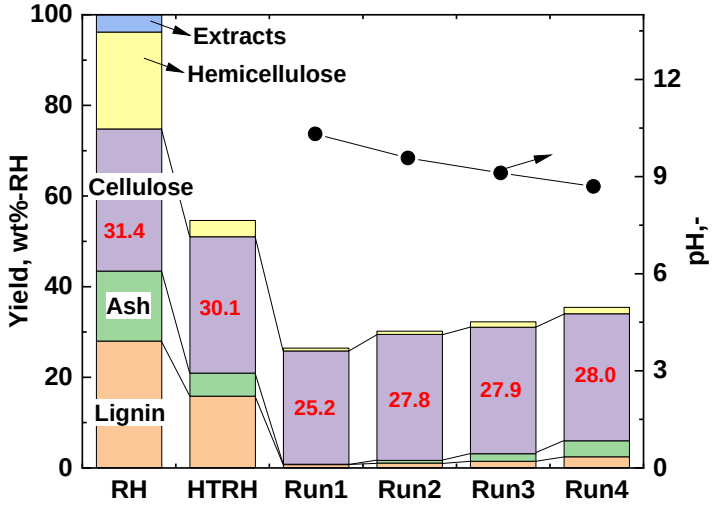

Figure 5.2. Components yield of the residue. (Condition: O_2 2 MPa, 120 min, filtrate, L/S = 40 mL/g, and 120 ℃)

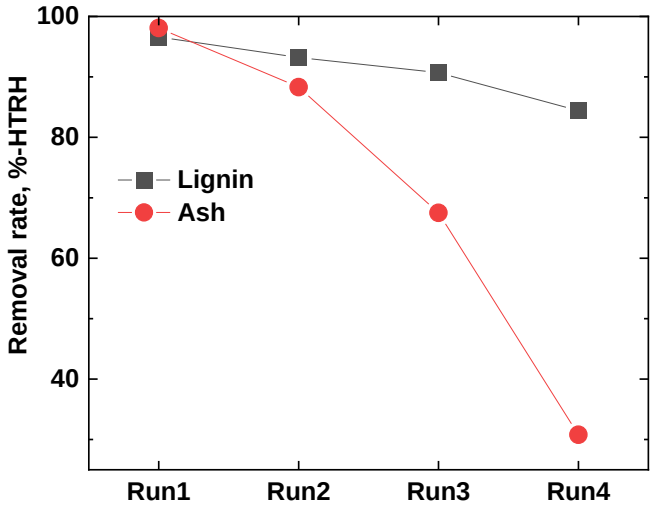

Figure 5.3. Removal rate of lignin and ash.

The dramatic deterioration in ash removal efficiency can be attributed to the pH decrease (10.3 to 8.6) and the accumulation of ash in the liquid product. The silicon in RH has good solubility in alkaline solution with pH > 10. [7] The pH decrease of the liquid product is mainly due to the formation of large amounts of organic acids (**Figure 5.4**). The decrease of pH has a great negative impact on the ash removal but a limited impact on lignin removal. The effective removal of lignin indicates that the effective oxidation reactions occurred even in the low pH liquid product. The alkaline dosage could be significantly reduced by reusing the filtrate.

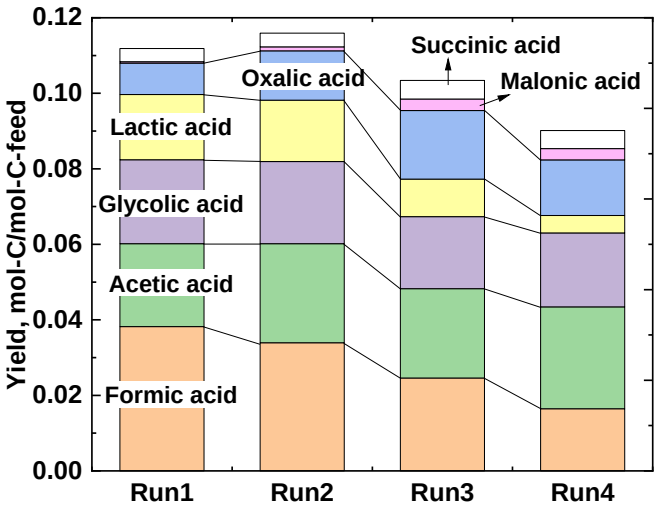

Figure 5.4. Carbon-based yields of organic acids.

5.3.3. Characterization of solid products

The macroscopic (photographs) and microscopic (SEM) visualizations of the RH evolution are shown in Figure 1. The original RH was light brown, and it changed to dark brown after hydrothermal treatment and white after alkaline wet oxidation. The inside surface became rougher after hydrothermal treatment, while no change was observed on the outside surface. It was found that the silicon in the RH is mainly concentrated around the dome-shaped protrusions on the outer surface, which makes it very stubborn. [16] The RH structure was completely destroyed after alkaline wet oxidation and the fiber bundles were separated into individual fibers with a diameter of about 5 μm. Cellulose fibers are not only used directly for material applications, but also as raw feedstock for the preparation of cellulose nanocrystals and nanofibers. [17]

The functional groups related to lignin or hemicellulose, such as the acetyl and ester groups C=O at 1730 cm^{-1} and the C=C stretching of aromatic ring at 1510 cm^{-1}, nearly disappeared in the cellulose fiber. [8] No significant differences were observed between HTRH and cellulose fiber in the 900–1500 cm^{-1}spectra range corresponding to cellulose. [18] The results showed that the cellulose molecular structure remained invariant after treatments.

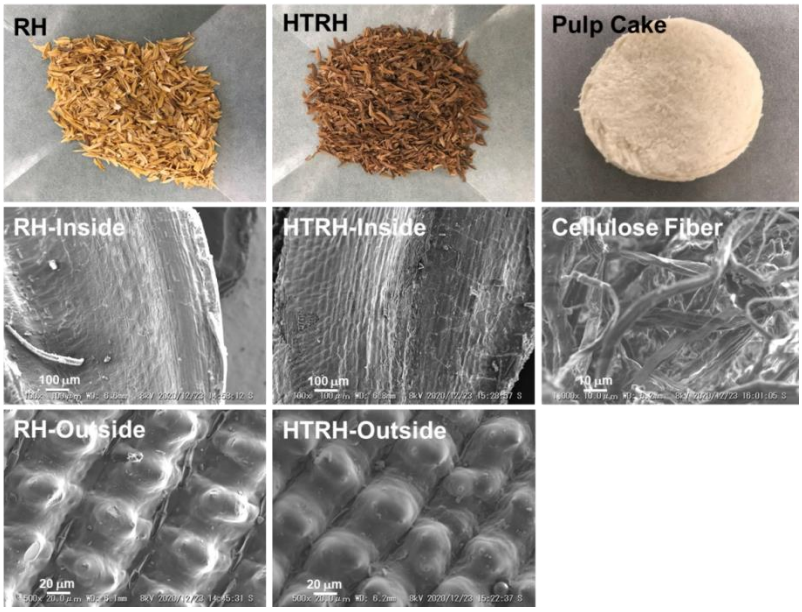

Figure 5.5. Photographs and SEM micrographs of RH, HTRH, and cellulose fibers.

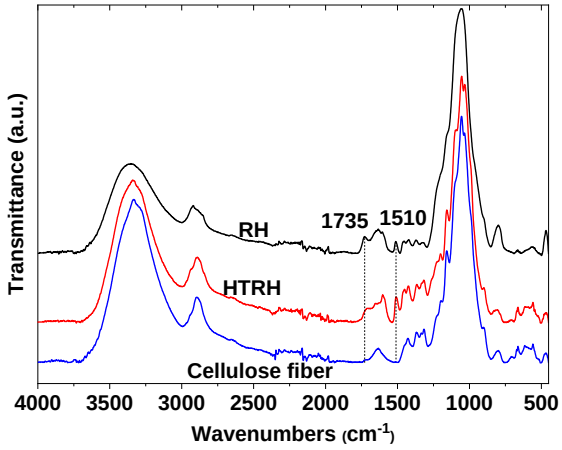

Figure 5.6. FTIR spectra recorded of RH, HTRH, and cellulose fibers.

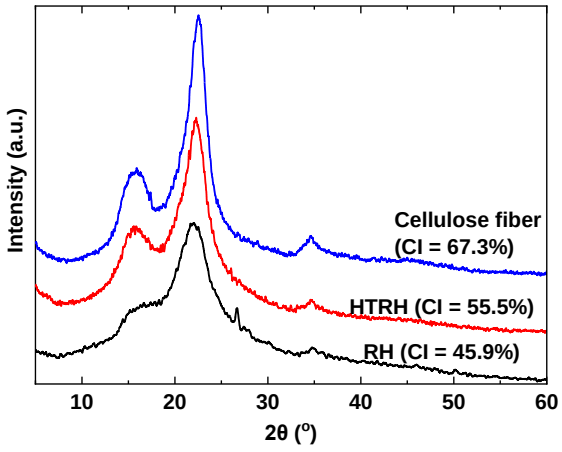

Figure 5.7. X-ray diffraction patterns of RH, HTRH, and cellulose fibers. (The crystallinity index was calculated by the Segal formula: CI = (I_{22} °–I_{18} °)/ I_{22} °× 100%)

Figure 5.7 shows the diffraction patterns of RH, HTRH, and cellulose fibers. They are typical of cellulose I with three well-defined crystalline peaks around $2\theta = 16^o$, 22^o, and 35^o. The peak at 22 ° represents both crystalline and amorphous region and the peak at 18 ° corresponds to the amorphous region in cellulosic materials. [19] The $2\theta = 22^o$ peak became more defined in cellulose fiber than in RH and HTRH. The crystallization index of RH was 45.9%, while the CI of cellulose fiber increased to 67.3%. The increased crystallinity was ascribed to the removal of amorphous non-cellulosic materials and cellulosic domains. The amorphous region of cellulose is more accessible resulting in hydrolytic cleavage of the glycosidic bond. [20] The crystallinity of cellulose obtained from other materials was about 66% for potato tuber, 68% for rice straw, and 71% for wood cellulose. [21] The RH cellulose obtained in this study has great potential to achieve high reinforcement of composites. [22]

5.4. Conclusion

Hydrothermal pretreatment significantly promoted the removal of hemicellulose, lignin, and ash in the subsequent alkaline wet oxidation process. Ash removal requires alkaline rather than oxidation while the lignin removal requires both alkaline and oxidation. Compared to NaOH, Na_2CO_3 surprisingly avoided the substantial loss of RH cellulose. High-purity cellulose fiber (98.1%) was obtained in a high yield (>83 wt%) by using Na_2CO_3 solution and O_2 at 120 ℃ for 120 min. The liquid product (filtrate obtained after reaction) maintained a good delignification effect (84%) even after being reused four times. The ash in the RH can only be effectively removed when the pH > 10 of the reaction solution. The cellulose fiber obtained in this study has a diameter of approximately 5 μm and a crystallinity of 67%.

5.5. References

[1] H.X. Zhang, X.F. Ding, X. Chen, Y.J. Ma, Z.C. Wang, X. Zhao, A new method of utilizing rice husk: consecutively preparing D-xylose, organosolv lignin, ethanol and amorphous superfine silica, *J. Hazard. Mater.*, 291 (2015) 65-73.

[2] K. Mochidzuki, A. Sakoda, M. Suzuki, J. Izumi, N. Tomonaga, Structural behavior of rice husk silica in pressurized hot-water treatment processes, *Ind. Eng. Chem. Res.*, 40 (2001) 5705–5709.

[3] Y. Li, X.F. Ding, Y.P. Guo, C.G. Rong, L.L. Wang, Y.N. Qu, X.Y. Ma, Z.C. Wang, A new method of comprehensive utilization of rice husk, *J. Hazard. Mater.*, 186 (2011) 2151-2156.

[4] T.N. Ang, G.C. Ngoh, A.S.M. Chua, Comparative study of various pretreatment reagents on rice husk and structural changes assessment of the optimized pretreated rice husk, *Bioresource Technol.*, 135 (2013) 116-119.

[5] G. Gallina, E.R. Alfageme, P. Biasi, J. Garcia-Serna, Hydrothermal extraction of hemicellulose: from lab to pilot scale, *Bioresource Technol.*, 247 (2018) 980-991.

[6] A. Mittal, R. Katahira, B.S. Donohoe, B.A. Black, S. Pattathil, J.M. Stringer, G.T. Beckham, Alkaline peroxide delignification of corn stover, *ACS Sustainable Chem. Eng.*, 5 (2017) 6310-6321.

[7] N. Soltani, A. Bahrami, M.I. Pech-Canul, L.A. González, Review on the physicochemical treatments of rice husk for production of advanced materials, *Chem. Eng. J.*, 264 (2015) 899-935.

[8] S.M.L. Rosa, N. Rehman, M.I.G. Miranda, S.M.B. Nachtigall, C.I.D. Bica, Chlorine-free extraction of cellulose from rice husk and whisker isolation, *Carbohyd. Polym.*, 87 (2012) 1131-1138.

[9] S.J. Eichhorn, A. Dufresne, M. Aranguren, N.E. Marcovich, J.R. Capadona, S.J. Rowan, et al., Review: current international research into cellulose nanofibres and nanocomposites, *J.of Mater. Sci.*, 45 (2010) 1-33.

[10] P. Jeetah, N. Golaup, K. Buddynauth, Production of cardboard from waste rice husk, *J. Environ. Chem. Eng.*, 3 (2015) 52-59.

[11] N. Johar, I. Ahmad, A. Dufresne, Extraction, preparation and characterization of cellulose fibres and nanocrystals from rice husk, *Ind. Crop. Prod.*, 37 (2012) 93-99.

[12] M.T. Amiri, G.R. Dick, Y.M. Questell-Santiago, J.S. Luterbacher, Fractionation of lignocellulosic biomass to produce uncondensed aldehyde-stabilized lignin, *Nat. Protoc.*, 14 (2019) 921-954.

[13] R.C. Francis, S.J. Shin, S. Omori, T.E. Amidon, T.J. Blain, Soda Pulping of hardwoods catalyzed by anthraquinone and methyl substituted anthraquinones, *J. Wood Chem. Technol.*, 26 (2006) 141-152.

[14] F.S. Chakar, A.J. Ragauskas, Review of current and future softwood kraft lignin process chemistry, *Ind. Crop. Prod.*, 20 (2004) 131-141.

[15] B.G. Frantisek Potucek, Katerina Hajkova, Soda pulping of rapeseed straw, *Cellulose Chem. Technol.*, 48 (2014) 683-691.

[16] B.-D. Park, S.G. Wi, K.H. Lee, A.P. Singh, T.-H. Yoon, Y.S. Kim, Characterization of anatomical features and silica distribution in rice husk using microscopic and

micro-analytical techniques, *Biomass Bioenerg.*, 25 (2003) 319-327.

[17] A. Sharma, M. Thakur, M. Bhattacharya, T. Mandal, S. Goswami, Commercial application of cellulose nano-composites-A review, *Biotechnol. Rep.*, 21 (2019) e00316.

[18] H.R. Lee, R.J. Kazlauskas, T.H. Park, One-step pretreatment of yellow poplar biomass using peracetic acid to enhance enzymatic digestibility, *Sci. Rep.*, 7 (2017) 12216.

[19] N. Reddy, Y. Yang, Structure and properties of high quality natural cellulose fibers from cornstalks, *Polymer*, 46 (2005) 5494-5500.

[20] M.M. de Souza Lima, R. Borsali, Rodlike cellulose microcrystals: Structure, properties, and applications, *Macromol. Rapid Comm.*, 25 (2004) 771-787.

[21] K. Abe, H. Yano, Comparison of the characteristics of cellulose microfibril aggregates of wood, rice straw and potato tuber, *Cellulose*, 16 (2009) 1017-1023.

[22] Q. Cheng, S. Wang, T.G. Rials, S.H. Lee, Physical and mechanical properties of polyvinyl alcohol and polypropylene composite materials reinforced with fibril aggregates isolated from regenerated cellulose fibers, *Cellulose*, 14 (2007) 593-602.

CHAPTER 6

General Conclusions

Biomass structure is complex and resistant, especially high lignin content biomass. Lignin is the main obstacle to the efficient conversion of carbohydrates. The alkaline wet oxidation is a potentially effective pretreatment and fractionation technology which can provide cellulose rich fraction and a soluble stream of hemicellulose/lignin. However, there are still problems such as severe loss of carbohydrates, unclear mechanism of biomass degradation, and the use of expensive or toxic reagents. Characteristics of the delignification are important for yield and property of resulting carbohydrates. With this perspective, this thesis carried out the alkaline wet oxidation of the high lignin content biomass using the green oxidant O_2 under mild conditions for delignification. The chemical mechanism was explored through the repetitive operation of a batch reactor and the continuous operation of a flow-through reactor.

Even at 90 ℃, O_2 greatly promotes the lignin dissolution while decomposing carbohydrates. Polysaccharides are decomposed into small molecules without forming monosaccharides. The chemical condensation of dissolved lignin fragments greatly impedes the delignification. Repeated short-time oxidation with renewal of alkaline water suppressed the condensation enhancing the delignification. Lignification consists of three stages (early, mid, and late stages). The late-stage delignification (rate >0.65) requires cellulose decomposition for making the lignin accessible to oxidizing agents. The target purity of the product cellulose should be determined in consideration of the unavoidable trade-off relationship between lignin and cellulose retentions.

The alkaline wet oxidation performed in a flow-through percolator rather than in a batch reactor, allows for analysis of the primary reaction by eliminating the secondary reactions of the extracts. The cedar consisted of three kinetic components (C1, C2, and C3) that underwent extraction in parallel following first-order kinetics with different rate constants. The chemical compositions of the kinetic components were mixtures of carbohydrates and lignin. C1 was converted most rapidly by non-oxidative reactions such as alkali-catalyzed hydrolysis, while C2 by oxidative degradation. The product distributions from C1 and C2 (CO_2, lower organic acids, oligosaccharides, acid-soluble and acid-insoluble lignins) were steady throughout

their conversion. C3 was the most refractory component, consisting mainly of glucan and very minimally of the lignin and hemicellulose.

Most hemicellulose in cedar was recovered as mannose-oligosaccharides by hydrothermal extraction using H_2O at 180 ℃. Compared to NaOH, Na_2CO_3 was more favorable for the oxidative depolymerization of lignin recovering a high-cellulose residue (98.8%) from cedar. Oxidative depolymerization and degradation are dominant reactions during lignin removal resulting 65-95% of the dissolved lignin was degraded into small lignin fragments and organic acids by Na_2CO_3.

Hydrothermal pretreatment significantly promoted the removal of hemicellulose, lignin, and ash from rice husk in the subsequent alkaline wet oxidation process. Na_2CO_3 effectively prevented the loss of cellulose and separated cellulose fiber from rice husk in high yield. The liquid product (filtrate obtained after reaction) maintained a good delignification effect even after being reused four times.

ACKNOWLEDGEMENTS

The present study was carried out at the Interdisciplinary Graduate School of Engineering Science in Kyushu University from 2017 to 2020. This experience ended painfully and cheerfully.

I would like to express my sincere gratitude to Prof. Jun-ichiro Hayashi, my supervisor, for his great patience, intelligent and careful guidance, and constructive feedback for this research. I have great admiration for his work enthusiasm. I was greatly inspired by his insights on research.

I would also like to thank Associate prof. Shinji Kudo, who has been of great help with his feedback, discussions, and opinions. In particular, I admire his concentration on research.

I am also grateful for the help given by Assistant prof. Shusaku Asano in both research and daily life. In particular, he gave me professional and detailed knowledge about writing and publishing papers.

Special thanks to Ms. Asuka Mori, Ms. Yasuyo Hachiyama, Mrs. NaoKo Sudo, and Mr. Kentaro Shima, for their great help in research and daily life. Special gratitude is also given to Mr. Tianlong Liu, Mr. Fu Wei, Ms. Yan Li, and Ms. Phatchada Santawaja for their encouragement when I was depressed. Their friendship is unforgettable for life.

Most importantly, I would like to thank my family, especially my girl Ms. Shengnan Liu, for their continued support and encouragement. What a long wait! Wish you all the best and I love you.

Also, I acknowledge the China Scholarship Council with financial support for my study and life in Japan.

Wang Jingxian

Chikushi Campus

February 14, 2021